NOAA Technical Memorandum NMFS-NWFSC-149

https://doi.org/10.25923/p0ed-ke21

Ecosystem Status Report of the California Current for 2019:

A Summary of Ecosystem Indicators Compiled by the California Current Integrated Ecosystem Assessment Team (CCIEA)

October 2019

U.S. DEPARTMENT OF COMMERCE

National Oceanic and Atmospheric Administration
National Marine Fisheries Service
Northwest Fisheries Science Center

NOAA Technical Memorandum Series NMFS-NWFSC

The Northwest Fisheries Science Center of NOAA's National Marine Fisheries Service uses the NOAA Technical Memorandum NMFS-NWFSC series to issue scientific and technical publications that have received thorough internal scientific review and editing. Reviews are transparent collegial reviews, not anonymous peer reviews. Documents within this series represent sound professional work and may be referenced in the formal scientific and technical literature.

The Northwest Fisheries Science Center's NOAA Technical Memorandum series continues the NMFS-F/NWC series established in 1970 by the Northwest and Alaska Fisheries Science Center, which subsequently was divided into the Northwest Fisheries Science Center and the Alaska Fisheries Science Center. The latter uses the NOAA Technical Memorandum NMFS-AFSC series.

NOAA Technical Memorandums NMFS-NWFSC are available from the NOAA Institutional Repository, https://repository.library.noaa.gov.

Any mention throughout this document of trade names or commercial companies is for identification purposes only and does not imply endorsement by the National Marine Fisheries Service, NOAA.

Cover image: Crowds razor clamming on a beach near Ocean Shores, Washington, spring 2007. Photograph by M. Coverdale via D. Ayres, WDFW.

Reference this document as follows:

Harvey, C., N. Garfield, G. Williams, N. Tolimieri, I. Schroeder, K. Andrews, K. Barnas, E. Bjorkstedt, S. Bograd, R. Brodeur, B. Burke, J. Cope, A. Coyne, L. deWitt, J. Dowell, J. Field, J. Fisher, P. Frey, T. Good, C. Greene, E. Hazen, D. Holland, M. Hunter, K. Jacobson, M. Jacox, C. Juhasz, I. Kaplan, S. Kasperski, D. Lawson, A. Leising, A. Manderson, S. Melin, S. Moore, C. Morgan, B. Muhling, S. Munsch, K. Norman, R. Robertson, L. Rogers-Bennett, K. Sakuma, J. Samhouri, R. Selden, S. Siedlecki, K. Somers, W. Sydeman, A. Thompson, J. Thorson, D. Tommasi, V. Trainer, A. Varney, B. Wells, C. Whitmire, M. Williams, T. Williams, J. Zamon, and S. Zeman. 2019. Ecosystem Status Report of the California Current for 2019: A Summary of Ecosystem Indicators Compiled by the California Current Integrated Ecosystem Assessment Team (CCEIA). U.S. Department of Commerce, NOAA Technical Memorandum NMFS-NWFSC-149.

https://doi.org/10.25923/p0ed-ke21

NOAA FISHERIES

Ecosystem Status Report of the California Current for 2019: A Summary of Ecosystem Indicators Compiled by the California Current Integrated Ecosystem Assessment Team (CCIEA)

Chris Harvey, Newell Garfield, Gregory Williams, Nick Tolimieri, Isaac Schroeder, Kelly Andrews, Katie Barnas, Eric Bjorkstedt, Steven Bograd, Richard Brodeur, Brian Burke, Jason Cope, Audrey Coyne, Lynn deWitt, Judy Dowell, John Field, Jennifer Fisher, Peter Frey, Thomas Good, Correigh Greene, Elliott Hazen, Daniel Holland, Matthew Hunter, Kym Jacobson, Michael Jacox, Christy Juhasz, Isaac Kaplan, Stephen Kasperski, Dan Lawson, Andrew Leising, Alex Manderson, Sharon Melin, Stephanie Moore, Cheryl Morgan, Barbara Muhling, Stuart Munsch, Karma Norman, Roxanne Robertson, Laura Rogers-Bennett, Keith Sakuma, Jameal Samhouri, Rebecca Selden, Samantha Siedlecki, Kayleigh Somers, William Sydeman, Andrew Thompson, Jim Thorson, Desiree Tommasi, Vera Trainer, Anna Varney, Brian Wells, Curt Whitmire, Margaret Williams, Thomas Williams, Jeannette Zamon, and Samantha Zeman

https://doi.org/10.25923/p0ed-ke21

October 2019

U.S. DEPARTMENT OF COMMERCE

National Oceanic and Atmospheric Administration
National Marine Fisheries Service
Northwest Fisheries Science Center

Contents

Figures

Tables

Executive Summary

This document is a companion to the ecosystem status report (ESR) provided by the California Current Integrated Ecosystem Assessment team (CCIEA team) to the Pacific Fishery Management Council (PFMC) in March of 2019 (Harvey et al. 2019). The CCIEA team provides ESRs annually to PFMC, as one component of the overall CCIEA goal of providing quantitative, integrative science tools, products, and synthesis in support of a more holistic (ecosystem-based) approach to managing marine resources in the California Current.

The ESR features a suite of indicators co-developed by the CCIEA team and PFMC. The suite of indicators was initially identified in 2009, and has been refined and updated over the years to best capture the current state of the California Current ecosystem. The analyses in this document thus represent our best understanding of environmental, ecological, and socioeconomic conditions in this ecosystem roughly through the end of 2018. Because the time required to process the data varies for different indicators, some of the resulting time series are slightly more up-to-date than others. Some indicators (snowpack, sea lion reproduction and pup growth, seabirds, fishery landings, fishery revenue, and non-fishing human activities) have been updated since the March 2019 report to PFMC (Harvey et al. 2019).

In terms of the natural biophysical system, we regarded 2018 as another transitional year, in which the CCE continued its recovery from the marine heat wave of 2013–16 and the major El Niño event of 2015–16. We similarly considered much of 2016 and all of 2017 to be transitional. By "transitional," we mean that many indicators suggest that the system has shifted away from the highly unusual conditions of the marine heat wave and El Niño events, which included very warm water temperatures, poor productivity across several trophic levels, and widespread occurrence of species normally associated with warmer southerly and/or offshore waters. However, some aspects of these conditions remain in the system. Also, some populations of long-lived fishes, seabirds and marine mammals may show the effects of the unusual warming events at lag times of months to years, even after physical conditions and characteristics of the base of the food web have returned to average or above-average conditions.

We acknowledge that calling this period "transitional" begs the question: transitioning to what? We are not confident in our answer to that question: the system may remain in this current state, where many indicators are close to (or oscillating around) their long-term averages, or it may shift toward a more definitive state of high productivity (as observed for much of 2008–13) or low productivity (as observed from 2014–16).

Many indicators in 2018 gave somewhat conflicting signs as to what conditions will prevail in the year to come. Several metrics indicated average or improving conditions in the CCE:

- Indicators of temperature in the North Pacific Ocean, the Equatorial Pacific, and along the West Coast were closer to long-term averages for much of 2018.
- Although there were signs that a new marine heatwave was forming in a large portion of the North Pacific in the fall of 2018, those signs dissipated by the end of the year.
- The community of copepods (tiny free-swimming crustaceans at the bottom of the food web) off Newport, Oregon shifted toward a cool-water, energy-rich assemblage, following many years of abundant warm-water, energy-poor species.

- Krill off of Trinidad Head, California grew to the largest sizes observed since 2014.
- Some important forage species, including anchovies (*Engraulis mordax*), market squid (*Doryteuthis opalescens*), and krill, had increasing and/or above average abundance in portions of the system.
- Catch rates of juvenile salmon, especially coho salmon (*Oncorhynchus kisutch*), increased off of Washington and Oregon.
- Abundance and growth rate of California sea lion (*Zalophus californianus*) pups at the San Miguel Island colony were above average, implying improved feeding conditions in that region for adult female sea lions.
- No mass seabird die-offs were observed that could be attributed to poor food availability.

However, other indicators from 2018 suggested ongoing unfavorable conditions:

- Equatorial temperatures indicated that the region was trending toward a weak El Niño at the end of 2018.
- An index of the volume of cool, productive subarctic water entering the CCE from the north declined to some of the weakest levels observed.
- Warmer-than-normal water masses persisted into 2018, particularly in the upper 50 m of the water column in the southern CCE.
- Widespread hypoxia occurred along the bottom of the continental shelf off Washington and Oregon in the summer and early fall. According to analyses that are new to this year's report, hypoxia of bottom waters is again forecast to occur in this region in 2019, along with conditions consistent with ocean acidification.
- Harmful algal blooms of the diatom *Pseudo-nitzschia* led to high concentrations of domoic acid in shellfish in Oregon and California, resulting in multiple fishery closures.
- Pyrosomes, free-swimming colonial gelatinous animals that normally prefer warmer waters found further to the south, remained abundant in the northern and central CCE.
- A number of biological and oceanographic indicators in 2017–18 projected below-average Chinook (*Oncorhynchus tshawytscha*) salmon returns to the Columbia River basin in 2019.
- Reports of whale entanglements in fixed fishing gear were above average for the fifth consecutive year, and were greater than in 2017.

Total commercial fishery landings have increased since a recent low point in 2015, and the increase mostly is attributable to Pacific hake (*Merluccius productus*). Conversely, recreational fishery landings have been declining since 2015. We continued to observe very low diversification of catch revenues by commercial fishing vessels of all size and revenue classes in all three coastal states; in other words, on average, vessels are relying on relatively few species to provide the bulk of their revenues. We are working to understand how the reliance of coastal communities on commercial and recreational fishing relates to those communities' overall social wellbeing and vulnerability.

How changes in the ecosystem affect the abundance, distribution, and condition of marine species is of great interest to commercial and recreational fishers, managers, conservation groups, and the broader public. In this year's report, we present new analyses that describe how shifts in the abundance and distribution of important groundfish make them more available to some fishing ports and less available to others. These patterns of changing availability can be compared to other metrics we are tracking, such as the amount of bottom fishing effort occurring in an area, the fleet diversification of a region, or social and

economic vulnerability of different coastal communities. These measures that connect environmental conditions and shifting target species populations to human activities and wellbeing may assist PFMC in achieving objectives under its "Climate and Communities Initiative,"[1] being undertaken to better understand how climate variability and climate change affect fish populations, and thereby affect coastal communities that rely on fishing as part of their economic, social and cultural wellbeing.

The sections that follow will go into greater detail about the status and trends of indicators summarized here; after a short Introduction, we include sections related to Climate and Ocean Drivers, the Focal Components of Ecological Integrity, Human Activities, and Human Wellbeing, followed by a brief Synthesis.

[1] https://www.pcouncil.org/ecosystem-based-fisheries-management/fishery-ecosystem-plan-initiatives/climate-and-communities-initiative

1. Introduction

1.1. Ecosystem-Based Fisheries Management and Integrated Ecosystem Assessment

Ecosystem-based management of fisheries and other marine resources has emerged as a priority in the U.S. (Ecosystem Principles Advisory Panel 1999, Fluharty et al. 2006, McFadden and Barnes 2009, NOAA 2018) and elsewhere (Browman et al. 2004, Sainsbury et al. 2014, Walther and Möllmann 2014, Long et al. 2015). The National Marine Fisheries Service (NOAA Fisheries) defines ecosystem-based fisheries management (EBFM) as

> a systematic approach to fisheries management in a geographically specified area that contributes to the resilience and sustainability of the ecosystem; recognizes the physical, biological, economic, and social interactions among the affected fishery-related components of the ecosystem, including humans; and seeks to optimize benefits among a diverse set of societal goals (NOAA 2018).

This definition encompasses interactions within and among fisheries, protected species, aquaculture, habitats, and human communities that depend upon fisheries and related ecosystem services. An EBFM approach is intended to improve upon traditional fishery management practices that primarily are focused on individual fished stocks.

Successful EBFM requires considerable effort and coordination due to the formidable amount of information required and uncertainty involved. In response, scientists throughout the world have developed many frameworks for organizing science and information to clarify and synthesize this overwhelming volume of data into science-based guidance for policymakers. NOAA Fisheries has adopted a framework called integrated ecosystem assessment (IEA; Levin et al. 2008, Levin et al. 2009), which can be summarized in five progressive steps (Figure 1):

1. Identifying and scoping ecosystem goals, objectives, targets, and threats.
2. Assessing ecosystem status and trends through the use of valid ecosystem indicators.
3. Assessing the risks of key threats and stressors to the ecosystem.
4. Analyzing management strategy alternatives and identifying potential tradeoffs.
5. Implementing selected actions, and monitoring and evaluating management success.

As shown in Figure 1, the IEA approach is iterative. Following the implementation of management actions, all other steps in the IEA loop must be revisited in order to ensure that a) evolving goals and objectives are clearly identified, b) monitoring plans and indicators are appropriate for the management objectives in mind, c) existing and emerging risks are properly prioritized, and d) management actions are objectively and regularly evaluated for success. The five steps of the IEA framework, plus its iterative nature, are very similar to and compatible with the core guiding principles of the NOAA EBFM Policy (NOAA 2016, Link 2017).

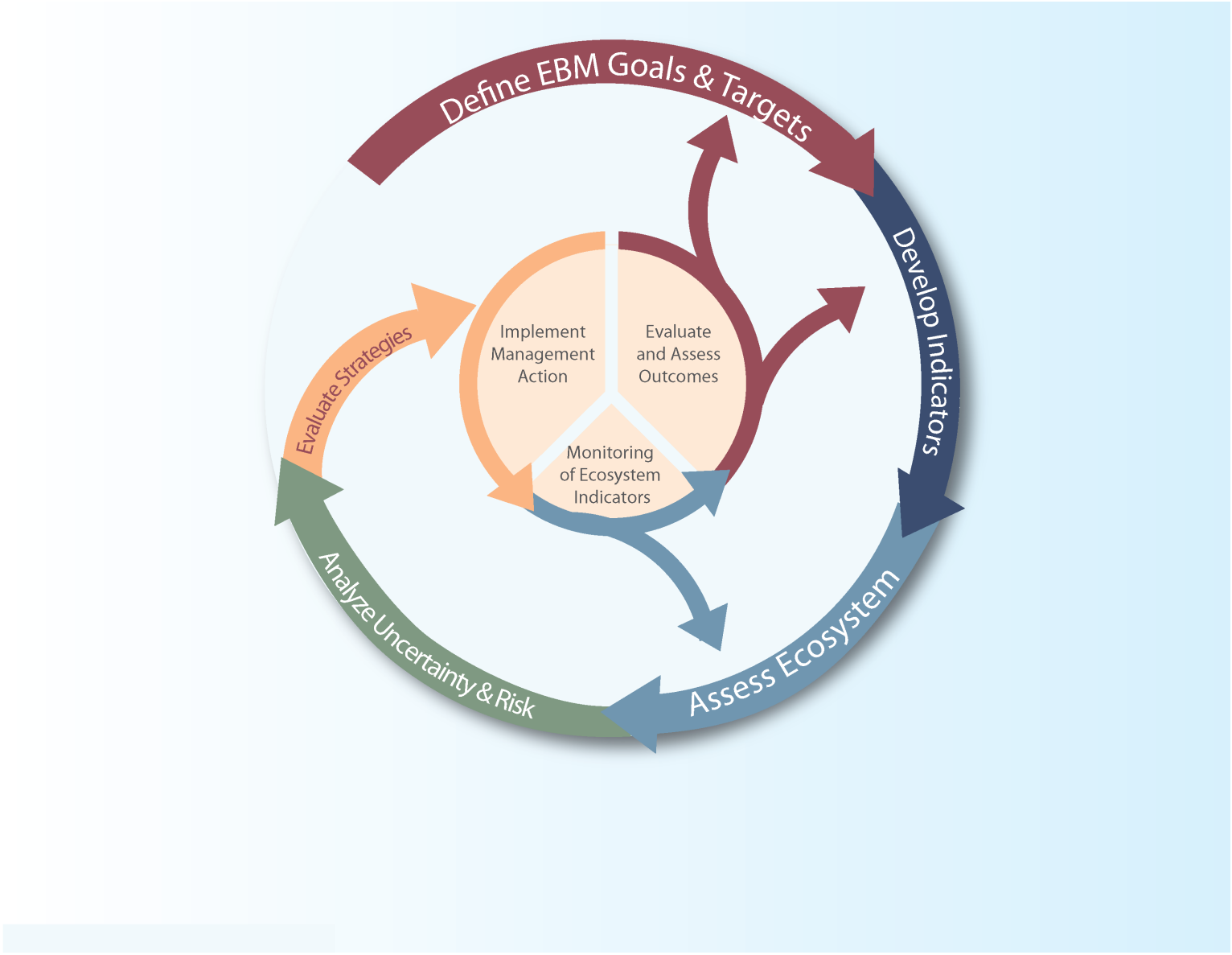

Figure 1. Loop diagram of the five progressive steps in iterations of the integrated ecosystem assessment (IEA) process. From Samhouri et al. (2014).

Figure 2. Conceptual model of the California Current social-ecological system. The model represents the complex and inextricable connections between natural components (left) and human components (center, right). These components are arranged in three tiers: focal ecosystem components, which are often associated with broad objectives such as ecological integrity and human wellbeing; mediating components, such as habitat and local social systems; and drivers and pressures, which are generally external forces on the ecosystem. Human activities are placed at the center to emphasize their broad extent and because they are where management actions are directly implemented in order to achieve objectives elsewhere in the system. From Levin et al. (2016).

In 2009, NOAA line offices along the U.S. West Coast initiated the California Current Integrated Ecosystem Assessment (CCIEA). The CCIEA team focuses on the California Current ecosystem (CCE) along the U.S. West Coast. In keeping with the principles of ecosystem-based management, the CCIEA team regards the CCE as a dynamic, interactive, social-ecological system with multiple levels of organization and diverse goals and endpoints that are both environmental and social in nature (Figure 2). The challenging task of assembling and interpreting information from this broad range of disciplines, locations, and time frames engages over 50 scientists from NOAA's Northwest and Southwest Fisheries Science Centers and other NOAA offices, as well as colleagues from other agencies, academia, and nongovernmental entities. Information on CCIEA research efforts, tools, products, publications, partnerships, and points of contact is available on the CCIEA website.[1]

The primary management partner of the CCIEA team to date has been the Pacific Fishery Management Council (PFMC),[2] which oversees federally managed fisheries and implementation of the Magnuson–Stevens Fishery Conservation and Management Act in the Exclusive Economic Zone off the U.S. West Coast. PFMC manages target species directly under policies outlined in its four fishery management plans (FMPs), and may incorporate nonbinding guidance from its Fishery Ecosystem Plan (FEP; PFMC 2013).[3]

Section 1.4 of the FEP outlined a reporting process wherein the CCIEA team provides PFMC with a yearly ecosystem status report (ESR) that describes the current status and trends of ecosystem attributes of the CCE. The purpose of the ESR is to provide PFMC with a general sense of ecosystem conditions as context for decision-making. ESRs include information on a range of attributes, including climate and oceanographic drivers, status of key species groups, fisheries-related human activities, and human wellbeing in coastal communities. ESRs track ecosystem attributes through ecosystem indicators, most of which were derived through a rigorous indicator screening process developed by Kershner et al. (2011); details of specific CCIEA indicator screening exercises are documented elsewhere (Levin and Schwing 2011, Levin et al. 2013, Harvey et al. 2014).

Since 2012, the CCIEA team has provided the PFMC with seven ESRs, most recently in March 2019. The ESRs are available as online sections of PFMC briefing books[4] for the meetings at which the CCIEA team has presented the reports (November 2012, then annually in March 2014–19), and are also available on the CCIEA website.[5] The contents of ESRs have evolved over the years through collaboration between the CCIEA team and PFMC and its advisory bodies, most notably through an FEP initiative[6] begun in 2015 to refine the indicators in the ESR to better reflect PFMC's needs. For example, PFMC has requested that the annual ESRs be confined to ~20 printed pages.

[1] https://www.integratedecosystemassessment.noaa.gov/regions/california-current
[2] https://www.pcouncil.org
[3] https://www.pcouncil.org/ecosystem-based-fisheries-management/fep
[4] https://www.pcouncil.org/council-operations/council-meetings/past-meetings
[5] https://www.integratedecosystemassessment.noaa.gov/regions/california-current/publications.html
[6] https://www.pcouncil.org/ecosystem-based-management/fishery-ecosystem-plan-initiatives/coordinated-ecosystem-indicator-review-initiative/

This technical memorandum is a companion document to the ESR delivered by the CCIEA team to the PFMC in March 2019 (Harvey et al. 2019), representing the status and trends of ecosystem indicators in the CCE through 2018 and, in some cases, early 2019. It is the third in an ongoing annual series of technical memorandums (following Harvey et al. 2017, Harvey et al. 2018) that will provide a more thorough ESR of the CCE than the page limit allows us to present to PFMC. We will continue to provide the annual report to PFMC, and this technical memorandum series will largely be based on that report. However, as this series evolves, the technical memorandums will incorporate more indicators and analyses covering a broader range of ecosystem attributes. This is because the CCIEA team looks to support other management partners in addition to PFMC, and our goal is for our annual ESR to feature information in support of ecosystem-based management (EBM) in other sectors and services in addition to fisheries (Slater et al. 2017). The technical memorandum format enables increased information content, contributions from a broader range of authors, and value to a wider range of audiences. It is our hope that an expanded ESR will lead to greater dialogue with potential partners and stakeholders; such dialogue and engagement is at the heart of the initial step of the IEA process (Figure 1), and is essential to every other step in all iterations as well.

1.2. Notes on Interpreting Time-Series Figures

Throughout this report, many data figures will follow one of two common formats, time-series plots or quad plots, both illustrated with sample data in Figure 3; see figure captions for details. Time-series plots generally contain a single dataset (Figures 3a,b), whereas quad plots are used to summarize the recent averages and trends for multiple time series in a single panel, as when we have time series of multiple populations that we want to compare in a simplified visual manner (Figure 3c). Some time-series plots now show thresholds beyond which we expect substantial changes in response variables, such as when a physiological tolerance to a physical or chemical variable is exceeded (Figure 3b). Where possible, we include estimates of error or uncertainty in the data. Generally, error estimates are standard deviations or standard errors in the observations.

1.3. Sampling Locations

Figure 4a shows the major headlands that demarcate potential biogeographic boundaries, in particular Cape Mendocino and Point Conception. We generally consider the region north of Cape Mendocino to be the "Northern CCE," the region between Cape Mendocino and Point Conception the "Central CCE," and the region south of Point Conception the "Southern CCE." Figure 4a also shows sampling locations for much of the regional climate and oceanographic data presented in this report. In particular, many of the physical and chemical oceanographic data are collected on the Newport Line off Oregon and the California Cooperative Oceanic Fisheries Investigations (CalCOFI) grid off California. Physical oceanography sampling is further complemented by basin-scale observations and models.

Freshwater habitats worldwide can be spatially grouped into "ecoregions" according to the designations of Abell et al. (2008). The freshwater ecoregions in the CCE are shown in Figure 4b, and are the basis by which we summarize freshwater habitat indicators relating to streamflow, stream water temperatures, and snowpack.

The map in Figure 4c represents sampling for most biological indicators, including zooplankton, forage species, California sea lions (*Zalophus californianus*), and seabirds. Zooplankton data are primarily reported from the Newport Line off Oregon and the Trinidad Head Line off northern California. The blue-, green-, and orange-shaded regions of coastal waters refer to the extent of major survey efforts that focus on forage species, juvenile salmon, and seabirds in shelf and slope habitats; in some cases, the surveys span both sides of the major zoogeographic boundaries of Cape Mendocino and Point Conception (especially the surveys represented by green shading), although the data we use in this report for those groups are mostly subsets drawn from areas that represent status and trends specific to the Northern, Central, and Southern regions. Groundfish bottom trawl sampling by the NOAA Fisheries West Coast Groundfish Bottom Trawl Survey (Keller et al. 2017) occurs in roughly the same area on the shelf and upper slope (depths of 55-1,280 m) as the blue- and green-shaded regions of Figure 4c.

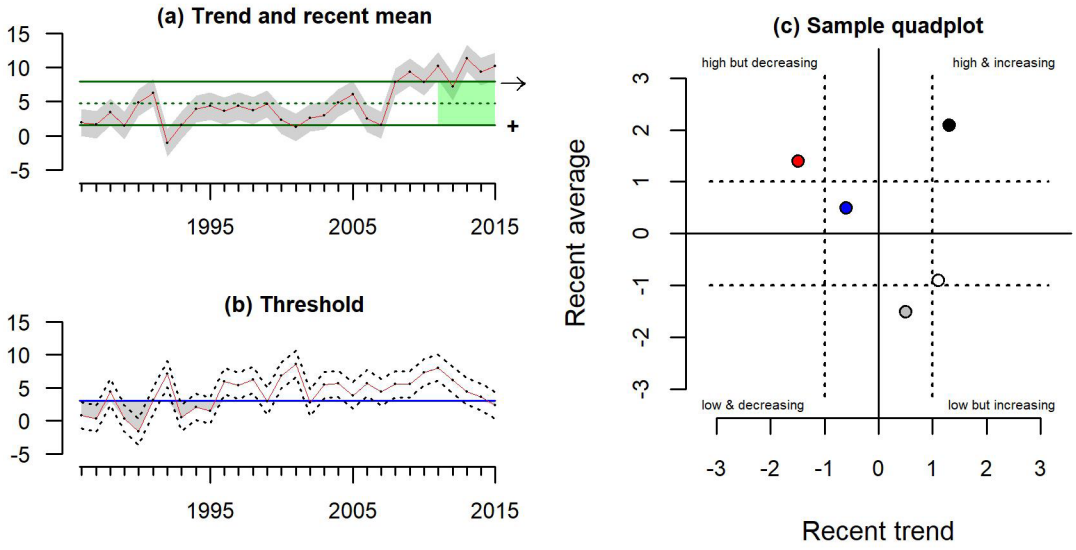

Figure 3. (a) Sample time-series plot, with indicator data relative to the mean (dashed line) and ±1.0 standard deviation (SD; solid lines) of the full time series. Arrow at right indicates if the trend over the most recent 5 years (shaded green) is positive (↗), negative (↘), or neutral (↔). Symbol at the lower right indicates if the recent mean was greater than (+), less than (-), or within 1 SD of (·) the long-term mean. When possible, time series indicate observation error (gray shading), which is standard error unless otherwise defined. (b) Sample time-series plot with the indicator plotted relative to a threshold value (blue line). Dashed lines indicate upper and lower observation error, again defined for each plot. (c) Sample quad plot. Each point represents one normalized time series. The position of a point indicates whether the recent years of the time series are above or below the long-term average, and if they are increasing or decreasing. Dashed lines represent ±1 SD of the full time series.

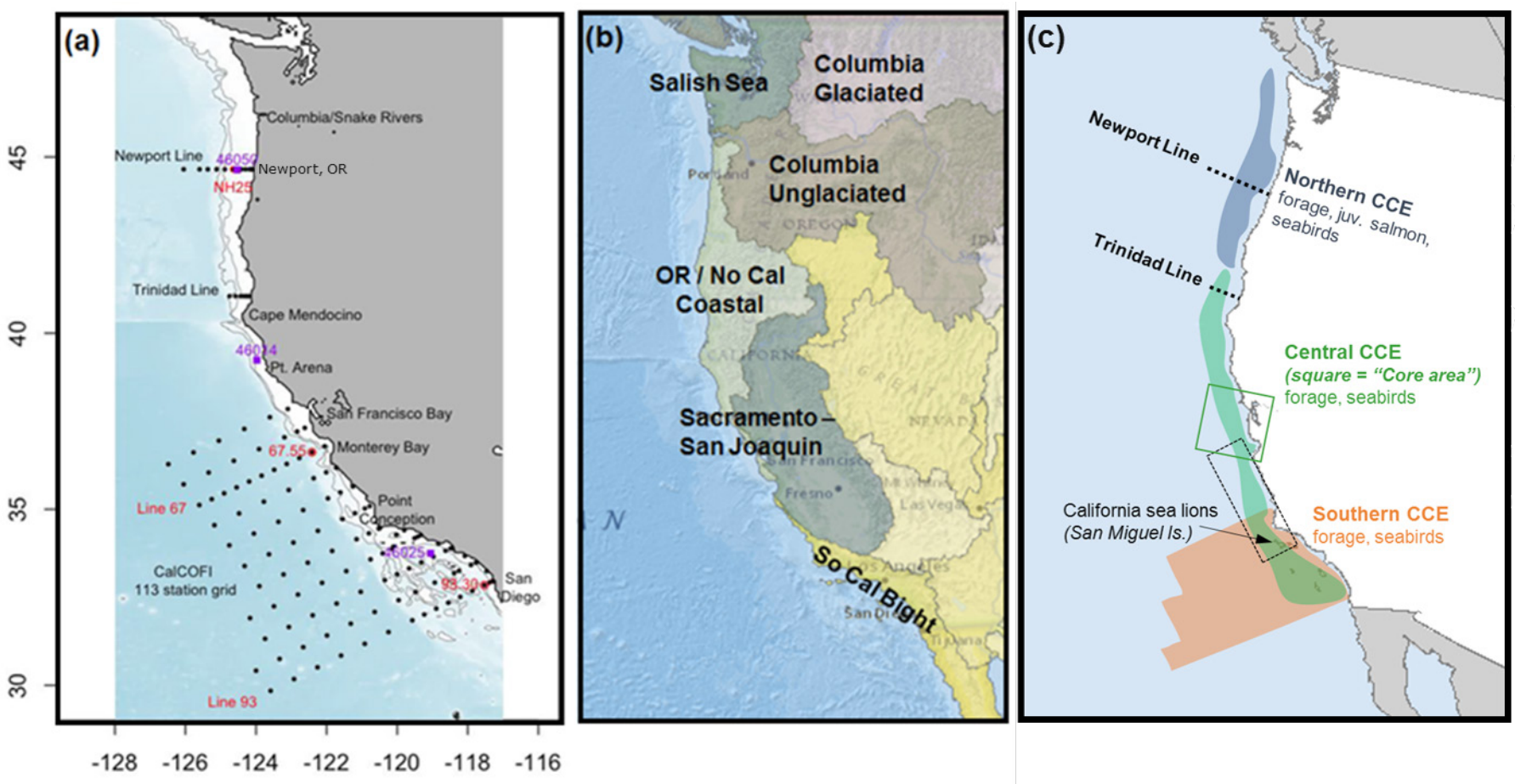

Figure 4. Maps of the California Current Ecosystem (CCE) and sampling areas. (a) Key geographic features and oceanographic sampling locations. (b) Freshwater ecoregions, where snowpack and freshwater indicators are measured. (c) Biological sampling areas for copepods and krill (Newport Line, Trinidad Line), pelagic forage, juvenile salmon, seabirds, and California sea lions. Solid box = the "core" sampling area for forage in the central CCE. Dotted box approximates the foraging area for adult female California sea lions from the San Miguel colony.

2. Climate and Ocean Drivers

The northeastern Pacific Ocean has experienced exceptional climate variability over the past five years, reaching new extremes for many indicators related to climate and ocean drivers. As we describe in this section, this variability has affected many aspects of the CCE, including water and air temperature, winds, currents, mixing of ocean waters, water chemistry, and precipitation. Climate and ocean indicators in the CCE reveal a climate system still in transition in 2018. The historically unprecedented North Pacific marine heat wave of 2013–16 and the strong El Niño event of 2015–16 gave way to cooler coastal waters, a succession of strong storms in the winter of 2016–17, and weak La Niña conditions by late 2017. However, by the end of 2018, mild El Niño conditions had returned, and the influx of cool, nutrient-rich subarctic water from the North Pacific Gyre had weakened to some of the lowest levels ever calculated. El Niño conditions and weak inputs from the North Pacific Gyre generally result in below-average productivity in the CCE. Superimposed on these large-scale climate and ocean drivers, regional indicators of upwelling, water chemistry, and stream conditions demonstrated their characteristically high spatiotemporal variability, resulting in patterns of local variation.

The following subsections provide in-depth descriptions of basin-scale, regional-scale, and hydrologic indicators of climate and ocean variability in the CCE.

2.1. Basin-Scale Indicators

The CCE is driven by atmosphere–ocean energy exchange that occurs on many temporal and spatial scales. To capture large-scale variability, the CCIEA team tracks three indices: the status of the equatorial El Niño–Southern Oscillation (ENSO), described by the Oceanic Niño Index (ONI); the Pacific Decadal Oscillation (PDO); and the North Pacific Gyre Oscillation (NPGO). Positive ONI and PDO values and negative NPGO values usually denote conditions that lead to low CCE productivity, whereas negative ONI and PDO values and positive NPGO values are associated with periods of high CCE productivity.

ENSO events impact the CCE by modifying the jet stream and storm tracks, changing the nearshore thermocline, and influencing coastal currents that affect poleward transport and distribution of equatorial and subequatorial waters (and species). A positive ONI indicates El Niño conditions, which usually means more storms to the south, weaker upwelling, and lower primary productivity in the CCE. A negative ONI means La Niña conditions, which usually lead to higher productivity. The PDO is related to sea surface temperature (SST), and is derived from sea surface temperature anomalies (SSTa) in the Northeast Pacific, which often persist in "regimes" that last for many years. In positive PDO regimes, coastal SSTa in the Gulf of Alaska and the CCE tend to be warmer, while those in the North Pacific Subtropical Gyre tend to be cooler. Positive PDO values are associated with lower productivity in the CCE. The NPGO is a low-frequency variation of sea surface height, indicating variations in the circulation of the North Pacific Subtropical Gyre and the Alaskan Gyre, which in turn relate to the source waters for the CCE. Positive NPGO values are associated with increased equatorward flow, along with increased surface salinities, nutrients, and chlorophyll-*a*. Negative NPGO values are associated with decreases in such values, implying less subarctic source water and generally lower productivity.

In 2018, the ONI began at negative values indicative of weak La Niña conditions, but increased to weak El Niño conditions by the end of the year (Figure 5, top). This El Niño is much weaker than the major El Niño of 2015–16. As of 13 June 2019, the NOAA Climate Prediction Center[7] had predicted a 66% chance of a weak El Niño persisting through the summer of 2019. PDO values were neutral to slightly positive for most of the year, consistently within 1 standard deviation (SD) of the long-term mean, and much lower than during the 2013–16 North Pacific marine heat wave (Figure 5, middle). However, NPGO values, which had been highly variable but generally negative in recent years, decreased during 2018 to some of the lowest values estimated over the entirety of the time series (Figure 5, bottom). Thus, the three basin-scale indices provide a mixed signal of general conditions in the CCE: the ONI and NPGO were consistent with lower productivity, while the PDO was neutral, implying average productivity.

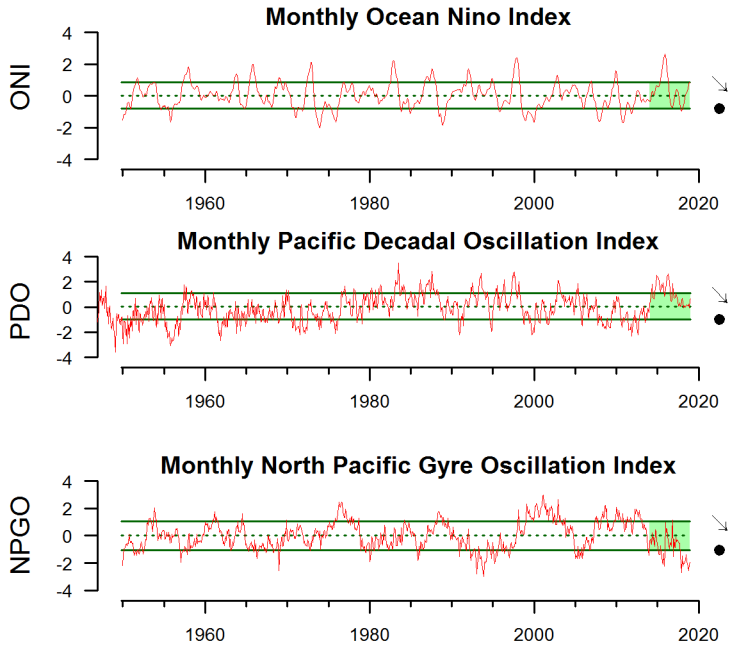

Figure 5. Monthly values of the Oceanic Niño Index (ONI), the Pacific Decadal Oscillation (PDO), and the North Pacific Gyre Oscillation (NPGO), from 1950–2018. Lines, colors, and symbols as in Figure 3a. Oceanic Niño Index information and data are from the NOAA Climate Prediction Center (https://origin.cpc.ncep.noaa.gov/products/analysis_monitoring/ensostuff/ONI_v5.php). Pacific Decadal Oscillation data are from N. Mantua, NMFS/SWFSC, and are served by the University of Washington Joint Institute for the study of the Atmospheric and Ocean (JISAO; http://research.jisao.washington.edu/pdo/). North Pacific Gyre Oscillation data are from E. Di Lorenzo, Georgia Institute of Technology (http://www.o3d.org/npgo/).

Seasonal SSTa values from 2018 reveal that CCE surface waters were warmer than average, although not nearly to the extent of the anomalously warm years of 2014–16. In early 2018, SSTa values were slightly (<1 SD) above average for much of the North Pacific, including waters along the U.S. West Coast (Figure 6, upper left). However, in the summer of 2018, SSTa values along the West Coast were patchier, with large, slightly cooler-than-average cells forming off Washington, Oregon and Central California, and a major warm area (SSTa >1 SD) in the Southern California Bight south of Point Conception (Figure 6, lower left). The influence of the 2013–16 marine heat wave and 2015–16 El Niño event remained evident in the five-year means (Figure 6, middle), with strongly positive anomalies in the majority of the domain in winter and summer. In contrast, the five-year trends for SSTa were strongly negative in nearly the entire region in both seasons (Figure 6, right); these negative trends reflect the overall cooling of the North Pacific following the anomalous warm events of 2013–16.

[7] https://www.cpc.ncep.noaa.gov/products/analysis_monitoring/enso_advisory/ensodisc.shtml

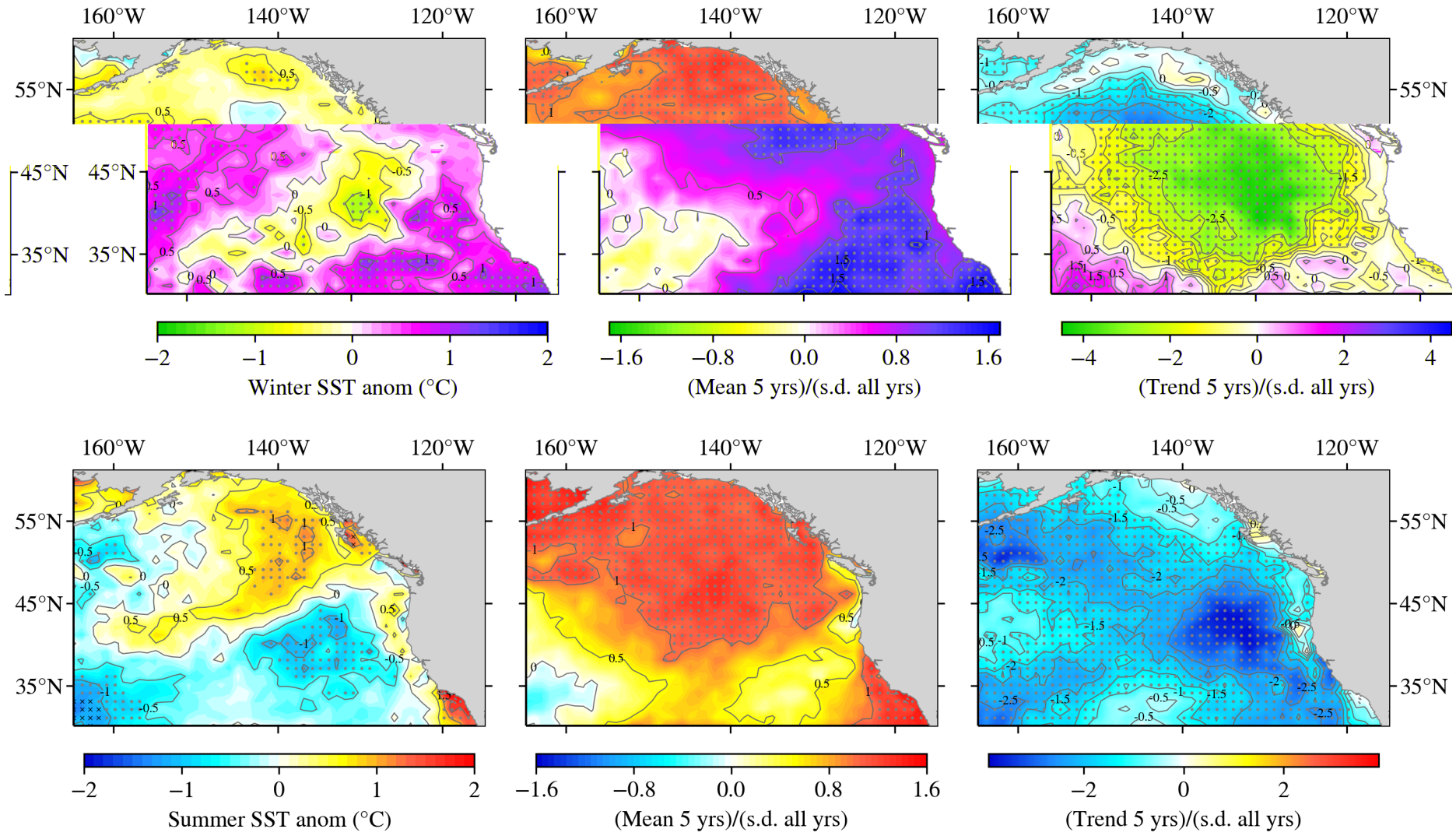

Figure 6. Sea surface temperature (SST) anomalies (2018; left), five-year means (2014–18; middle), and five-year trends (2014–18; right) in winter (Jan–Mar; top) and summer (Jul–Sep; bottom). The time series at each grid point began in 1982. Black circles mark cells where the anomaly was >1 SD above the long-term mean. Black x's mark cells where the anomaly was the highest of the time series. SST maps are optimally interpolated, remotely sensed temperatures (Reynolds et al. 2007). The daily optimal interpolated AVHRR SST can be downloaded from ERDDAP, https://coastwatch.pfeg.noaa.gov/erddap/index.html. Dataset ID: `ncdcOisst2Agg`.

Depth profiles of water temperatures off of Newport, Oregon and San Diego, California demonstrate the extent of recent warm and cool anomalies into the water column, as well as the spatial and temporal dynamics of those anomalies. Both areas of the coast experienced severe warming in the upper 50 m of the water column in 2014–15 and deeper warming in 2015–16 (Figure 7). Off Newport (Figure 7, top), temperature anomalies at depth followed similar patterns in 2017 and 2018: temperature anomalies in the upper 50 m of the water column gradually became negative (cooler than average), which is consistent with the negative SSTa off Oregon in the summer of 2018 (Figure 6, lower left). Deeper than 50 m, however, temperature anomalies off Newport remained slightly positive (Figure 7, top). In contrast, CalCOFI station 93.30 off San Diego experienced notably cooler waters at depth in 2017 (Figure 7, bottom). Then in 2018, station 93.30 experienced strong warming down to about 50 m; this is consistent with the warm SSTa during summer 2018 in the Southern California Bight (Figure 6, lower left). This warming was generally surface-oriented; below 100 m, waters were average or slightly cooler-than-average (Figure 7, bottom).

In late 2018, news media reported that, based on satellite imagery of SST, a marine heatwave similar to the "Blob" of 2013–16 may be reforming in the northeast Pacific. Based on an analysis of SSTa from 1985–2016, a marine heatwave has the potential to cause impacts in the CCE that are comparable to those from the 2013–16 event if the anomalous feature: 1) has statistically normalized SSTa >2 SD of the long-term SSTa time series at a particular location; 2) is greater than 500,000 km^2 in area; and 3) lasts for >60 days.[8] Many features have occurred in the North Pacific in recent decades that surpassed one or two of these thresholds, but typically not all three. Some years have experienced multiple events; however, none of the other events match the combined duration and intensity of the 2013–16 event (Figure 8). In the fall of 2018, the widely reported warm feature in the North Pacific surpassed the area threshold (Figure 9, left, black outlined regions), but did not surpass the duration threshold, largely dissipating by December 2018 (Figure 9, middle). However, analysis of SSTa data showed that in late spring/early summer of 2019, another anomalously warm feature had developed in the waters offshore of Oregon and Washington. By July 2019, the feature had surpassed the strength and area thresholds, was nearing the duration threshold, and was rapidly approaching the coast (Figure 9, right). At the time this report was finalized (August 2019), the feature had continued to strengthen and expand, and exceeded the duration threshold (Figure 8, far right region of time series). It may also move closer to shore as upwelling relaxes going into the fall. We will continue to monitor this marine heatwave to determine if it has discernible impacts on the CCE.

In summary, following the 2013–16 marine heat wave and the 2015–16 El Niño event, basin-scale temperatures moderated during 2017–18, with notable exceptions such as the very warm patch of water off Southern California in the summer of 2018 (Figure 6, lower left) and the brief warm anomaly in the North Pacific in late 2018 (Figures 8 and 9). While the PDO was essentially neutral in early 2019, indicating average SSTs in the subarctic North Pacific, we are concerned that the weak El Niño and strongly negative NPGO are indicative of poor conditions for overall system productivity in the CCE in 2019. Additional information on recent dynamics in the CCE is provided in the thorough summaries done by Leising et al. (2015), McClatchie et al. (2016), Wells et al. (2017), and Thompson et al. (2018).

[8] https://www.integratedecosystemassessment.noaa.gov/regions/california-current/cc-projects-blobtracker

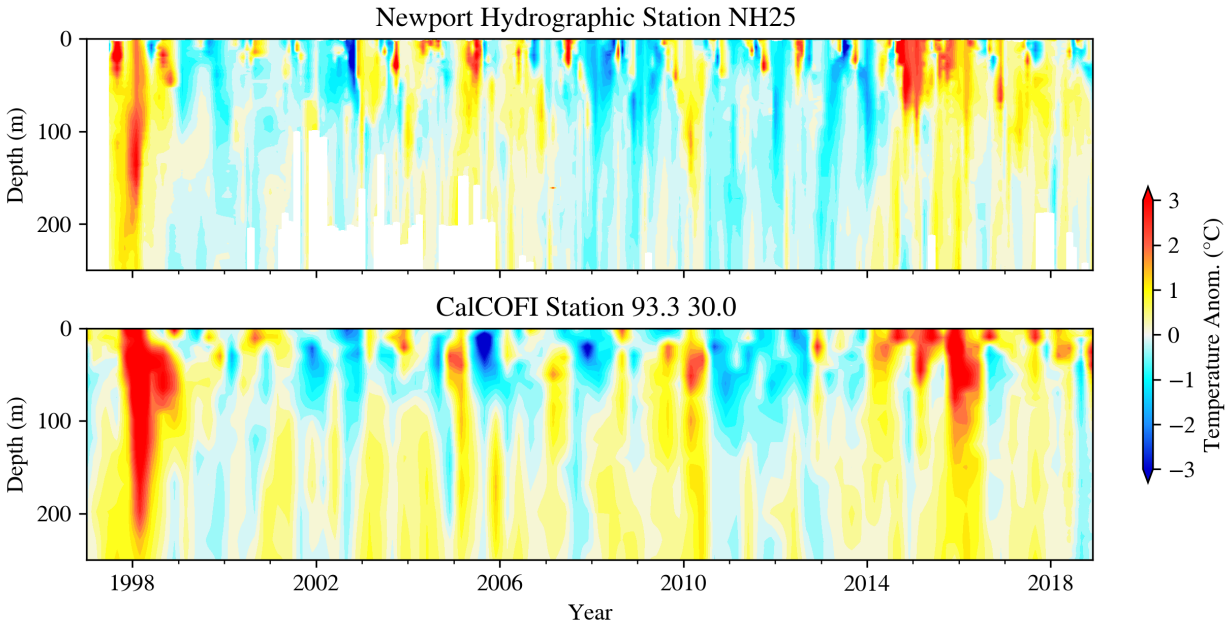

Figure 7. Time–depth temperature anomalies for hydrographic stations NH25 (July 1997 to December 2018) and CalCOFI 93.30 (January 1997 to August 2018). The NH25 (top plot) temperature anomalies are monthly means and the time interval is one month (i.e., 12 values per year); white vertical lines indicate when months were not sampled. The CalCOFI (bottom plot) temperature anomalies are quarterly means and the time intervals are seasons (i.e., four values per year). For the locations of these stations, see Figure 4a. Newport Hydrographic (NH) line temperature data are from J. Fisher, NMFS/NWFSC, OSU. CalCOFI hydrographic line data are from http://calcofi.org/data.html (request permission to access). CalCOFI data from January 1997–October 2018 are from the bottle data database, while the remaining 2018 data are preliminary conductivity, temperature, and depth data from the recent CTD database.

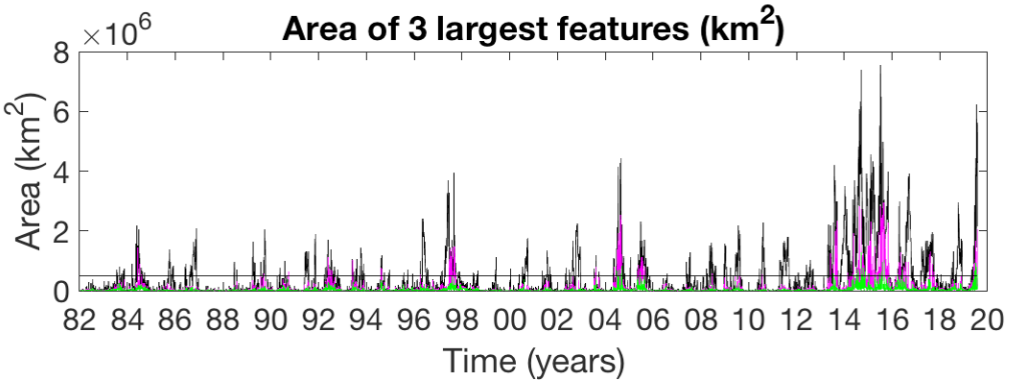

Figure 8. Retrospective analysis of sea surface temperature anomalies in the California Current region, 1982–2019, showing the relatively higher strength, size, and duration of warm-water events during the 2014–16 time period, as well as the most recent 2019 event. Colored time series represent the three largest warm events occurring in the region at a given time: black (largest), magenta (second-largest) and green (third-largest). Horizontal line represents the area threshold for finding features likely to impact the coastal region.

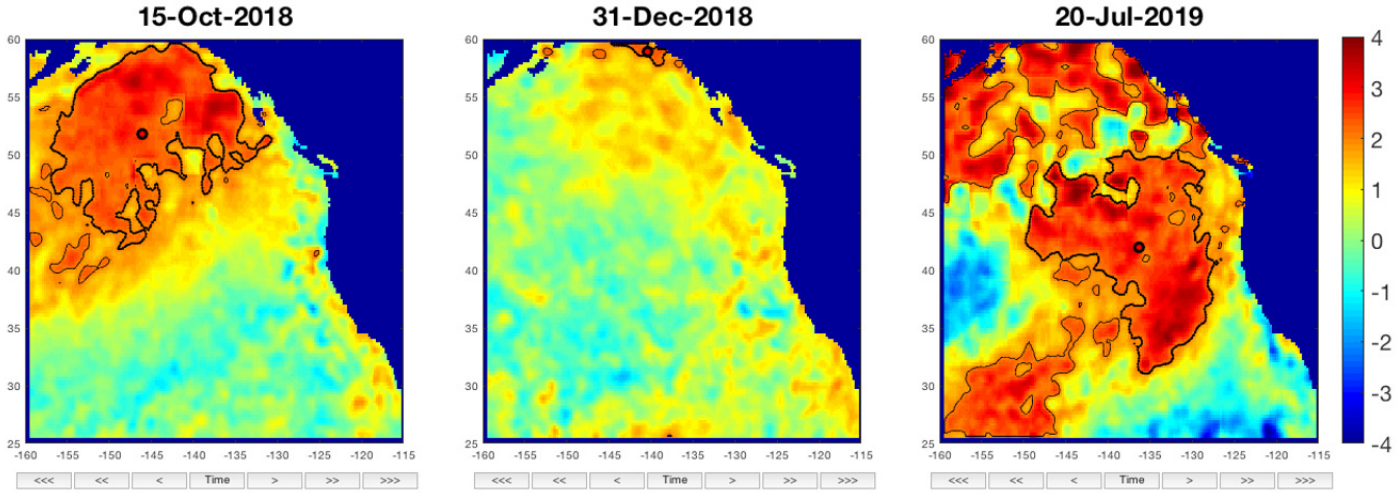

Figure 9. Standardized sea surface temperature anomalies (SSTa) across the Northeast Pacific Ocean for late 2018 and mid-2019. Dark contours denote regions that meet the criteria of a marine heat wave (see text). The October 2018 image (left) has the largest (by area) marine heatwave detected during 2018; this event had largely dissipated by December 2018 (middle). However, in summer 2019, a new marine heatwave emerged in the Northeast Pacific (right). The standardized SSTa is defined as SSTa divided by the SD of SSTa at each location calculated over 1985–2016, thus taking into account spatial variance in the normal fluctuation of SSTa.

2.2. Regional Upwelling Indices

Seasonal cross-shore gradients in sea level atmospheric pressure produce the alongshore winds that drive coastal upwelling and downwelling in the CCE. Upwelling, driven by equatorward-blowing winds, is a physical process of lifting cold, nutrient-rich water from deep in the ocean to the surface, which fuels the high seasonal primary production at the base of the CCE food web. The timing, strength, and duration of upwelling vary greatly along the coast. In the past, we have summarized upwelling timing and intensity using the well-established Bakun Upwelling Index, estimated at 3° latitudinal intervals along the coast (see Schwing et al. 1996 for a review of the Bakun Index). The Bakun Index, derived from a U.S. Navy Fleet Numerical Meteorology and Oceanography Center sea level pressure product, provided information on the onset of upwelling-favorable winds ("spring transition"), a general indication of the strength of upwelling, relaxation events, and the end of the upwelling season at a given location. However, the Bakun Index does not take into consideration the underlying ocean structure (e.g. ocean stratification), which can have considerable influence on the nutrient content of the upwelled water, nor does it consider the influence of ocean

circulation that can impact upwelling. In addition, assumptions of the Bakun Index break down off of central and southern California due to features of coastal geography, leading to poor wind (and therefore upwelling) estimates there. Jacox et al. (2018) developed new estimates of coastal upwelling, specifically for the vertical water volume transport (Coastal Upwelling Transport Index; CUTI) and the vertical nitrate flux (Biologically Effective Upwelling Transport Index; BEUTI). These indices are derived from a CCE configuration of the Regional Ocean Modeling System (ROMS) model with data assimilation (Neveu et al. 2016). We will use these indices to describe upwelling in the CCE in this and future reports, as they better represent surface winds, ocean circulation, and subsurface variability. CUTI provides more accurate estimates of vertical transport of water, whereas BEUTI provides valuable additional information about the nature of the upwelled water (e.g., its nitrate content) that can be linked to ecological processes such as productivity (Jacox et al. 2018).

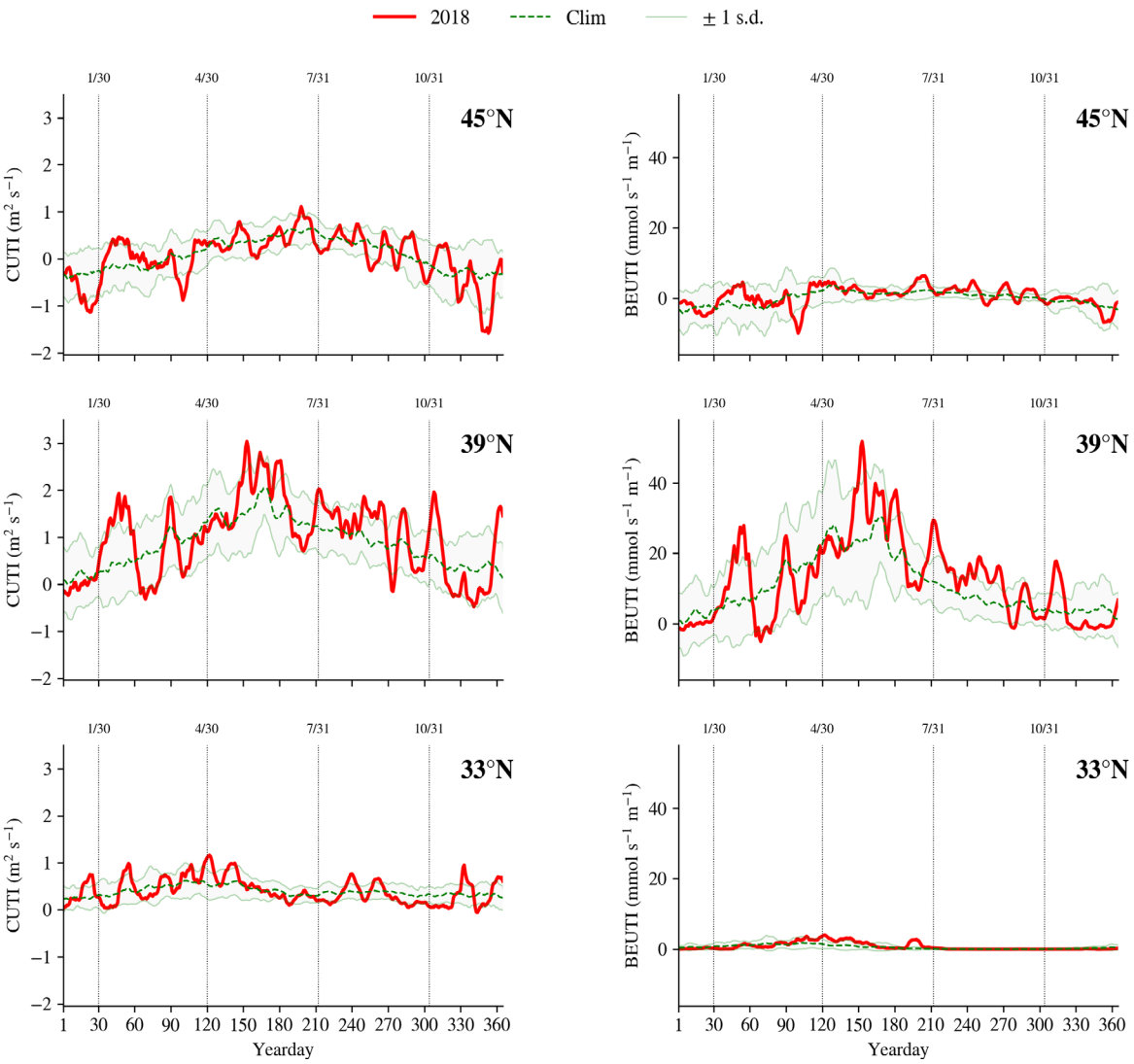

Figure 10. Daily values of Coastal Upwelling Transport Index (CUTI; left) and Biologically Effective Upwelling Transport Index (BEUTI; right) during 2018, relative to the 1988–2018 climatology average (green dashed line), ±1 SD (shaded area), at lats 33°N, 39°N, and 45°N. Daily data are smoothed with a 10-day running mean. Vertical lines mark the ends of Jan, Apr, July, and Oct. Daily 2018 values of CUTI and BEUTI are derived from numerical model outputs described in Jacox et al. (2018); detailed information about these indices can be found at https://mjacox.com/upwelling-indices/.

In the CCE, the timing of peak upwelling (CUTI) varies by latitude, with northern latitudes having a later onset of maximum upwelling (Figure 10 left, shaded areas). The maximum climatological value of CUTI (Figure 10 left, dashed line) is at the end of April at lat 33°N (Southern California), the middle of June at 39°N (Point Arena, CA), and the end of July at 45°N (Newport, OR). The magnitude of vertical nitrate flux (BEUTI) also varies greatly by latitude (Figure 10 right, shaded areas). At 39°N, BEUTI is about an order of magnitude larger than at either the northern station at 45°N or the southern station at 33°N. At 45°N, and to a lesser extent at 39°N, downwelling occurs in the winter due to poleward-blowing winds (note that a negative value of BEUTI accompanying downwelling suggests removal of nitrate, but a source is not identified).

During 2018, CUTI and BEUTI in the CCE as a whole were near their long-term averages, with a brief late-winter period of negative anomalies followed by strong upwelling and higher nitrate flux in the spring (Figure 10, heavy solid lines). The total upwelling and nutrient flux in 2018 were higher than in recent years (in particular the marine heatwave years of 2014–16), but were still well below peak values (e.g., ~50% less than the strong upwelling year of 2013). In general, temporal variations in CUTI and BEUTI were coherent along the U.S. West Coast in 2018, though the magnitude of fluctuations was greatest off central and northern California where seasonal upwelling is strongest.

2.3. Hypoxia and Ocean Acidification

Nearshore dissolved oxygen (DO) depends on many processes, including currents, upwelling, air–sea exchange, and community-level production and respiration in the water column and benthos. DO is required for organismal respiration; low DO can compress habitat and cause stress or die-offs for sensitive species. Waters with DO levels <1.4 mL/L (2 mg/L) are considered to be hypoxic; such conditions may occur on the shelf following the onset of spring upwelling, and continue into the summer and early fall months until the fall transition mixes shelf waters. Upwelling-driven hypoxia occurs because upwelled water from deeper ocean sources tends to be low in DO, and microbial decomposition of organic matter in the summer and fall increases overall system respiration and oxygen consumption, particularly closer to the seafloor.

Low DO was a serious issue in the northern CCE in 2018, apparently to a greater extent than was observed in 2017 (Harvey et al. 2018). At station NH05 (5 nautical miles off of Newport, Oregon), water near bottom over the continental shelf was below the hypoxia threshold from late July until early September (Figure 11, top) before its seasonal rebound

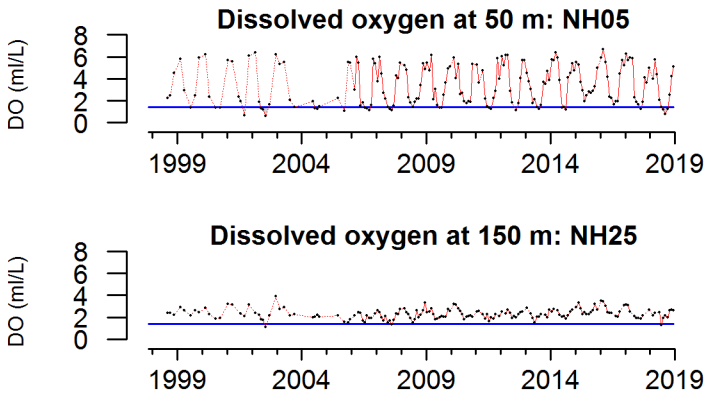

Figure 11. Dissolved oxygen (DO) at 50 m and 150 m depths off Newport, OR, through 2018. Stations NH05 and NH25 are 9 and 46 km from shore, respectively. The blue line is the hypoxic threshold of 1.4 mL dissolved oxygen per L. The dotted red line indicates missing data. Lines, colors, and symbols are as in Figure 3b. Newport Hydrographic (NH) line DO data are from J. Fisher, NMFS/NWFSC, OSU.

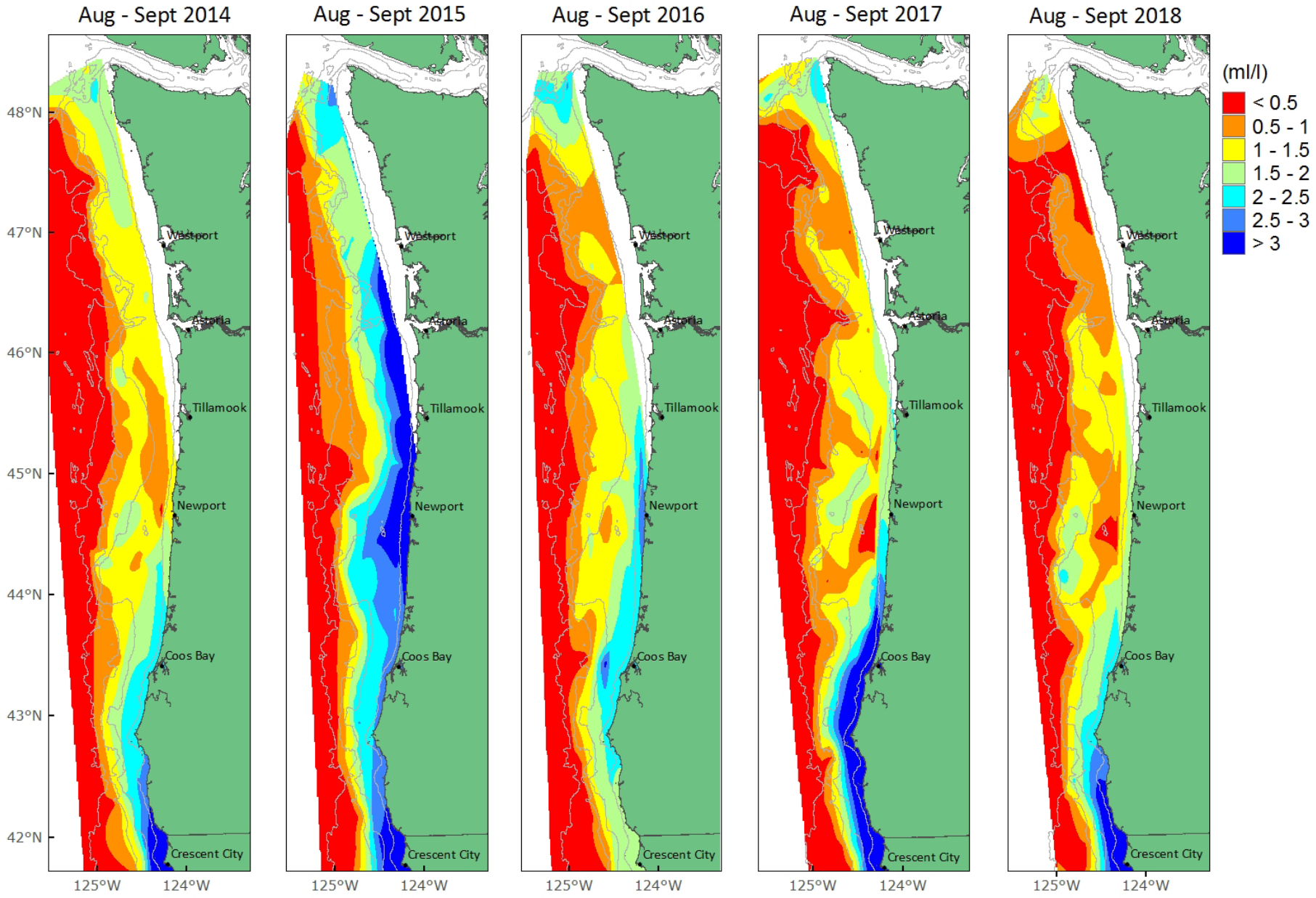

Figure 12. Annual maps of near-bottom dissolved oxygen levels (mL/L) during the months of Aug–Sept from 2014 (far left) through 2018 (far right). NOAA Fisheries/NWFSC FRAM Division West Coast Groundfish Bottom Trawl Survey.

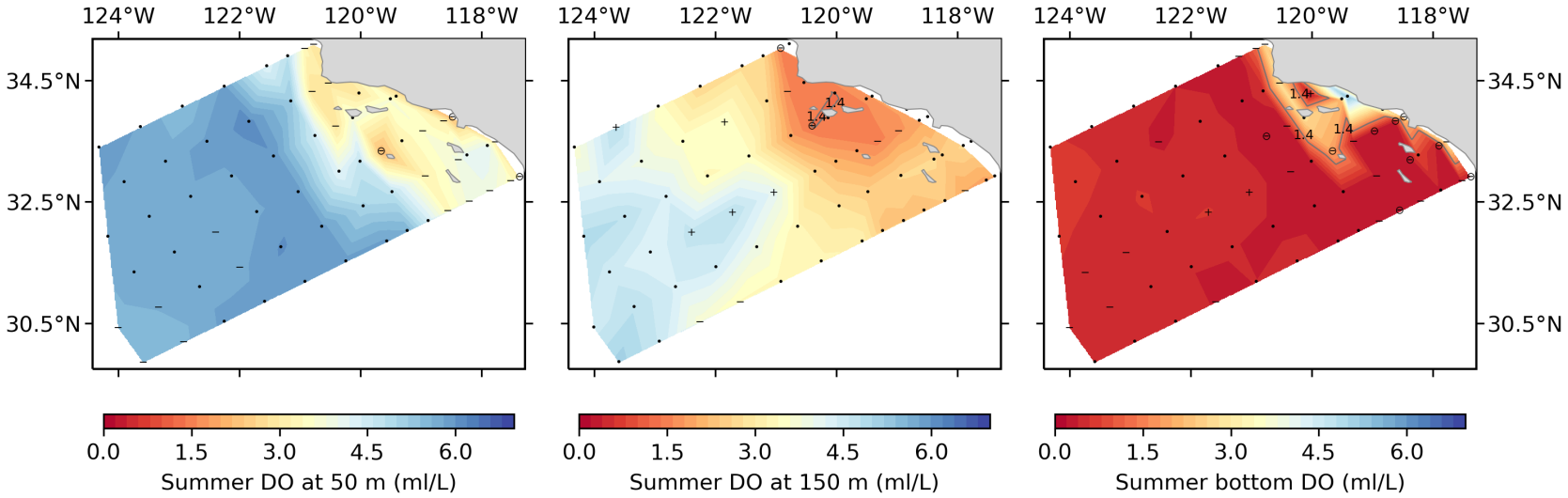

Figure 13. Summer 2018 dissolved oxygen (DO) observations during the quarterly CalCOFI survey of the southern CCE at: 50 m (left), 150 m (middle), and the bottom of the hydrographic cast (right). DO was sampled at hydrographic stations (marked with black dots). Hydrographic casts extended to the bottom or to a maximum depth of 500 m; only a small number of stations near shore or islands have bottom depths less than 500 m. The black dots are changed to either a minus (-) or plus (+) if the measured value was less or greater than 1 s.d. above the long-term mean, respectively. Also, if the measured value is the smallest or largest value ever sampled since 1984 the symbol is surrounded by a black circle. The 1.4 ml/L contour level is labeled if it exists.

in fall. Observed DO levels in the middle of the water column 25 nautical miles offshore of Newport (station NH25) were mostly above the 1.4 mL/L threshold, except for one reading in June (Figure 11, bottom). The 2018 hypoxic event affected major portions of the near-bottom waters over the continental shelf off of Washington and Oregon in the summer, as indicated by DO readings taken from the NOAA Fisheries West Coast Groundfish Bottom Trawl Survey (Figure 12). The 2018 event appeared even more severe and spatially extensive than the 2017 event, and caused widespread die-offs of crabs and other benthic invertebrates and redistribution of groundfish (data not shown). Similar responses to hypoxic events have been observed previously among the benthic and demersal community (Grantham et al. 2004, Chan et al. 2008, Keller et al. 2010, Keller et al. 2017).

In the CalCOFI region of the southern CCE (see Figure 4a), summer DO values displayed strong inshore-offshore and depth gradients, with higher values measured farther offshore and lower values measured at depth. The southern CCE DO levels in the upper 150 m measured during the summer 2018 CalCOFI survey had levels above the hypoxic threshold (Figure 13). In general, the DO measured during the summer cruise was lower than average, with many stations, especially nearshore and

around islands, having DO values <1 SD below the long-term mean. DO values at 500 m depths were well below the 1.4 ml/L hypoxic threshold. However, in the area around the Channel Islands and for stations adjacent to shore, DO values near the seafloor were above the hypoxic threshold (Figure 13, right).

Ocean acidification (OA), caused by anthropogenically increased levels of atmospheric CO_2, reduces pH and carbonate ion levels in seawater. A key indicator of OA is aragonite saturation state, a measure of the availability of aragonite (a form of calcium carbonate). Aragonite saturation <1.0 indicates corrosive conditions that have been shown to be stressful for many CCE species, including oysters, crabs, and pteropods (Barton et al. 2012, Bednaršek et al. 2014, Marshall et al. 2017, Hodgson et al. 2018). Upwelling, which drives primary production in the CCE, also transports hypoxic, acidified waters from offshore onto the continental shelf, where increased community-level metabolic activity can further exacerbate OA (Chan et al. 2008, Feely et al. 2008, Feely et al. 2018). As a result, aragonite saturation levels tend to be lowest during and following upwelling in the spring and summer, and highest during the winter. Rivers in the region tend to be undersaturated and may contributed further to corrosivity (Feely et al. 2018).

Aragonite saturation levels off Newport in 2018 were fairly typical, and lower than in the anomalous years of 2014–15 (Figure 14). At the nearshore station (NH05), aragonite levels at 50 m depth were saturated (>1.0) in winter and spring, then fell below 1.0 in the summer and fall, as is typical. At station NH25, aragonite saturation state at 150 m depth followed the same seasonal cycle but across a narrower range; conditions at this site and depth in 2018 were always corrosive (<1.0). At station NH25, the horizon for corrosive water (i.e., the isocline at which aragonite saturation state = 1.0) came close to the upper 50 m of the water column in late summer and fall of 2018, which is comparable to many other years in recent decades (Figure 15).

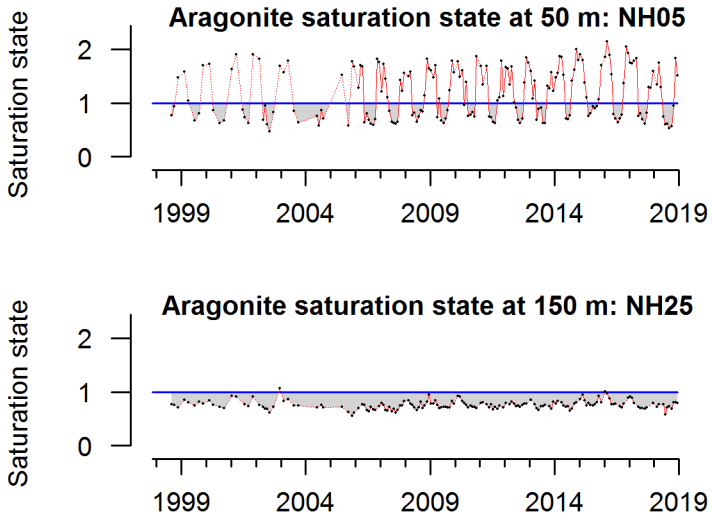

Figure 14. Monthly aragonite saturation values off Newport, OR, 1998–2018. The blue line is the threshold value of 1.0 for aragonite saturation state. Lines, colors, and symbols are as in Figure 3b. Aragonite saturation state data were provided by J. Fisher, NMFS/NWFSC, OSU.

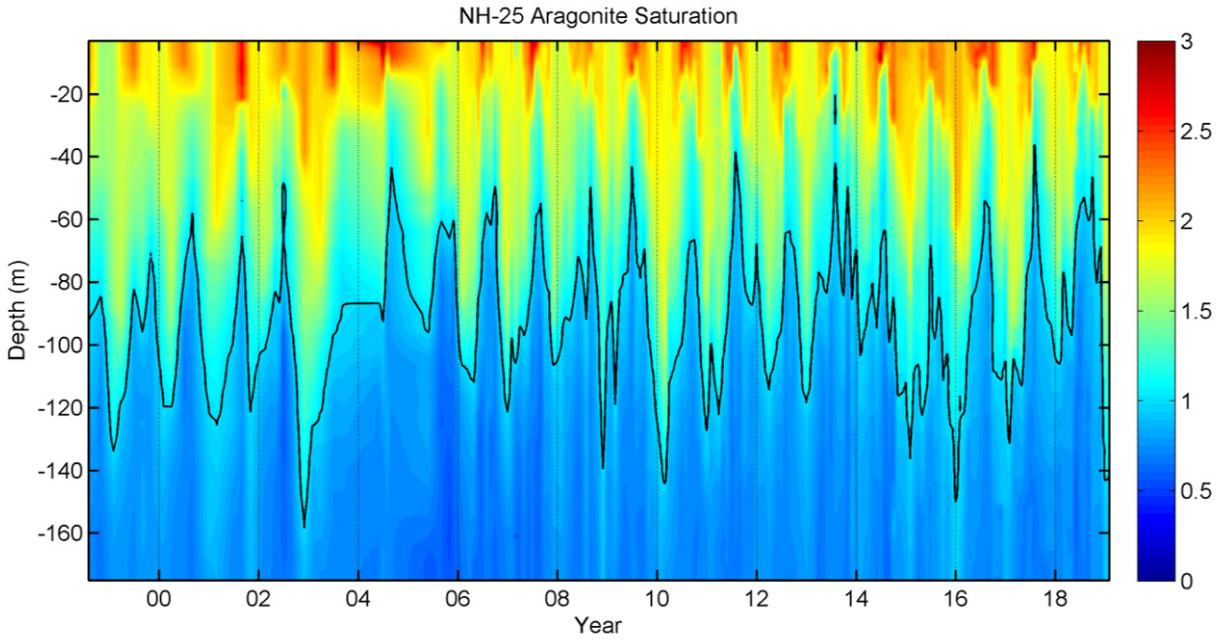

Figure 15. Aragonite saturation state versus depth at station NH25 along the Newport Hydrographic Line, 1998–2018. Dark line indicates the threshold value of 1.0 for aragonite saturation state. Lines, colors, and symbols are as in Figure 3a. Data were provided by J. Fisher, NMFS/NWFSC, OSU.

2.4. Hydrologic Indicators

Freshwater habitat conditions are critical for salmon populations, and for estuaries that support many marine species. Indicators are reported based on a hierarchical spatial framework and are summarized by freshwater ecoregion (Figure 4b, as derived from Abell et al. [2008] and Freshwater Ecoregions of the World[9]) or, where possible, by salmon evolutionarily significant units (ESUs, sensu Waples 1995). Within ecoregions, we summarized data by Chinook salmon ESUs. Status and trends for all freshwater indicators are estimated using space–time models (Lindgren and Rue 2015), which account for temporal and spatial autocorrelation.

The freshwater indicators presented here focus on salmon habitat conditions as related to snowpack, streamflow, and temperature. Snow-water equivalent (SWE) is the total water content in snowpack, which provides a steady source of cool, fresh water that is vital for salmon in the warm summer months (Munsch et al. 2019). Maximum streamflows in winter and spring are important for habitat formation, and in California can be important for removing a polychaete worm that is the obligate host of the salmon parasites *Ceratonova shasta* and *Parvicapsula minibicornis* (Alexander et al. 2014, True et al. 2017); however, high flows can also cause scouring of eggs from salmon redds (DeVries 1997), thereby reducing abundance and productivity (Greene et al. 2005, Zimmerman et al. 2015). Minimum streamflows in summer and fall can restrict habitat for instream juveniles and migrating adults (Bradford and Heinonen 2008), and high summer water temperatures can cause impaired physiology and increased mortality for both juveniles (Marine and Cech 2004, Richter and Kolmes 2005) and adults (Jeffries et al. 2012). All freshwater indicators are influenced by climate and weather patterns, and intensifying climate change is expected to exacerbate high temperatures, low SWEs, and extreme flow events.

[9] http://www.feow.org/

SWE in 2018 exhibited some differences from north to south, and some changes relative to 2017. SWE was close to average in the Salish Sea, Columbia Glaciated and Columbia Unglaciated ecoregions (Figure 16; see Figure 4b for locations of freshwater ecoregions). This was the third consecutive winter of roughly average SWE in these three ecoregions. In contrast, SWE was nearly 1 SD below the long-term averages in the Oregon & Northern California Coast ecoregion and the Sacramento & San Joaquin ecoregion, each representing a strong decline relative to 2017, though not to the extreme extent of 2015 (Figure 16). Because the official SWE estimate is made on 1 April for each calendar year, SWE for the 2018–19 winter is not represented in Figure 16, which was presented to the PFMC in March 2019. However, the updated map in Figure 17 indicates that SWE on 1 April 2019 was above average in much of the region, particularly in the southern Cascade Range and the Sierra Nevada Range, due in large part to a series of powerful winter storms in January, February and March.

Streamflow indicators are derived from active U.S. Geological Survey (USGS) stream gages with records of at least 30 years' duration. We use standardized anomalies of streamflow time series from 213 individual gages. Daily means were used to calculate annual one-day maximum and seven-day minimum flows, corresponding to flow parameters to which salmon populations are most sensitive. Seven-day minimum flow anomalies in the Salish Sea, Columbia Glaciated and Columbia Unglaciated ecoregions were close to long-term averages (Figure 18), as was also the case with SWE in those ecoregions in 2018. Minimum flows in the Oregon & Northern California Coast ecoregion decreased from 2017 to 2018 (also similar to SWE in that ecoregion), but the 2018 minimum flow anomaly was close to zero

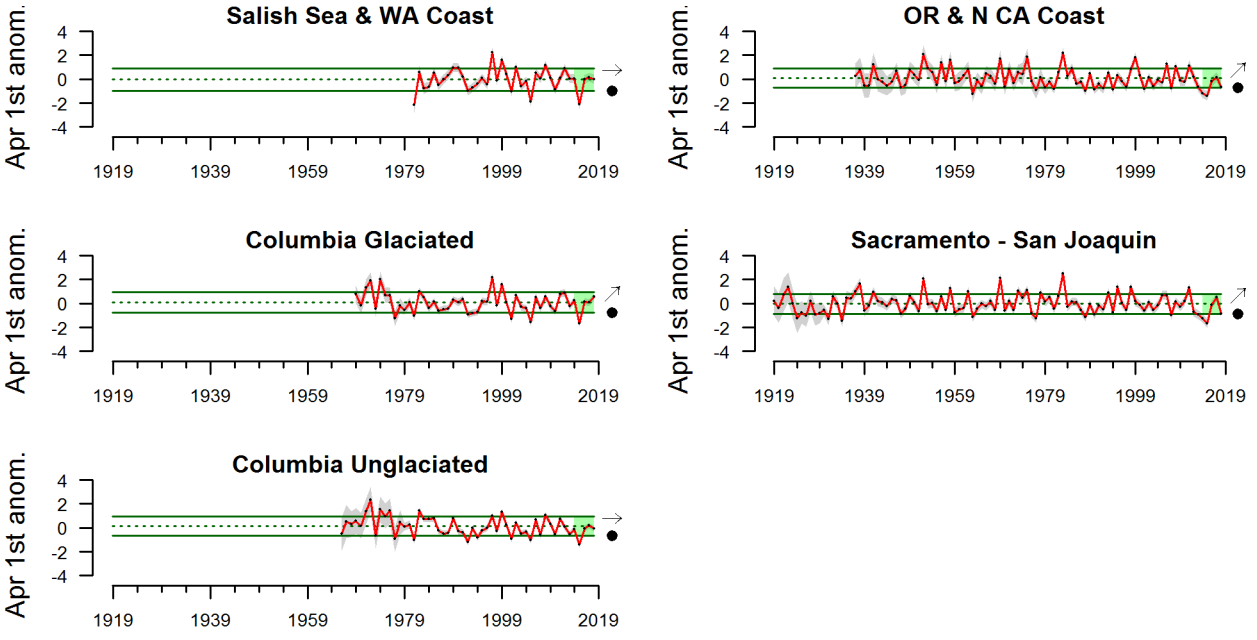

Figure 16. Anomalies of 1 April snow-water equivalent (SWE) in five freshwater ecoregions of the CCE through 2018. Lines, colors, and symbols as in Figure 3. Ecoregions are mapped in Figure 4b. SWE data were derived from the California Department of Water Resources snow survey (http://cdec.water.ca.gov/) and the Natural Resources Conservation Service's SNOTEL sites in WA, OR, CA, and ID (http://www.wcc.nrcs.usda.gov/snow/).

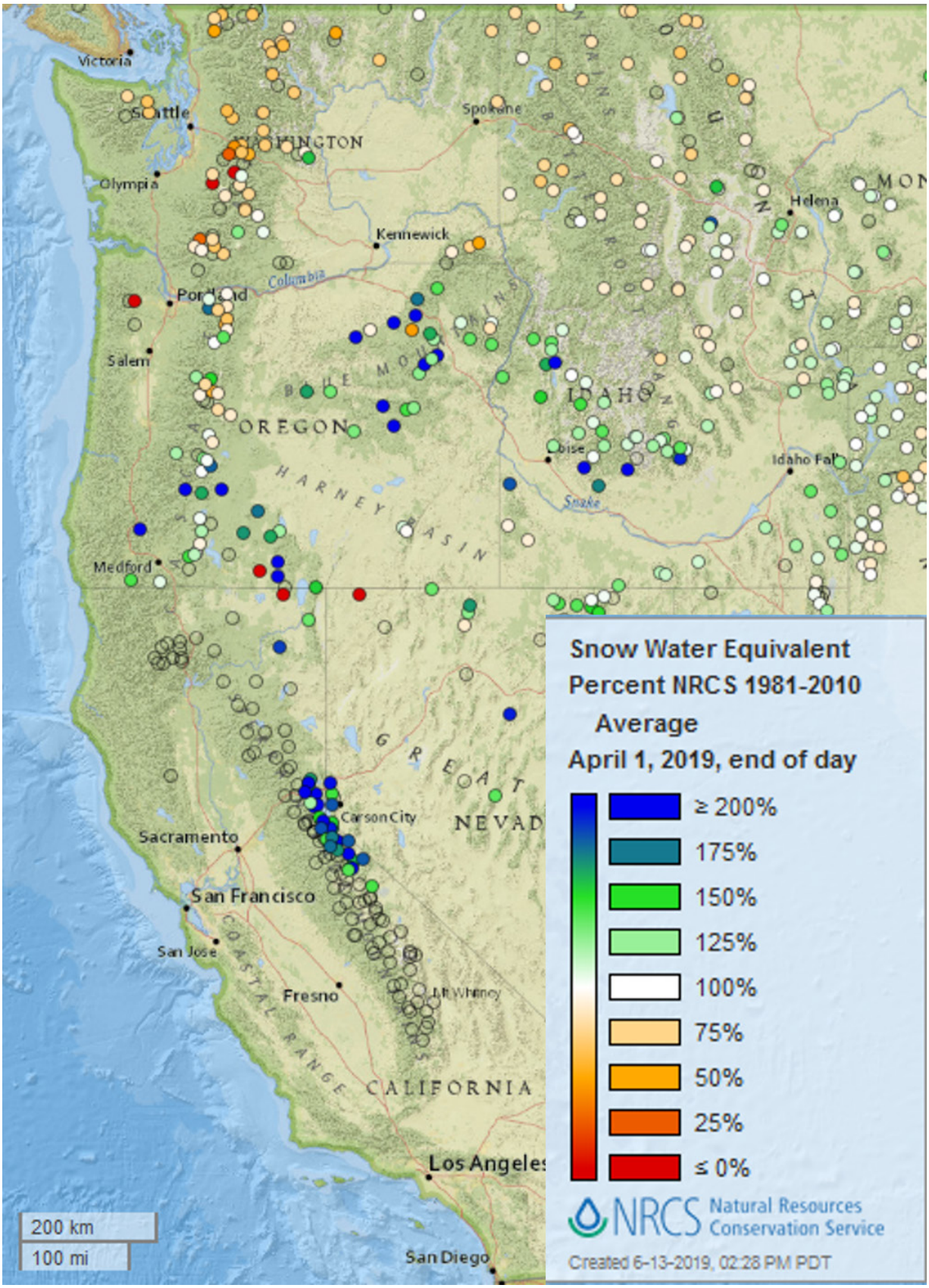

Figure 17. Mountain snowpack on 1 April 2019 at select monitoring sites relative to average values from 1981–2010. Snowpack data were obtained from interactive map products produced by the NRCS Natural Resources Conservation Service, presented as snow-water equivalent, percentile compared to period of record (https://www.wcc.nrcs.usda.gov/snow/snow_map.html).

following the noticeable peak in 2017 (Figure 18). Both the Sacramento & San Joaquin and Southern California Bight ecoregions experienced little change from 2017 to 2018, although the Southern California Bight anomaly has been negative by >1 SD for six years (Figure 18). We note that members of the PFMC have expressed concern that the minimum annual flow estimates for some ecoregions (especially in the Upper Columbia watershed) could be derived from winter conditions when streams were frozen. A follow-up analysis of data from the Salish Sea and Snake River catchments indicates the majority of low flow data came from fall (S. Munsch, NOAA, unpublished data), so we believe these results to be robust (though imperfect) indicators of low-flow events that could be detrimental to juvenile and adult salmon due to constrained habitat, warm water, and hypoxia. In future reports, we will work to further refine these indicators to best represent late-summer and fall low-flow periods.

One-day maximum flows had several distinct trends across the six ecoregions. The clearest individual trend was the Columbia Glaciated ecoregion: maximum flows increased over the past five years (Figure 19, top right), which is consistent with the 5-year trend of SWE in that ecoregion. The remaining ecoregions had considerable interannual variation in recent years, from which two inverse patterns appear to emerge: in the Salish Sea/Coastal Washington region, maximum flows dipped in 2017 but increased slightly in 2018; the remaining ecoregions experienced relatively high peak flows in 2017 but then declined in 2018 (Figure 19). These patterns were not strictly consistent with SWE patterns in the same ecoregions, which may be due to interannual variation in the speed and intensity with which snowmelt occurs in different locations.

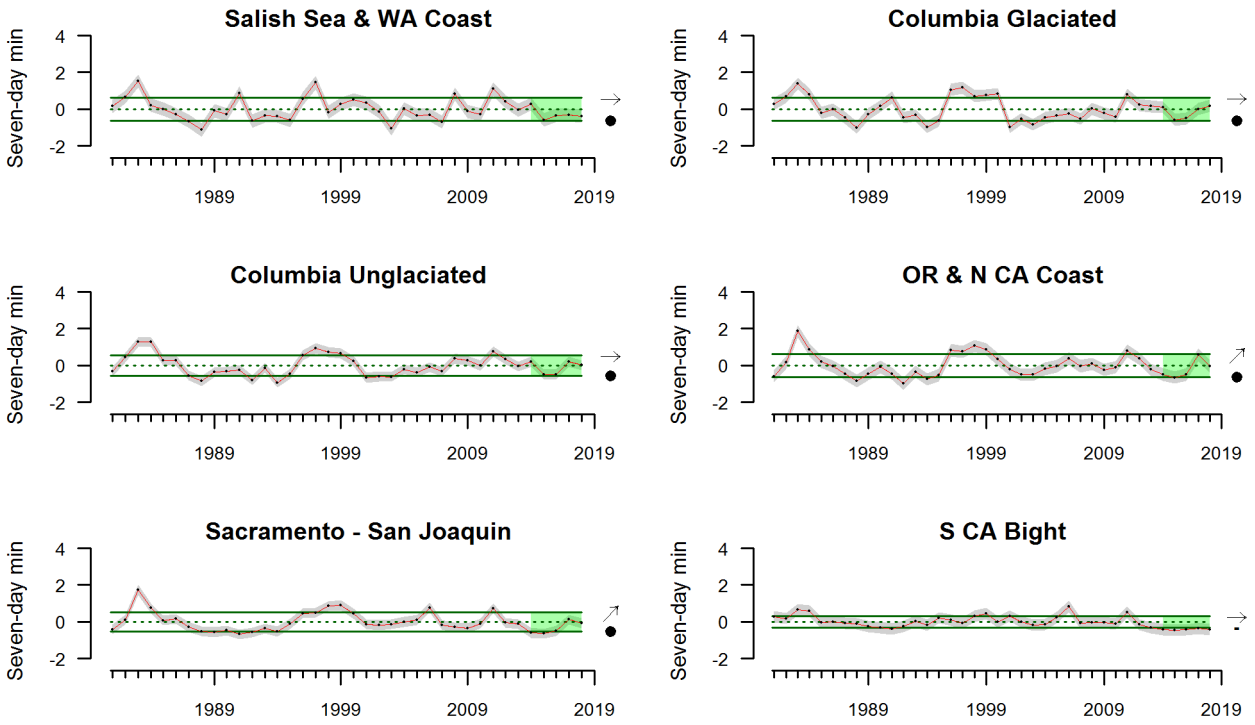

Figure 18. Anomalies of the 7-day minimum streamflow measured at 213 gages in six ecoregions from 1981–2018. Gages include both regulated (subject to hydropower operations) and unregulated systems, although trends were similar when these systems were examined separately. Lines, colors and symbols are as in Figure 3a. Streamflow data were provided by the U.S. Geological Survey (http://waterdata.usgs.gov/nwis/sw).

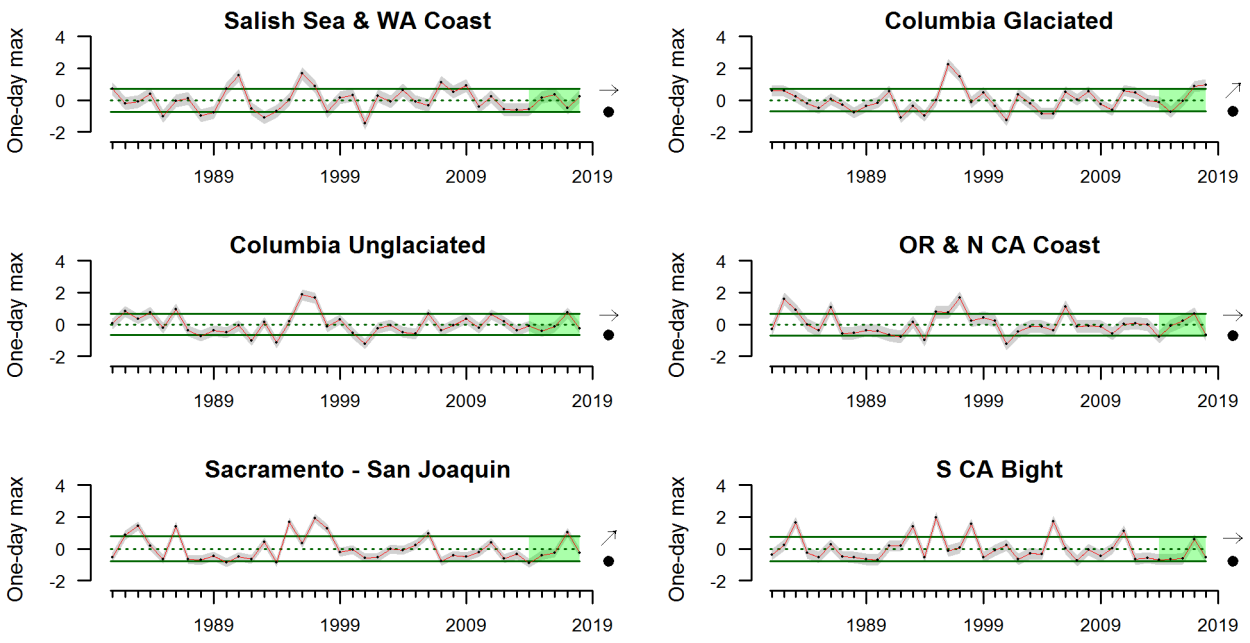

Figure 19. Anomalies of the 1-day maximum streamflow measured at 213 gages in six ecoregions from 1981–2018. Gages include both regulated (subject to hydropower operations) and unregulated systems, although trends were similar when these systems were examined separately. Lines, colors and symbols are as in Figure 3a. Streamflow data were provided by the U.S. Geological Survey (http://waterdata.usgs.gov/nwis/sw).

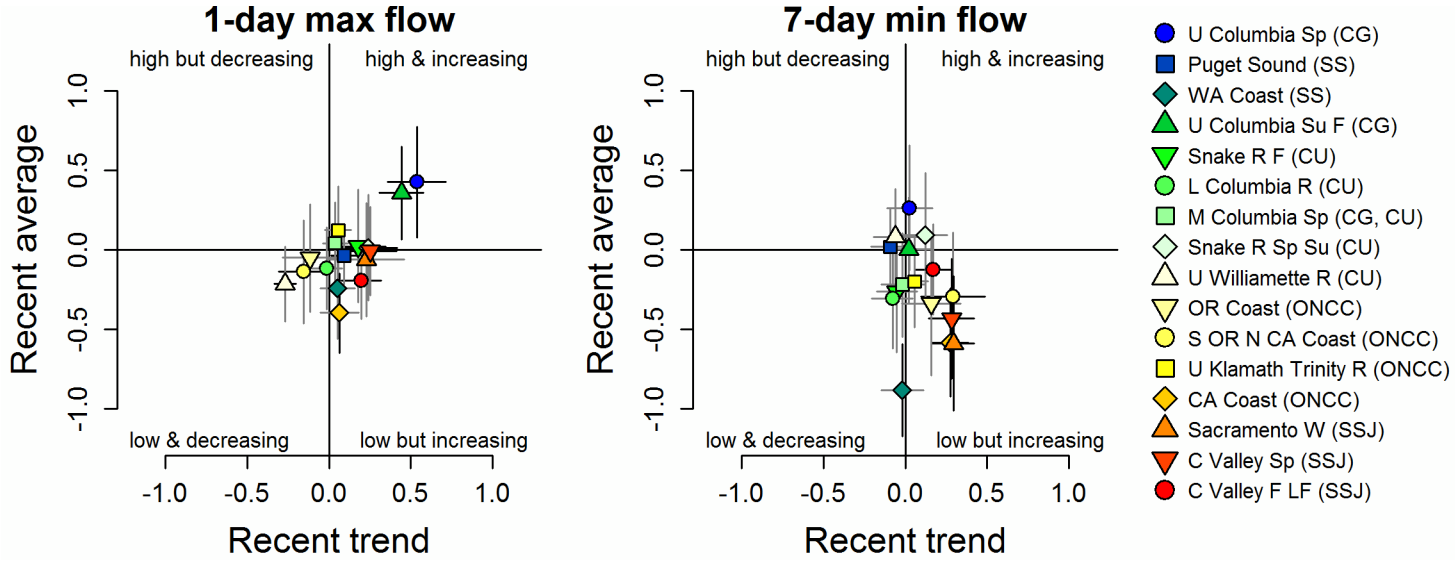

Figure 20. Recent (5-year) trend and average of maximum and minimum streamflow anomalies in 16 freshwater Chinook salmon ESUs through 2018. Symbols of ESUs are color-coded from north (blue) to south (red). Error bars represent the 2.5% and 97.5% upper and lower credible intervals. Grey error bars overlap zero, while heavy black error bars differ from zero. Abbreviations in the legend refer to the ESU's freshwater ecoregion shown in Fig. 4b (CG = Columbia Glaciated; SS = Salish Sea; CU = Columbia Unglaciated; ONCC = OR/No Cal Coastal; SSJ = Sacramento/San Joaquin). Lines and symbols are as in Figure 3c. Streamflow data were provided by the U.S. Geological Survey (http://waterdata.usgs.gov/nwis/sw).

We also used quad plots to summarize streamflow at the finer spatial scale of individual Chinook salmon ESUs (Figure 20). Points indicate the average and trend for a particular ESU from 2014-2018. The error bars describe 95% credible intervals of river flow, allowing us to determine which ESUs have short-term trends or averages strongly greater than zero or the long-term mean, respectively; these credible intervals are narrower than in last year's report (Harvey et al. 2018, their Figure 17) because the analysis now takes into account spatial correlations between different gages within a given ESU (S. Munsch, NOAA, unpublished data). Maximum flow events were generally clustered close to the center, with credible intervals overlapping zero, indicating that the recent average anomalies were not statistically different from zero and that recent trends were neutral (Figure 20, left). There were many exceptions, however; the Upper Columbia Spring and Upper Columbia Summer/Fall ESUs both experienced above average and increasing maximum flow events. Additionally, several California ESUs and Snake River ESUs showed increasing trends in maximum flow, although their overall average anomalies were very close to zero. The increasing trends observed in the above ESUs likely reflect very low flow years in either 2014 or 2015 that were followed by average or above average flows in more recent years. In contrast, maximum flow in the Upper Willamette River ESU had a negative trend over the past five years, and the California Coast ESU had below-average maximum flow but no trend. Minimum flow anomalies, which may signal the potential for stress related to temperature, oxygen, or space, were below average for a number of California ESUs, although many of these had increasing trends, suggesting that 7-day minima may be recovering toward long-term averages in these systems (Figure 20, right). The Washington coastal ESU was also below average, though with a neutral trend.

Maximum August stream temperature is derived from 446 USGS gages with temperature monitoring capability. While these gages did not necessarily operate simultaneously throughout the period of record, at least two gages provided data in all ecoregions each year. Stream temperature records are limited in California, so two ecoregions were combined. Maximum August stream temperature patterns differed markedly by ecoregion (Figure 21). The Salish Sea and Washington Coast ecoregion had higher temperatures in the last five years compared to the period of record, while the two Columbia ecoregions were closer to average. Decreasing five-year trends occurred in both the Oregon/California Coast ecoregion and the combined Sacramento/San Joaquin and Southern California Bight ecoregions.

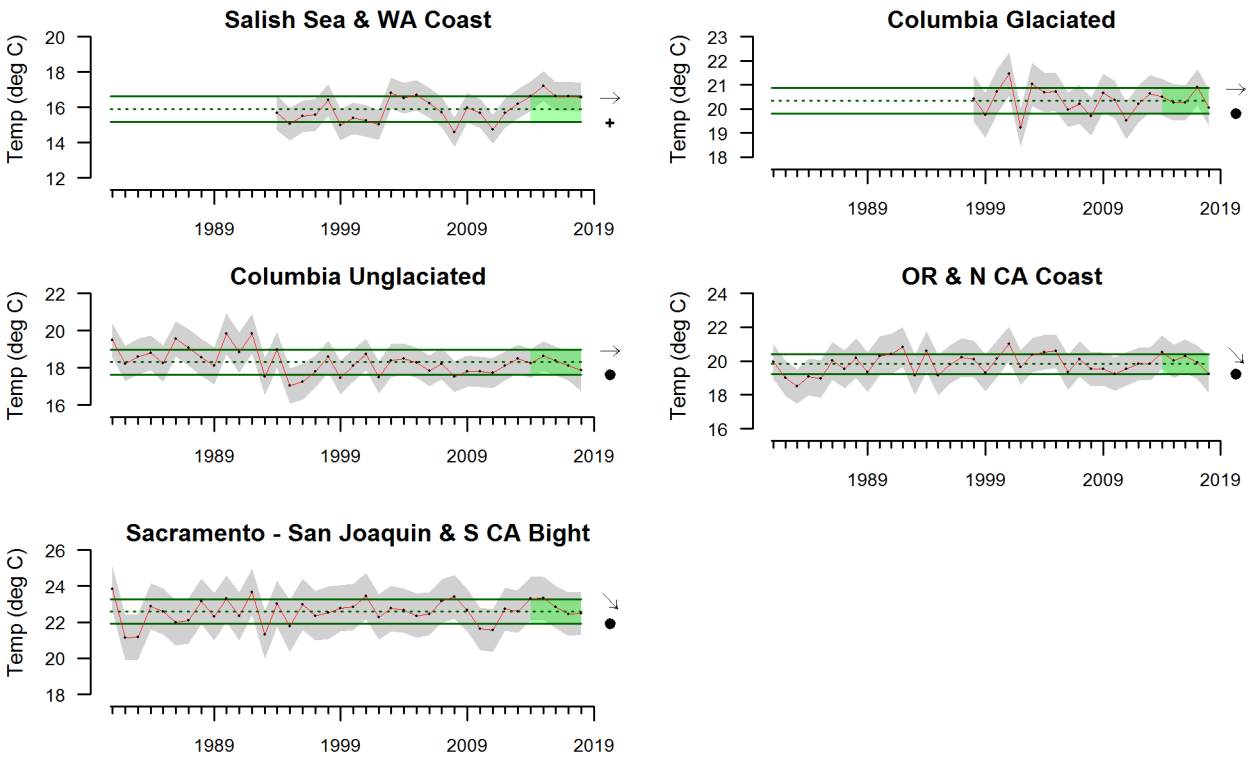

Figure 21. Mean maximum stream temperature in August in six ecoregions from 1981–2018. Gages include both regulated (subject to hydropower operations) and unregulated systems, although trends were similar when these systems were examined separately. Lines, colors, and symbols as in Figure 3a. Stream temperature data were provided by the U.S. Geological Survey (http://waterdata.usgs.gov/nwis/sw).

3. Focal Components of Ecological Integrity

The CCIEA team examines many indicators related to the abundance and condition of key species, the dynamics of community structure, and ecological interactions. Many CCE species and processes respond very quickly to changes in ocean and climate drivers, while other responses may lag by many years. These dynamics are challenging to predict. Between 2014 and 2016, many ecological metrics indicated conditions of poor productivity at lower trophic levels and poor foraging conditions for many predators. In 2017, there were some signs that indicator species abundance, condition and composition were returning to more average conditions, although there were many exceptions that implied residual effects of the anomalous warming events. In 2018, we observed additional signs that the ecology was returning to more average conditions, albeit with some lingering evidence of the recent warm anomalies in pelagic waters throughout the CCE. We describe these indicators below; how these species will respond in 2019 to the mixed physical signals outlined in the previous chapter is yet to be seen.

3.1. Northern Copepod Biomass Anomaly

Copepod biomass anomalies represent interannual variation for two groups of copepod taxa: "northern copepods," which are cold-water species rich in wax esters and fatty acids that appear to be essential for pelagic fishes, and "southern copepods," which are warm-water species that are smaller and have lower fat content and nutritional quality. In summer, northern copepods usually dominate the coastal zooplankton community observed along the Newport Hydrographic Line (see Figure 4), while southern copepods dominate during winter. El Niño events and positive PDO regimes can promote higher biomass of southern copepods (Keister et al. 2011, Fisher et al. 2015). Threshold values for the anomalies have not been set, but positive values of northern copepods in summer are correlated with stronger returns of Chinook salmon to Bonneville Dam, and values >0.2 are associated with better survival of coho salmon (Peterson et al. 2014).

From the start of the anomalous warm period in fall 2014 until spring 2017, copepod anomaly patterns strongly favored southern copepods. In late June 2017, the northern copepod anomaly increased from strongly negative to relatively neutral values, where it has essentially remained (Figure 22, top). In contrast, the southern copepod anomaly declined from strongly positive to neutral values in mid 2017; then, after a small spike

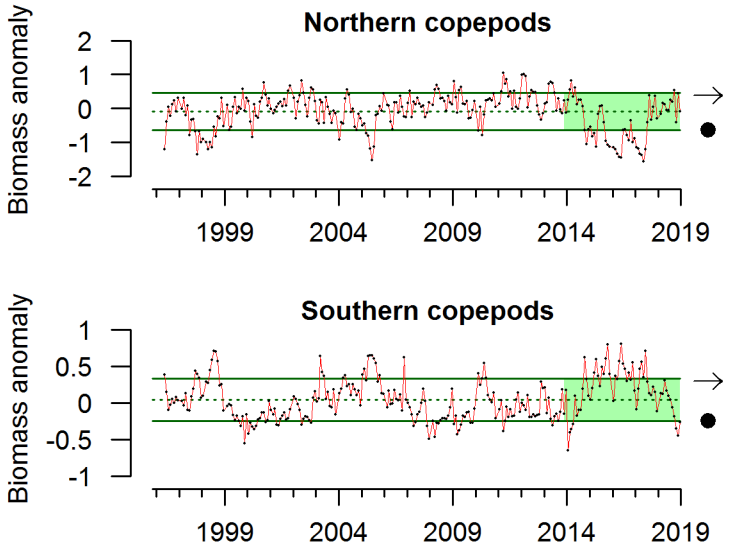

Figure 22. Monthly northern and southern copepod biomass anomalies at station NH05 off Newport, OR, 1996-2018. Lines, colors, and symbols as in Figure 3a. Copepod biomass anomaly data provided by J. Fisher, NMFS/NWFSC, OSU.

in early 2018, southern copepods declined sharply over the remainder of 2018 (Figure 22, bottom). Thus, the overall ratio of northern to southern copepods shifted to favor northern copepods, which may suggest better feeding conditions for small pelagic fishes that are, in turn, preyed upon by juvenile coho and Chinook salmon. Furthermore, while several rare or previously unrecorded copepods were observed on the Newport Line between fall 2014 and spring 2015 (when the marine heat wave moved onshore) and again in 2016 (possibly related to the marine heat wave and the strong 2015–16 El Niño event), these rare and new species were absent from 2017 samples (K. Jacobson/J. Fisher, NOAA/OSU, unpublished data). While these changes may suggest a transition away from the unproductive conditions observed in recent years in this region of the CCE, the lack of a dominant northern copepod signal suggests possible lingering effects of shifts in the northern copepod source population and/or weaker alongshore transport delivering fewer northern copepod species to the CCE. This may, for example, require the stronger degree of southward transport that occurs during the negative phase of the PDO (Bi et al. 2011, Keister et al. 2011, Di Lorenzo et al. 2013).

3.2. Euphausiid Size off Trinidad Head

In this year's report, we have added an indicator of lower trophic level productivity: the condition of euphausiids (krill) off of Trinidad Head, California (see Figure 4). Euphausiids are among the most important and ubiquitous taxa in the diets of fishes in the CCE, and are also key prey for many seabirds and marine mammals. Two species of particular importance are *Thysanoessa spinifera* and *Euphausia pacifica*. *E. pacifica* has been sampled multiple times per season off of Trinidad Head since late 2007. Here, we show mean body length of *E. pacifica* by sampling date as an indicator of euphausiid size, condition and energy content for predators. Within any given year, length of *E. pacifica* cycles from relatively short individuals in winter to longer individuals by summer (Figure 23). At an interannual scale, *E. pacifica* lengths were often above the time series mean in 2008 and 2009, then cycled around the mean between 2011 and 2014. (A data gap in summer and fall 2010 limits our assessment of the full annual cycle in that year.) *E. pacifica* length dropped sharply in late 2014 and early 2015 (Figure 23), concurrent with the onset of the warm anomalies along the West Coast, and remained unusually low through 2016. *E. pacifica* length increased modestly in 2017, and the annual cycle in 2018 resembles the pattern from prior to 2014. Thus, the size and condition of krill off of Northern California appears to have increased over the past several years; this information, coupled with above-average catches of krill further to the south off of Monterey Bay (see Harvey et al. 2019, Appendix G.2), imply that krill production in the northern and central portions of the CCE has improved since the warm conditions of 2014–16.

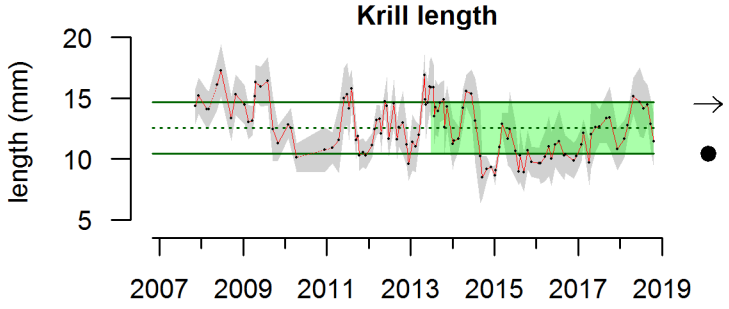

Figure 23. Mean krill length at stations along the Trinidad Head Hydrographic Line, 2007–18. The grey shaded region indicates ±1 SD. Lines, colors, and symbols are as in Figure 3a. Krill (*Euphausia pacifica*) data were provided by E. Bjorkstedt, NMFS/SWFSC, Humboldt State University (HSU), and R. Robertson, Cooperative Institute for Marine Ecosystems and Climate (CIMEC) at HSU. Krill were collected at monthly intervals from the Trinidad Head Line (Figure 4); krill body length (BL) was measured in mm from the back of the eye to the base of the telson.

3.3. Harmful Algal Blooms

In response to requests from various PFMC advisory bodies, this year we are adding a new indicator of the occurrence of harmful algal blooms (HABs). While many taxa produce HABs along the West Coast, blooms of the diatom genus *Pseudo-nitzschia* have been of particular concern in recent years. Certain species of *Pseudo-nitzschia* produce the toxin domoic acid, which can then be taken up by filter feeders and enter the food web of coastal waters. Domoic acid can cause amnesic shellfish poisoning in birds, various marine mammals, and humans. To protect human health, fisheries that target shellfish (including razor clam *Siliqua patula*, Dungeness crab *Metacarcinus magister,* rock crab *Cancer* spp., and spiny lobster *Panulirus interruptus*) are closed when concentrations exceed regulatory thresholds for human consumption, resulting in tens of millions of dollars in lost revenue and a range of cultural impacts in coastal communities (Dyson and Huppert 2010, NMFS 2016, Ritzman et al. 2018). Harmful or lethal effects of domoic acid extend through food webs to people as well as to marine predators such as marine mammals and seabirds (Lefebvre et al. 2002, McCabe et al. 2016). These impacts to coastal food webs, human health, and fishing opportunities are influenced by ocean conditions: extremely toxic HABs of *Pseudo-nitzschia* coincide with or closely follow El Niño events or positive PDO regimes and track regional anomalies in southern copepod species (McCabe et al. 2016, McKibben et al. 2017, Peterson et al. 2017). A widespread *Pseudo-nitzschia* bloom in 2015 was the most toxic ever recorded and coincided with the North Pacific marine heatwave (McCabe et al. 2016, Peterson et al. 2017); this event caused extensive closure of multiple fisheries along the West Coast, resulting in over $60M in federal disaster relief funds for salmon and crab fisheries.

Razor clams are good indicators of HAB dynamics in the coastal ocean. They provide an accurate record of the arrival and intensity of HAB events on beaches, and they can accumulate and retain domoic acid for up to a year following HABs of *Pseudo-nitzschia*. They are closely monitored by local, state, tribal and federal agencies, in order to ensure healthy seafood for commercial, recreational and tribal harvesters.

In 2018, domoic acid levels in razor clams varied sharply by region. Along the Washington coast, monthly maximum domoic acid concentrations in razor clams from six sites are shown in Figure 24 (top). Domoic acid levels at or exceeding the Federal Drug Administration (FDA) alert level of 20 parts per million trigger closures of razor clam harvests; such events occurred most recently in 2015, 2016 and 2017, coincident with the anomalous warming events in the CCE. In 2018, the low levels of domoic acid detected in Washington razor clams and Dungeness crabs did not trigger fishery closures at any of the sites.

In stark contrast to Washington, razor clams in Oregon had unsafe levels of domoic acid in 2018, and in fact have shown continuous, elevated domoic acid levels over the most recent 4 years, with maximum tissue concentrations as high as or higher than any peaks seen in decades prior (Figure 24, bottom). In 2018, razor clam harvesting in Oregon was closed several times due to domoic acid accumulation above 20 ppm. Most of the Oregon coast, from Cascade Head to the Oregon-California border, was closed at the end of 2017 and that closure extended into the middle of April 2018 from the Umpqua River south to Cape Arago. For the remainder of 2018, the fishery experienced a series of openers and closures, by time and area. From Cape Blanco to the Oregon–California border, razor clam harvest has been closed since 29 August 2014.

Recreational and commercial Dungeness crab fisheries in Oregon during 2018 were also interrupted due to domoic acid detections above the FDA alert level of 30 ppm for crab viscera (data not shown). The openings of both the 2017–18 and 2018–19 commercial ocean Dungeness crab seasons (from December to August) were delayed along the southern portions of the coast. Elevated domoic acid levels in crab viscera along the southern portion of the coast were detected after the 2017–18 crab season opened, which required all crab harvested for commercial purposes to be eviscerated for a period of time. The recreational crab fishery was closed in all of these same areas and times.

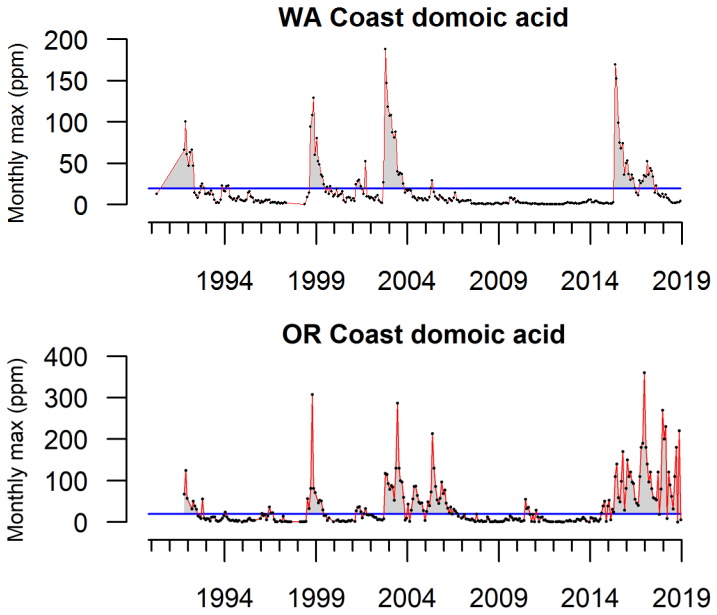

Figure 24. (top) Monthly maximum domoic acid concentration (parts per million; ppm) in razor clams through 2018 for the Washington State coast. The blue line is the domoic acid management threshold of 20 ppm. Lines, colors, and symbols are as in Figure 3b. Data compiled by the Washington Department of Health (WDOH) from samples collected and analyzed by a variety of local, tribal, and state partners. (bottom) Monthly maximum domoic acid concentration (ppm) measured in razor clam tissues from sites in Oregon, 1991–2018. Tissue sampling is conducted twice monthly from multiple sites across the Oregon coast, year-round, and domoic acid concentrations are determined from analyses conducted by the Oregon Department of Agriculture (ODA) using High Pressure Liquid Chromotography (HPLC).

California also experienced widespread closures of multiple nearshore fisheries due to *Pseudo-nitzschia* blooms and domoic acid in 2018, and those impacts have spilled forward into shellfish fisheries in 2019 (data not shown). Dungeness crab support one of the top two fisheries in the state (Rogers-Bennett and Juhasz 2014), and are tested for domoic acid at 18 sites near the major fishery ports of Crescent City and Morro Bay prior to the scheduled start of crabbing season. The longest closure to date of the California Dungeness crab fishery occurred during the 2015–16 fishing season amidst the highly toxic *Pseudo-nitzschia* bloom during the marine heatwave, leading to >$25M in federal disaster relief. The 2018–19 commercial Dungeness crab fishery was delayed by about three weeks between Bodega Head and the Sonoma–Mendocino County line and approximately 10 days between Patrick's Point, Humboldt County, and the California–Oregon border. The 2018–19 recreational Dungeness crab fishery was delayed approximately 2.5 months between Patrick's Point and the California–Oregon border. The 2018–19 commercial spiny lobster fishery was closed for one month around Santa Cruz and Anacapa Islands in Santa Barbara County. The commercial rock crab fishery north of Bodega Head, Sonoma County, was closed due to domoic acid beginning in 2015 and continuing into 2018. Potential fishery participants were able to provide rock crab for testing in Northern California; the fishery reopened in stages from south to north in Sonoma and Mendocino counties during January through April, 2018, but remained closed from Humboldt County north to the California–Oregon border. Finally, the recreational razor clam fishery remains closed since April 2016 in Humboldt and Del Norte counties.

The California Department of Public Health (CDPH) has monitored California state fisheries for domoic acid since 1991; they issue human health consumption advisories based on their findings.[10] Information on California fishery closures due to health advisories can be found at the California Department of Fish and Wildlife.[11]

3.4. Regional Forage Availability

This section describes trends in forage availability, based on spring/summer research cruises that have been conducted independently in three different regions (see Figure 4c) for decades. The CCE forage community is a diverse portfolio of species and life-history stages, varying in behavior, energy density, and availability to predators. Years with abundant pelagic fish, market squid, and krill are generally associated with cooler waters, strong upwelling, and higher productivity (Santora et al. 2014). The species shown below represent a substantial portion of the available forage in the regions sampled by the cruises. *We consider these regional indices of relative forage availability and variability, not indices of absolute abundance of coastal pelagic species* (CPS). Absolute abundance estimates should come from stock assessments and comprehensive monitoring programs. Although there is coastwide monitoring of CPS, currently absolute or total abundance estimates are limited to those resulting from stock assessments for sardine (*Sardinops sagax*) and Pacific mackerel (*Scomber japonicus*) (PFMC 2019).

The three regional surveys that produce forage community indicator data use different methods (e.g., gear selectivity, timing, frequency, and survey objectives); thus, the amplitudes of a given species' time series from a particular region are not necessarily comparable to that species' time series from the other regions. This problem has confounded the CCIEA team in past reporting because effectively analyzing and communicating the composition and status of a diverse forage assemblage spread across three regions with different sampling methods is very difficult. Past approaches have included presenting stacks of standard time series plots grouped by region, or use of quad plots; however, we have long felt that these placed an undue interpretive burden on readers, and also failed to address the challenge of making informed cross-regional comparisons. For 2018, we used a new approach that employs two forms of cluster analysis: one part of the analysis groups species that tend to co-occur in each region, and the other part of the analysis groups consecutive years of statistically similar species compositions. This allows us to identify years in which the forage community made a significant transition from one set of species to another. It also allows us to compare regions to see if significant transitions occurred at the same time, which may help us identify if concurrent changes in the rest of the system (climate, oceanography, fisheries, predators, etc.) are related to the forage community. The analysis also adds non-metric multidimensional scaling (NMDS) to look across all years and identify the key forage species and assemblages in each survey. Analytical methods for this approach are described in Thompson et al. (2019).

[10] https://www.cdph.ca.gov/Programs/CEH/DFDCS/Pages/FDBPrograms/FoodSafetyProgram/DomoicAcid.aspx
[11] https://www.wildlife.ca.gov/fishing/ocean/health-advisories

3.4.1. Northern CCE

Data from the northern CCE come from a NOAA survey off Washington and Oregon (see Figure 4c) called the Juvenile Salmon and Ocean Ecosystem Survey (JSOES). JSOES uses a surface trawl to target juvenile salmon (*Oncorhynchus* spp.), and also catches pelagic fishes, squid, and gelatinous zooplankton (Brodeur et al. 2005, Morgan et al. 2019). Because JSOES is a daytime survey that employs a surface trawl, it is not suitable for effective quantitative monitoring of pelagic species that undergo diet vertical migration (DVM) or that tend to be deeper in the water column. Thus, to avoid sampling bias, we focused on surface-oriented or non-DVM species like salmon, market squid, juvenile rockfish, and juvenile sablefish (*Anoplopoma fimbria*). We excluded data from midwater and DVM species such as sardine, anchovy, whitebait smelt (*Allosmerus elongatus*), jack mackerel (*Trachurus symmetricus*) and Pacific herring (*Clupea pallasii*).

Overall, the cluster analysis (Figure 25, right) shows that the forage community sampled by JSOES has been defined primarily by abundant catches of market squid nearly every year since 2014, while fish catches have undergone several changes in the same period, most recently an increase of yearling Chinook and coho salmon in 2018. These trends are depicted by the colors and lines within the grid. The relative abundance of a group over the course of the time series is indicated by color, from very rare (dark blue) to very abundant (dark red) relative to the group's time series mean (white). Horizontal lines separate the community into subgroups that tend to co-occur (e.g., the upper horizontal line in Figure 25 indicates that young-of-year sablefish, young-of-year rockfish, and subyearling Chinook salmon tended to be abundant at the same time in samples from the Northern CCE). Vertical lines indicate years in which a statistically significant shift in forage composition occurred (e.g., the heavy vertical line between 2013 and 2014 indicates a pronounced shift in dominant forage taxa, in this case from yearling salmon to market squid). The dendrograms indicate the hierarchical clustering of co-occurring species groups (dendrogram to left of grid) and of years with statistically similar forage community compositions (dendrogram above the grid), following the methods of Thompson et al. (2019).

On the left of Figure 25, a nonmetric multidimensional scaling (NMDS) plot arranges individual years along two standardized multivariate axes that represent significant tendencies in community composition (as described in Thompson et al. 2019). Thus, years with similar community compositions tend to occur close to one another on the plot. The names of species appear on the plot as well, with their position indicating their loadings on the two NMDS axes. The community sampled by JSOES in 2018 appears in the upper right quadrant, in roughly the same area as the community from 2003, 2014 and 2015 (all of which had high catches of market squid and moderate to high catches of at least one type of yearling salmon; see also Figure 25, right). The 2018 data point in the NMDS plot differed dramatically from the 2017 point, which was influenced primarily by market squid and represented very low catches of salmon (Figure 25, left).

As a final note regarding forage community composition in the northern CCE, extreme numbers of the pyrosome *Pyrosoma atlanticum*, a pelagic tunicate associated with warmer waters, were observed in a related survey in 2018, the second straight year of such exceptional densities (Figure 26). This is a continuation of a dramatic shift of pyrosomes into waters north of Cape Mendocino and into cooler areas of the NE Pacific; that shift began during the 2014–16 marine heat wave (Sutherland et al. 2018) and was accompanied by other changes to the pelagic community composition of this region (Brodeur et al. 2019, Morgan et al. 2019).

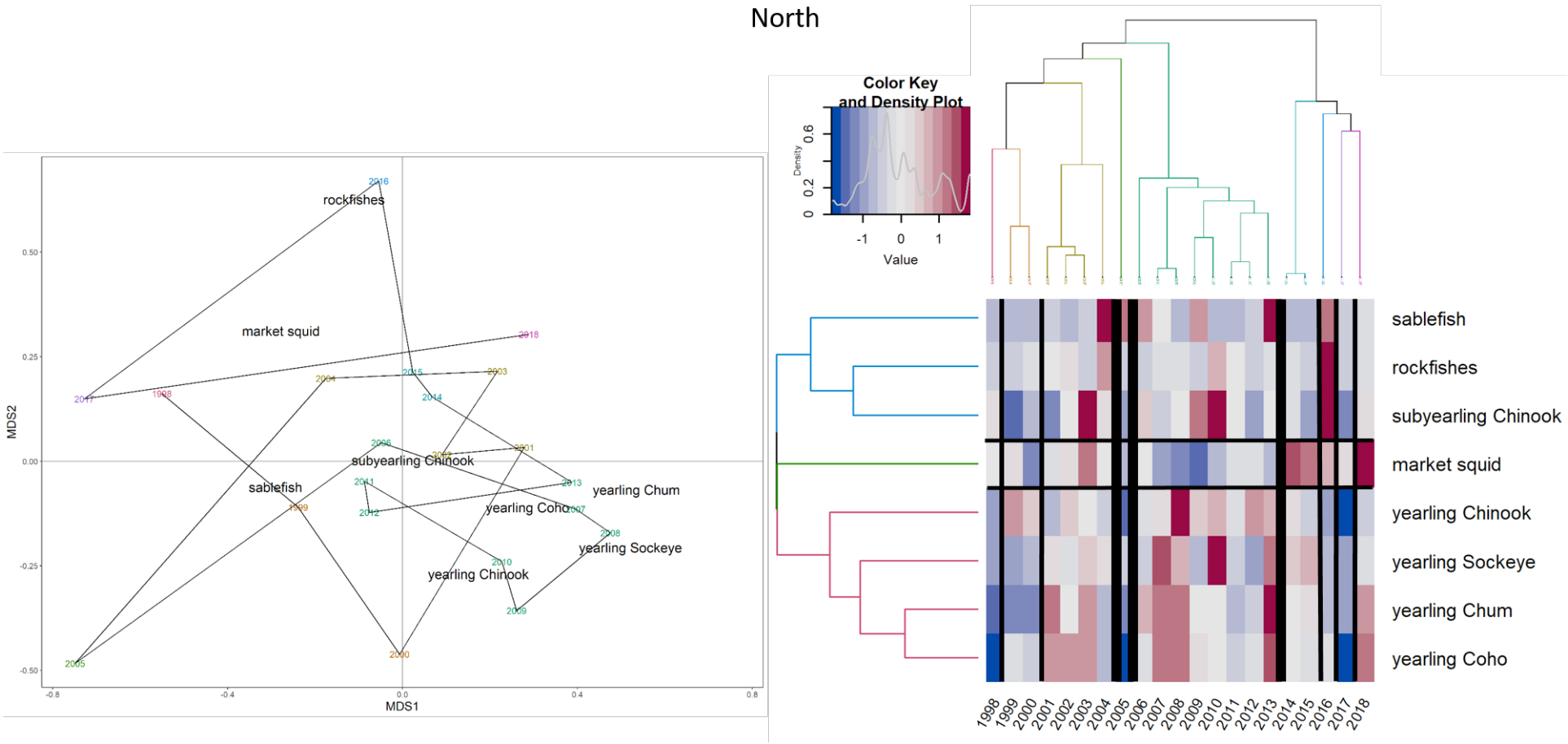

Figure 25. Multivariate analyses of forage dynamics in the northern CCE through 2018. The plot on the left depicts NMDS results where years are color coded to correspond with the horizontal chronological clustering branches on the top right. In the center, the dendrogram with horizontal lines indicates clusters of typically co-occurring species; vertical lines indicate temporal shifts in community structure. The heat map on the right is colored based on the Z-score for each taxon, with colors indicating relative abundance (red = abundant, blue = rare); dark vertical bars demarcate deep breaks in assemblage structure between years. Pelagic forage data from the Northern CCE were provided by B.Burke, NMFS/NWFSC and C. Morgan, NMFS/NWFSC, OSU. Data are derived from surface trawls taken in June during the NWFSC Juvenile Salmon & Ocean Ecosystem Survey (JSOES; https://www.nwfsc.noaa.gov/research/divisions/fe/estuarine/oeip/kb-juvenile-salmon-sampling.cfm).

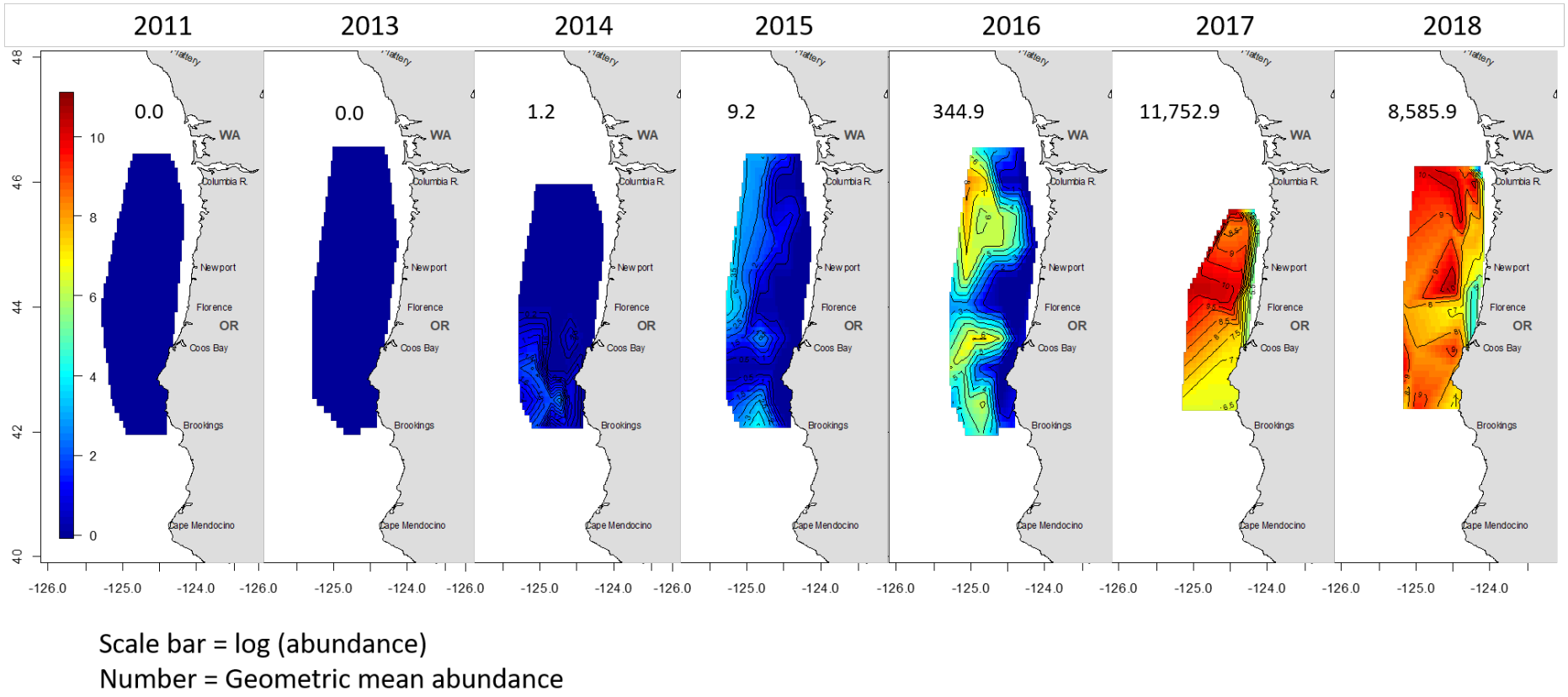

Figure 26. Catch of pyrosomes in the annual prerecruit survey in May and June off the Oregon and Washington coasts. Catches are standardized to 30-minute tows and shown in contours on a log scale. Number above the mapped data in each graph is the geographic mean catch in a 30-minute tow. R. Brodeur, unpublished, NMFS/NWFSC.

3.4.2. Central CCE

Data presented here are from the "core area" of a NOAA midwater trawl survey (see Figure 4c) called the Juvenile Rockfish Recruitment and Ecosystem Assessment Survey (JRREAS), which targets pelagic young-of-the-year (YOY) rockfishes (*Sebastes* spp.), but also samples other pelagic fish, market squid and zooplankton (Sakuma et al. 2016).

Somewhat surprisingly, there have been no statistically significant temporal shifts since 2013 (Figure 27, right), despite the considerable changes in climate and oceanography during that period with the onset of the anomalous warm conditions in 2014 and the relaxation of that warming after 2016. Since 2013, the cluster of forage that includes YOY rockfish, YOY sanddabs (*Citharichthys* spp.), YOY Pacific hake, market squid, juvenile sardine and juvenile anchovy has consistently been present, although the most prevalent groups within that cluster have varied from year to year; for example, YOY rockfish were abundant in 2013–17 but not 2018, and market squid were uncommon in 2016 but otherwise abundant from 2013–2018 (Figure 27, right). Since 2016, the cluster of forage that includes adult anchovy, adult sardine, and several mesopelagic fishes has become more prevalent, though not enough to result in a statistically significant temporal shift; the species driving this increase are adult anchovy, deep sea smelt (family Bathylagidae) and blue lanternfish (*Tarletonbeania crenularis*). Each of these taxa, along with California smoothtongue (*Leuroglossus stilbius*), was abundant in 2018.

In the NMDS plot for the central CCE forage community, the 2018 data grouped in the upper right quadrant, most closely associated with 2016 (Figure 27, left). The two groups with the strongest loadings in this quadrant were juvenile anchovy and juvenile sardine, both of which were abundant in 2018 catches relative to their respective time series, which are each characterized by near-zero catches in most years (Harvey et al. 2019, Appendix G.2). The placement of 2018 on the NMDS plot is also close to 2009, with both years characterized by relatively high abundances of mesopelagic species like deep sea smelt, blue lanternfish, and other lanternfishes (Figure 27, left).

There were other noteworthy findings from JRREAS (data not shown). Krill catches were above average for the second consecutive year, as alluded to in Euphausiid size off Trinidad Head, implying good foraging conditions in this area (see Appendix G.2 in Harvey et al. 2019). Also, catches of *Aurelia* and *Chrysaora fuscescens* jellyfish were among the highest observed in this survey's nearly 30-year time series, and this follows several years of very poor catches of jellies during the anomalous warm years (Harvey et al. 2019, Appendix G.2). Finally, pyrosomes were relatively abundant in the Central CCE for the fifth year in a row, although their numbers have declined steadily over the past 4 years and were near the long-term survey mean in 2018 (Harvey et al. 2019, Appendix G.2).

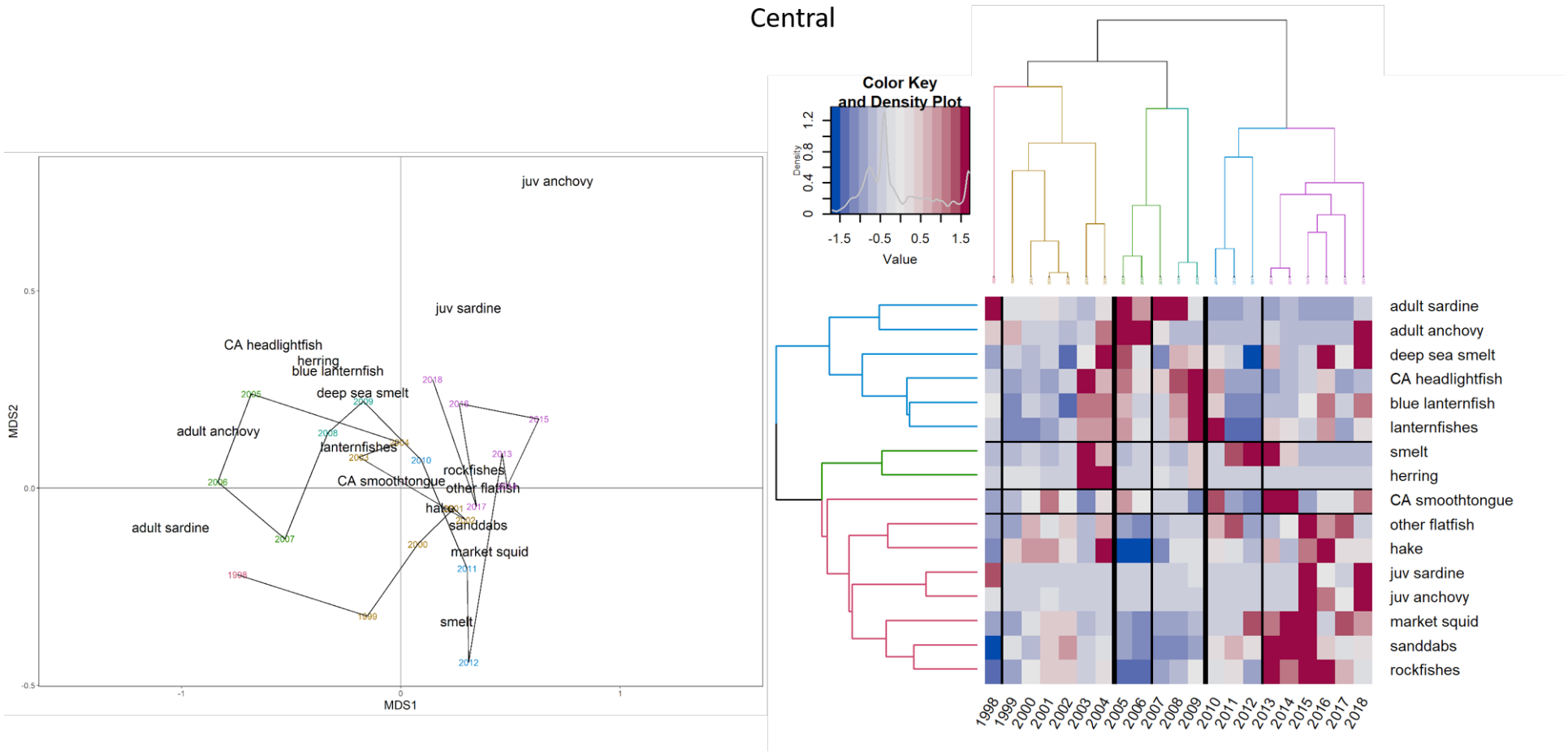

Figure 27. Multivariate analyses of forage dynamics in the central CCE through 2018. The plot on the left depicts NMDS results where years are color coded to correspond with the horizontal chronological clustering branches on the top right. In the center, the dendrogram with horizontal lines indicates clusters of typically co-occurring species; vertical lines indicate temporal shifts in community structure. The heat map on the right is colored based on the Z-score for each taxon, with colors indicating relative abundance (red = abundant, blue = rare); dark vertical bars demarcate deep breaks in assemblage structure between years. Pelagic forage data from the Central CCE were provided by J. Field and K. Sakuma, NMFS/SWFSC, from the SWFSC Rockfish Recruitment and Ecosystem Assessment Survey (https://swfsc.noaa.gov/textblock.aspx?Division=FED&ParentMenuId=54&id=20615).

3.4.3. Southern CCE

Forage indicators for the Southern CCE come from CalCOFI larval fish surveys conducted in the spring across all core stations of the CalCOFI survey (see Figure 4c), using oblique vertical tows of fine mesh Bongo nets to 212 m depth (McClatchie 2014). The survey collects a variety of fish and invertebrate larvae (<5 days old) from several taxonomic and functional groups. Larval biomass is assumed to correlate with regional abundance of mature forage fish.

Several statistically significant temporal shifts occurred over the most recent five years, including shifts coinciding with the onset of the warm anomalies (post-2014) and the relaxation of the warm anomalies (post-2016) (Figure 28, right). Since the last shift after 2016, the dominant species cluster has been larval anchovy and California smoothtongue. Species such as rockfishes and mackerels that had been abundant prior to 2017 were less common; other commercially important species such as market squid and sanddabs have not been abundant in the larval survey catches since 2014; larval sardine have been relatively rare since 2010.

According to the NMDS plot, the southern CCE larval forage community in 2018 continued a progressive shift in composition, and the trajectory of the shift in 2017 and 2018 appears to be toward larval anchovy (Figure 28, left).

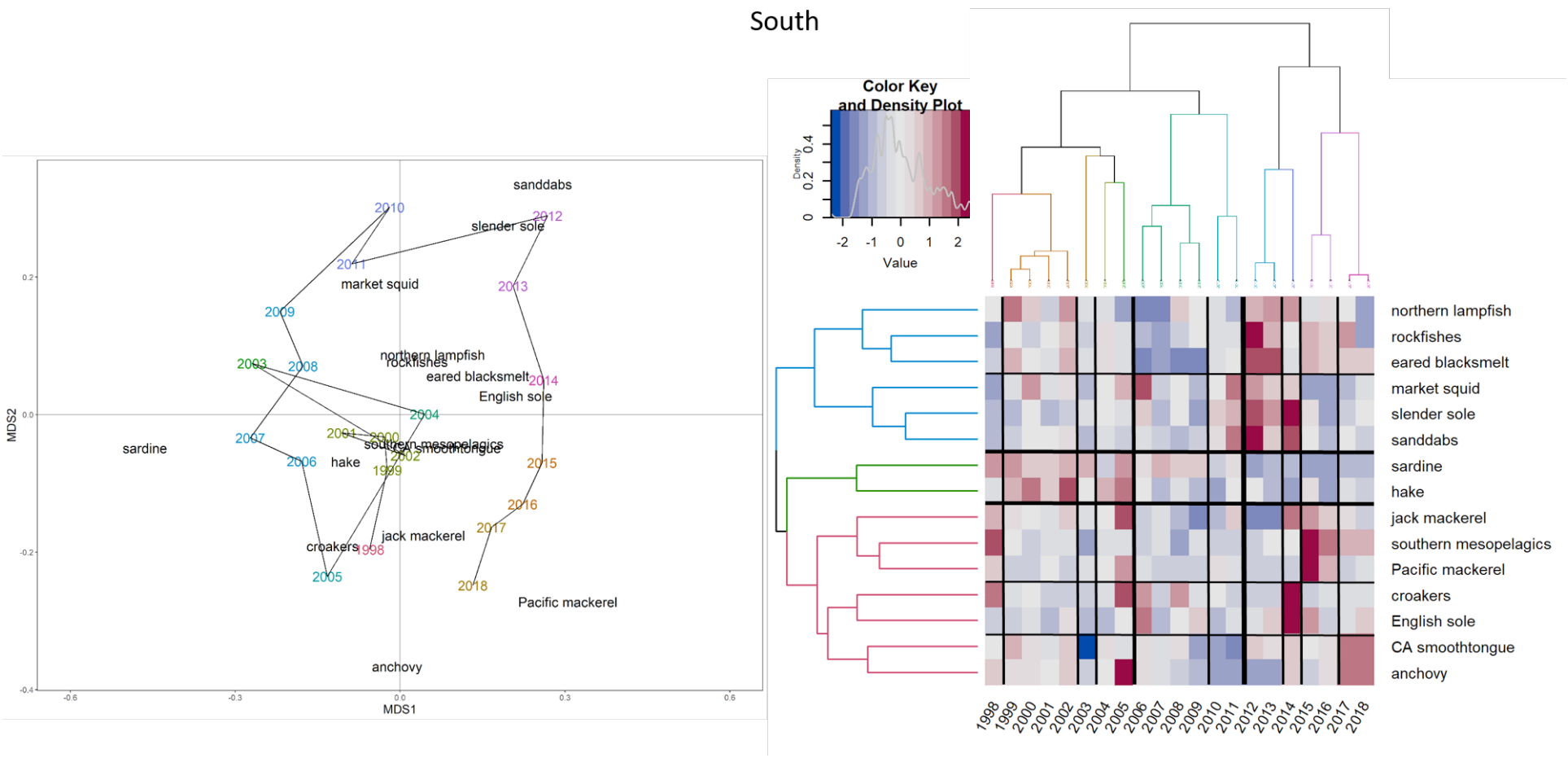

Figure 28. Multivariate analyses of forage dynamics in the southern CCE through 2018. The plot on the left depicts NMDS results where years are color coded to correspond with the horizontal chronological clustering branches on the top right. In the center, the dendrogram with horizontal lines indicates clusters of typically co-occurring species; vertical lines indicate temporal shifts in community structure. The heat map on the right is colored based on the Z-score for each taxon, with colors indicating relative abundance (red = abundant, blue = rare); dark vertical bars demarcate deep breaks in assemblage structure between years. Pelagic forage larvae data from the Southern CCE were provided by A. Thompson, NMFS/SWFSC, and derived from spring CalCOFI surveys (https://calcofi.org/).

3.5. Salmon

For indicators of the abundance of Chinook salmon populations, we compare the trends in natural spawning escapement along the CCE to evaluate the coherence in production dynamics, and also to get a more complete perspective of their status across the greater portion of their range. When available, we use escapement time series back to the 1970s; however, some populations have shorter time series (for example, Central Valley spring starts in 1995, Central Valley winter starts in 2001, and Coastal California starts in 1991). We summarize escapement trends in quad plots (see Figure 3); time series are available in Appendix H of Harvey et al. (2019), and trends are evaluated for the most recent 10-year period in order to capture population dynamics across multiple generations. We have also added a time series of juvenile salmon catches from a NOAA survey conducted in the Northern CCE off Oregon and Washington (see Figure 4c).

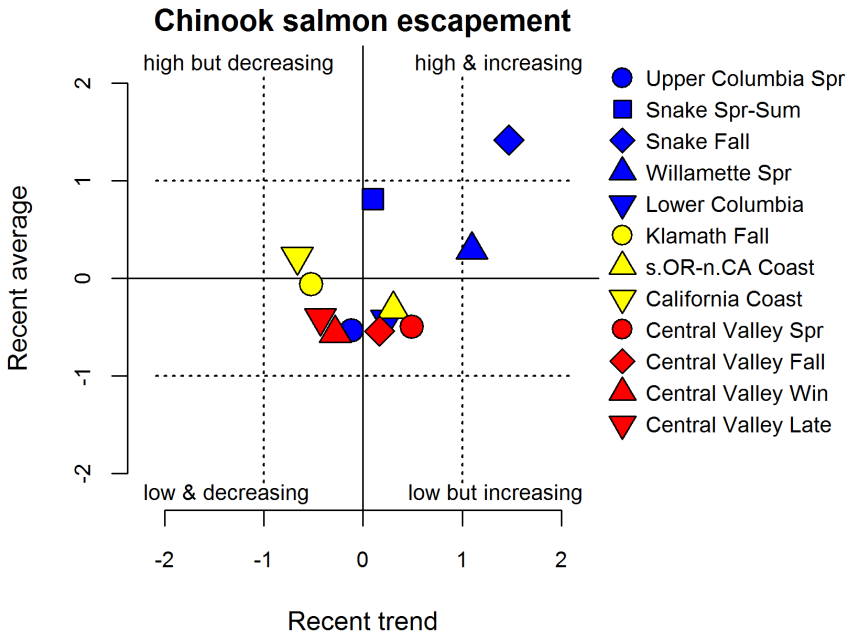

Figure 29. Recent (10-year) trend and average of Chinook salmon escapement through 2017. Recent trend indicates the escapement trend from 2007–17. Recent average is mean natural escapement (includes hatchery strays) from 2007–17. Lines and symbols as in Figure 3c. Chinook salmon escapement data were derived from the California Department of Fish and Wildlife (https://www.dfg.ca.gov/fish/Resources/Chinook/CValleyAssessment.asp), Pacific Fishery Management Council preseason reports (https://www.pcouncil.org/salmon/stock-assessment-and-fishery-evaluation-safe-documents/review-of-2017-ocean-salmon-fisheries/), and NOAA Fisheries/NWFSC's "Salmon Population Summary" database (https://www.webapps.nwfsc.noaa.gov/sps), with data provided directly from the Nez Perce Tribe, the Yakama Nation Tribe, and from Streamnet's Coordinated Assessments database (https://cax.streamnet.org), with data provided by the Oregon Department of Fish and Wildlife, Washington Department of Fish and Wildlife, Idaho Department of Fish and Game, Confederated Tribes and Bands of the Colville Reservation, Shoshone-Bannock Tribes, Confederated Tribes of the Umatilla Indian Reservation, and U.S. Fish and Wildlife Service.

Most Chinook salmon escapement data are updated through 2017. Generally, escapements of California Chinook salmon ESUs over the last decade of available data were within 1 SD of long-term averages (Figure 29), although 2017 escapements were among the lowest on record in several ESUs (Harvey et al. 2019, Appendix H). California Chinook salmon stocks had neutral trends over the last decade (Figure 29), and annual variation was generally high relative to the available time series (Harvey et al. 2019,

Appendix H). In Washington, Oregon and Idaho, most escapements were within 1 SD of the time series average for the past decade (Figure 29); the exception was Snake River Fall Chinook after a series of escapements since 2009 that were above the time series average (Harvey et al. 2019, Appendix H). Escapement trends for northern stocks were mostly neutral, but Willamette Spring and Snake River Fall Chinook had positive trends over the most recent decade of data (Figure 29). Escapements in 2017 ranged from above the time series average (Willamette Spring) to below the time series average (Upper Columbia Spring, Lower Columbia; Harvey et al. 2019, Appendix H).

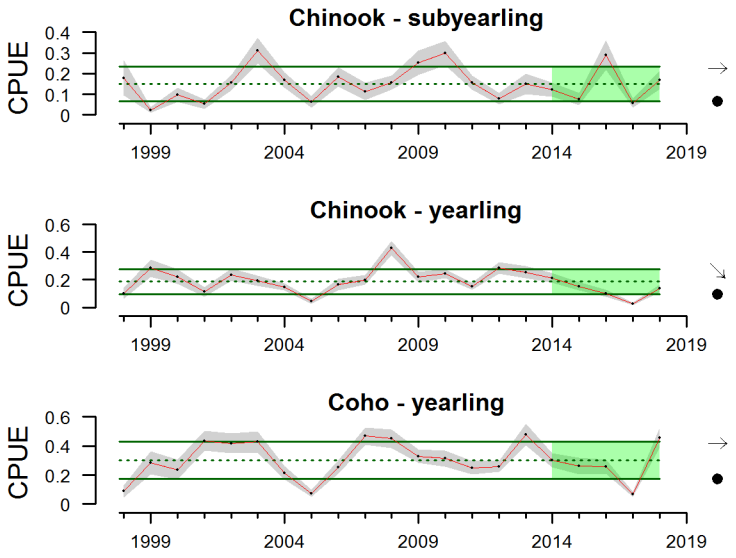

Figure 30. At-sea juvenile Chinook and coho salmon catch ($\log_{10}$[number/km + 1]) in June, 1998–2018, off Washington and Oregon. Lines, colors, and symbols as in Figure 3a. Data for at-sea juvenile salmon provided by B. Burke, NMFS/NWFSC, with additional calculations by C. Morgan, NMFS/NWFSC, OSU. Data are derived from surface trawls taken during NWFSC's Juvenile Salmon and Ocean Ecosystem Survey (JSOES).

Catches of juvenile Chinook and coho salmon in June off the coasts of Washington and Oregon can serve as indicators of survival during their first few weeks at sea. Catches of subyearling and yearling Chinook salmon were close to long-term averages in 2018, one year removed from near-historic lows; catches of yearling coho in 2018 were among the highest observed (Figure 30). These data suggest that some negative impacts of the marine heatwave on salmon survival have subsided. However, as discussed below, other aspects of the ecosystem have not completely returned to normal, suggesting that indirect impacts on survival may still occur. The recent catch trend for yearling Chinook in this region remains negative, while trends for subyearling Chinook and yearling coho salmon are neutral and more variable.

A suite of relevant ecosystem indicators of physical and biological processes suggests some modest improvements in returns of salmon to parts of the Pacific Northwest in 2019. Long-term associations between oceanographic conditions, food web structure, and salmon productivity (Burke et al. 2013, Peterson et al. 2014) support forecasts of returns of Chinook salmon to Bonneville Dam and smolt-to-adult survival of Oregon Coast coho salmon. Indicators of conditions for smolts that went to sea between 2015 and 2018 are generally consistent with below-average returns of Chinook and average returns of coho salmon to these freshwater systems in 2019, as depicted in the "stoplight chart" in Table 1; this includes many indicators in this report, such as PDO, ONI, Copepod Biomass Anomalies and Juvenile Salmon Catch. For comparison, the stoplight chart in last year's report indicated below-average returns in 2018 for fall Chinook and spring Chinook to Bonneville Dam and also below-average returns of coho to Oregon coast streams (Harvey et al. 2018). As we move away from the poor conditions of the marine heatwave and El Niño event, some conditions may be moderating and supporting modest improvements to salmon survival.

Table 1. "Stoplight" table of basin-scale and local/regional conditions for smolt years 2015-2018 and likely adult returns in 2019 for coho and Chinook salmon that inhabit coastal Oregon and Washington waters during their marine phase. Green/circle = favorable conditions, i.e., rank in the top third of all years examined. Yellow/square = intermediate conditions, i.e., rank in the middle third of all years examined. Red/diamond = poor conditions, i.e., rank in the bottom third of all years examined. Courtesy of J. Fisher, S. Zeman, and C. Morgan, NMFS/NWFSC, OSU.

	Smolt year				Adult return outlook	
Scale of indicators	**2015**	**2016**	**2017**	**2018**	**Coho, 2019**	**Chinook, 2019**
Basin-scale						
PDO (May–Sep)	◆	◆	◆	■	■	◆
ONI (Jan–Jun)	◆	◆	■	●	●	■
Local and regional						
SST anomalies	◆	◆	●	◆	◆	●
Deep water temperature	◆	■	◆	◆	◆	◆
Deep water salinity	◆	■	●	●	●	●
Copepod biodiversity	◆	◆	◆	■	■	◆
Northern copepod anomaly	◆	◆	◆	●	●	◆
Biological spring transition	◆	◆	◆	◆	◆	◆
Winter ichthyoplankton biomass	●	●	●	●	●	●
Winter ichthyoplankton community	◆	◆	◆	◆	◆	◆
Juvenile Chinook catch (Jun)	■	◆	◆	■	■	◆
Juvenile coho catch (Jun)	■	■	◆	●	●	◆

A quantitative model related to the stoplight chart (Table 1) also predicts a reasonable probability of modest increases in returns of Fall Chinook and coho in 2019 relative to 2018, but comparable returns of Spring Chinook. In this analysis, annual Chinook salmon counts at Bonneville Dam (Figure 31, top and middle) and Oregon coast coho smolt-to-adult survival (Figure 31, bottom) over the last two decades are regressed against the aggregate mean ranking of indicators in the stoplight table, with 1-year lag for coho and 2-year lag for Chinook. The highest ranking years at the left tend to produce the highest returns and survival. The 2017 stoplight indicators had a relatively low mean rank of 14.5, which would predict relatively low counts of 101,500 Spring and 277,400 Fall Chinook salmon at Bonneville Dam in 2019 (Figure 31, top and middle panels, solid arrows). The 2018 stoplight indicators had a higher mean rank of 11.6, which would predict smolt-to-adult survival of 2.2% for Oregon coast coho in 2019 (Figure 31, bottom, solid arrow). A stoplight indicator ranking of 11.6 in 2018 also corresponds to 2020 Bonneville counts of 127,100 Spring Chinook and 356,800 Fall Chinook (Figure 31, top and middle, dashed arrows). The relationships of past salmon returns to stoplight means explain between 32% (coho) and 55% (Fall Chinook) of variance. This is a fairly simple analysis, however, given that each indicator in the stoplight table is given equal weight, which is a tenuous assumption given both the differences in functional importance among different indicators and the high degree of correlation between some indicators.

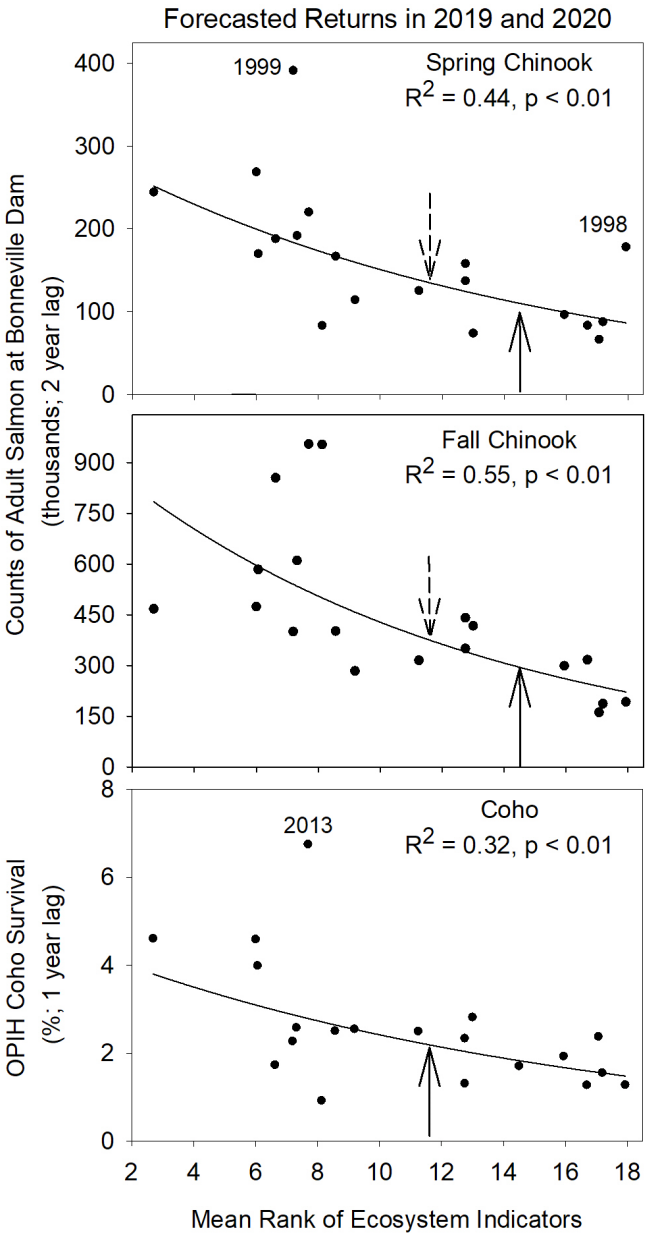

Figure 31. Salmon returns versus the mean rank of ecosystem "stoplight" indicators from Table 1. Arrows show the forecasted returns of Chinook salmon to Bonneville Dam in 2019 (solid) and 2020 (dashed), and of coho salmon to Oregon coast streams in 2019 (solid). Data courtesy of B. Burke, NMFS/NWFSC; "stoplight" indicator table courtesy of J. Fisher, S. Zeman, and C. Morgan, NMFS/NWFSC, OSU.

To address these caveats, we include a more robust quantitative analysis that uses an expanded set of ocean indicators plus principal components analysis and dynamic linear modeling to produce salmon forecasts for the same systems. The principal components analysis essentially is used for weighted averaging of the ocean indicators, reducing the total number of indicators while retaining the bulk of the information from them. The dynamic linear modeling technique relates salmon returns to the principal components of the indicator data, and the approach used here also incorporates dynamic information from sibling regression modeling. The model fits very well to data for Spring Chinook, Fall Chinook and coho salmon at the broad scales of the Columbia River and the Oregon coast (Figure 32). Forecasts with 95% confidence intervals suggest 2019 Bonneville counts of Spring Chinook salmon that are similar to 2018 (Figure 32, top), and potential increases of Fall Chinook at Bonneville and coho in the Oregon coast area (Figure 32, middle and bottom). Although these analyses represent a general description of ocean conditions, we must acknowledge that the importance of any particular indicator will vary among salmon species/runs. NOAA scientists and partners are working toward stock-specific salmon forecasts by using methods that can optimally weight the indicators for each response variable in which we are interested (Burke et al. 2013).

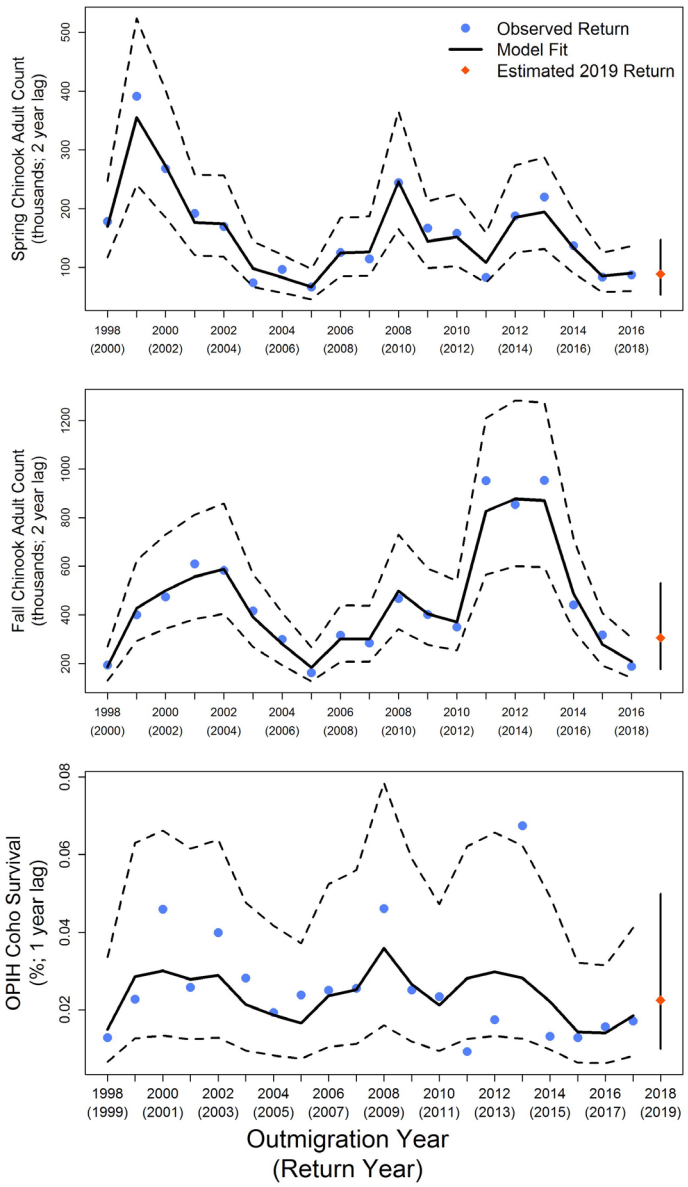

Figure 32. Time series of observed spring Chinook salmon adult counts (top), fall Chinook salmon adult counts (middle), and coho salmon smolt-to-adult survival (bottom) by out-migration year. In each plot, the dark line represents the model fit and lighter lines represent 95% confidence intervals. Forecasts were created from a DLM (Dynamic Linear Model) with log of sibling counts (for the Chinook models only) and first principal component of ocean indicators as predictor variables. Courtesy of B. Burke, NMFS/NWFSC.

3.6. Groundfish Stock Abundance and Community Structure

The CCIEA team regularly presents the status of groundfish biomass and fishing pressure based on the most recent stock assessments. Because only one groundfish stock assessment (Pacific hake) was updated in 2018 and was relatively unchanged, this year's groundfish stock indicators are identical to last year's report (Harvey et al. 2018). All groundfish assessed since 2007 were above biomass limit reference points (LRPs); thus, no stocks were considered "overfished" (Figure 33, x-axis), although previously overfished yelloweye rockfish (*Sebastes ruberrimus*) and cowcod (*S. levis*) were still rebuilding toward target reference points. "Overfishing" occurs when catches exceed overfishing limits (OFLs), but not all stocks are managed by OFLs. For summary purposes, our best alternative is to compare fishing rates to proxy rates that are based on a stock's spawner potential ratio (SPR; Figure 33, y-axis). Washington and California stocks of black rockfish (*S. melanops*) and the California stock of China rockfish (*S. nebulosus*) were being fished above the SPR proxy in their most recent assessments from 2015. These three stocks' fishing rates appear to be over the targets due to recent changes in how the targets are calculated in the assessments, not because of changes in management or fishery practices. Because many groundfish stock assessments are being done or updated in 2019, this summary of groundfish population status should change broadly next year.

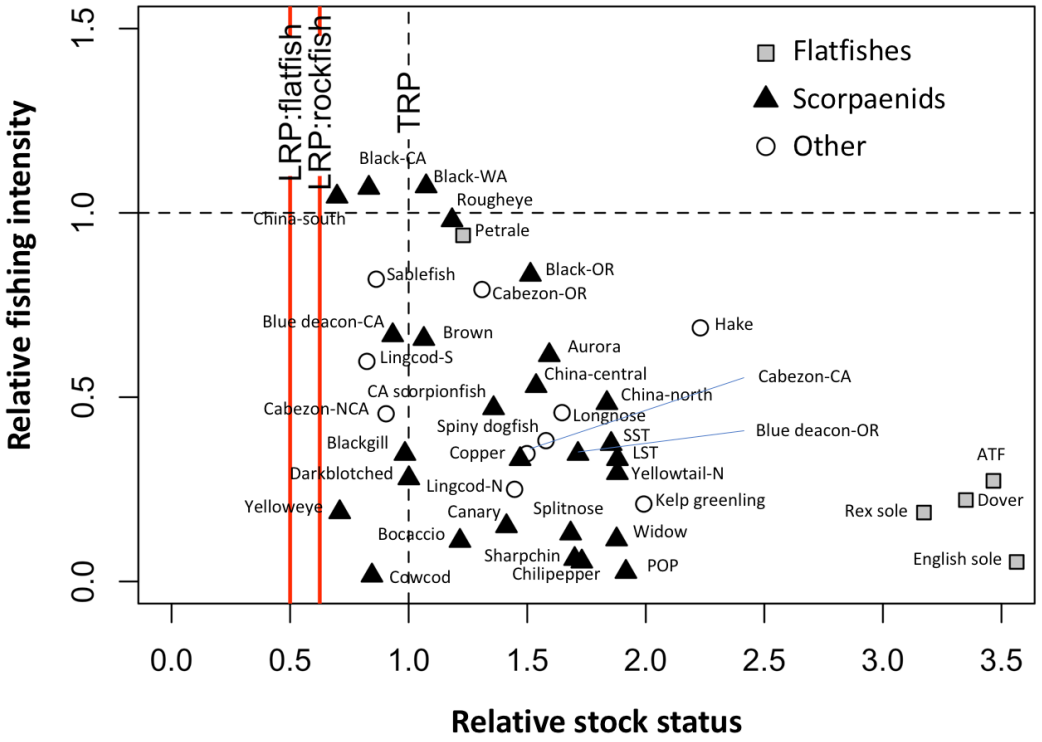

Figure 33. Stock status of CCE groundfish. X-axis: Relative stock status is the ratio of spawning output (in millions of eggs) of the last to the first years in the assessment. Y-axis: Relative fishing intensity uses the Spawner Potential Ratio (SPR) and is defined as (1-SPR)/1-(SPRMSY proxy), where the SPRMSY proxy is stock specific. The horizontal line is the fishing intensity rate reference; above the line would be above the reference level. Vertical lines are the biomass target reference points (TRP; dashed line) and limit reference points (LRP; solid lines); left of this line indicates overfished status. Symbols indicate taxonomic group. All points represent values from the most recent PFMC-adopted stock assessments. Groundfish stock status data were provided by J. Cope, NMFS/NWFSC, and were derived from NMFS stock assessments.

As noted above in Regional Forage Availability, YOY rockfish were highly abundant in the central CCE in 2013–17, and results from other NOAA surveys also revealed large numbers of pelagic and post-settled juvenile rockfish along the Washington coast in 2016. Given the warm and unproductive conditions of 2014–16, these findings ran counter to what we expected from conceptual models linking climate and productivity conditions to groundfish populations. The apparent mechanism for this surge in YOY rockfish was oceanographic conditions, particularly the presence of upwelled pockets of source water that was sufficiently cool, oxygenated, and fresh, all of which provided favorable conditions for adult female rockfish that were bearing larvae in the northern portion of the CCE (Schroeder et al. 2019). As of 2018, rockfish in these cohorts likely had not grown large enough to have been caught in bottom trawl surveys conducted by NOAA Fisheries or to have recruited into fisheries; thus, we will have to wait to determine how groundfish populations respond long-term to the recent climate anomalies.

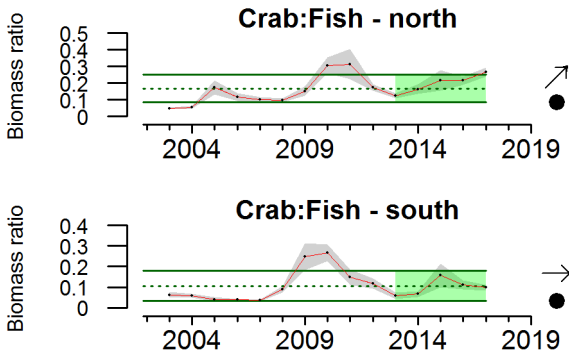

Figure 34. Ratio of crab biomass to finfish biomass for the NWFSC West Coast Groundfish Bottom Trawl Survey, 2003–17. Lines, colors, and symbols as in Figure 3a.

We are also tracking the abundance of groundfish relative to Dungeness and Tanner crabs (*Chionoecetes* spp.) as a metric of seafloor community structure and trophic status. This ratio may also relate to opportunities for vessels to participate in different fisheries. Data are area-weighted mean crab:finfish biomass ratios from NMFS trawl survey sites north and south of Cape Mendocino (Figure 34). The ratio has varied by region and time; in the north, the crab:finfish biomass ratio has been increasing steadily since 2013 and is approaching levels last seen in 2010–11. In contrast, the ratio in the south peaked in 2010, a year earlier than in the north, then declined steadily until 2013; since then, it has mostly varied around the long-term average with no significant trend between 2013 and 2017.

3.7. Highly Migratory Species

Biomass and recruitment patterns for highly migratory species (HMS), including several stocks managed by the PFMC, are derived from the most recent assessments of key HMS target stocks. Here, we present recent averages and trends of biomass and recruitment as quad plots (Figure 35); time series for these indicators are found in Appendix I of Harvey et al. (2019), mostly derived from stock assessments conducted from 2015–18. Average biomass of two stocks (eastern Pacific swordfish [*Xiphias gladius*] and skipjack [*Katsuwonus pelamis*]) over the most recent five years was >1 SD above the long-term mean, while blue marlin (*Makaira mazara*) and bigeye tuna (*Thunnus obesus*) were >1 SD below their long-term means (Figure 35, left). Bigeye tuna, bluefin tuna (*T. orientalis*), and blue marlin biomasses appeared to be near historic lows. Only bluefin tuna are thought to be overfished and experiencing overfishing at the scale of their full range, although uncertainty exists for other stocks, particularly bigeye tuna (see Appendix I of Harvey et al. 2019). Biomass trends were neutral for all species except skipjack, which were increasing. Recruitment indicators varied widely: recruitment appears to be increasing for skipjack, albacore (*Thunnus alalunga*), and yellowfin tuna (*T. albacares*) and neutral for other stocks (Figure 35, right). There was an apparent increase in age-0 bluefin in 2016 (Appendix I of Harvey et al. 2019). These trends generally reflect pan-Pacific changes in biomass and recruitment for these HMS species, not trends in their availability to fishers in the CCE, which represents a small portion of their total range. In future CCIEA reports, we hope to add indicators that are related to the dynamics and drivers of HMS ecology and distribution in the CCE.

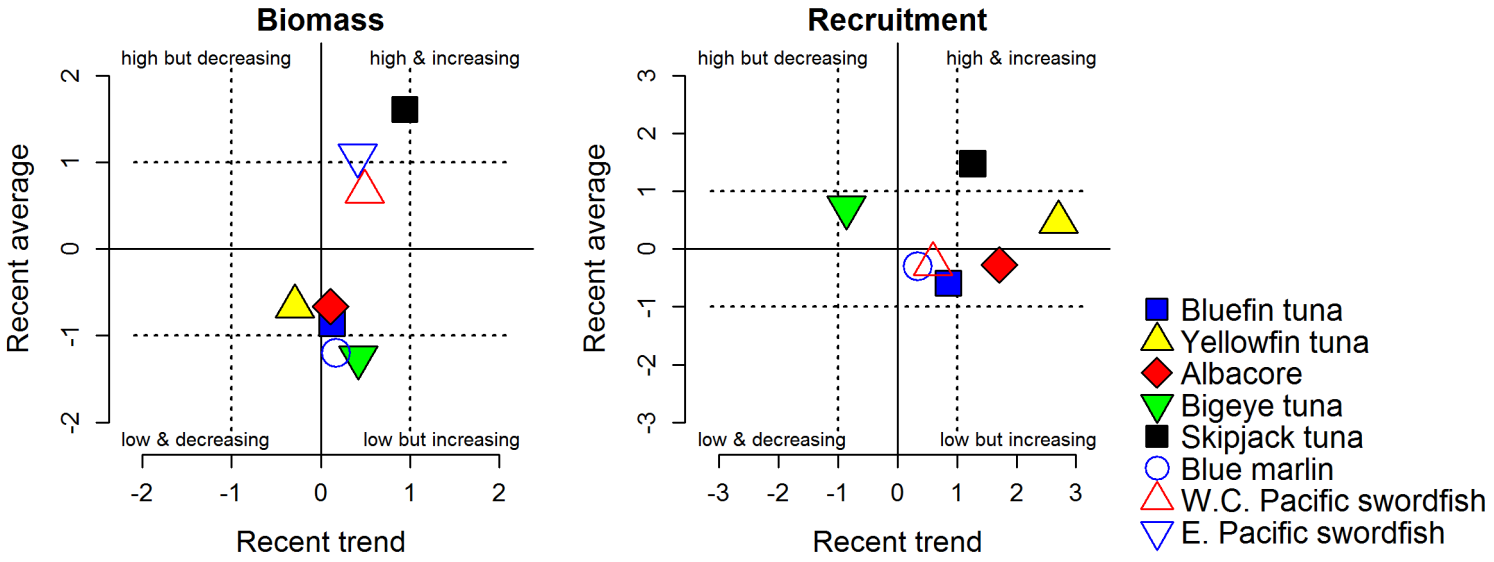

Figure 35. Recent (5-year) trend and average of biomass and recruitment for highly migratory species (HMS) in the CCE from the 2014–18 stock assessments. Data are total biomass for swordfish, relative biomass for skipjack tuna, spawning biomass for bluefin tuna, and female spawning biomass for all other species. Lines and symbols as in Figure 3c. Highly migratory species data provided by B. Muhling, NMFS/SWFSC, and D. Tommasi, NMFS/SWFSC, UCSC. Data are derived from stock assessment reports for the International Scientific Committee for Tuna and Tuna-like Species in the North Pacific Ocean (ISC; http://isc.fra.go.jp/reports/stock_assessments.html) or the Inter-American Tropical Tuna Commission (IATTC; https://www.iattc.org/PublicationsENG.htm).

3.8. Marine Mammals

3.8.1. Sea lion production

California sea lions are permanent residents of the CCE, breeding in the California Channel Islands and feeding throughout the CCE in coastal and offshore habitats. They are also indicators of prey availability in the central and southern CCE (Melin et al. 2012). Two indices are particularly sensitive measures of prey availability to California sea lions: pup production and pup growth during the period of maternal nutritional dependence. Sea lion pup count at San Miguel Island is a result of successful pregnancies, and relates to prey availability and nutritional status for adult females from October to June. Pup growth from birth to age seven months is related to prey availability to adult females during lactation from June to February.

In 2018, California sea lion pup births at San Miguel Island were about 1 SD above the long-term mean for the second consecutive year, representing a sharp increase from pup counts in 2015-16 and leading to an overall increasing short-term trend (Figure 36, top). Furthermore, pup growth rates for the 2016, 2017 and 2018 cohorts were at or above the long-term average (Figure 36, bottom). These indicators represent a substantial improvement in feeding conditions for the San Miguel colony relative cohorts in 2012–15; those cohorts experienced unusually high stranding rates associated with poor foraging conditions for nursing females in the central and southern CCE during the period of pup nutritional dependence (Wells et al. 2013, Leising et al. 2014, Leising et al. 2015, McClatchie et al. 2016). The improved growth of pups in the recent cohorts indicates that nursing females experienced better foraging conditions during 2016–18, coinciding with higher frequencies of anchovy and hake in their diets, compared to a diet rich in juvenile rockfish and market squid during the periods of poor survival.

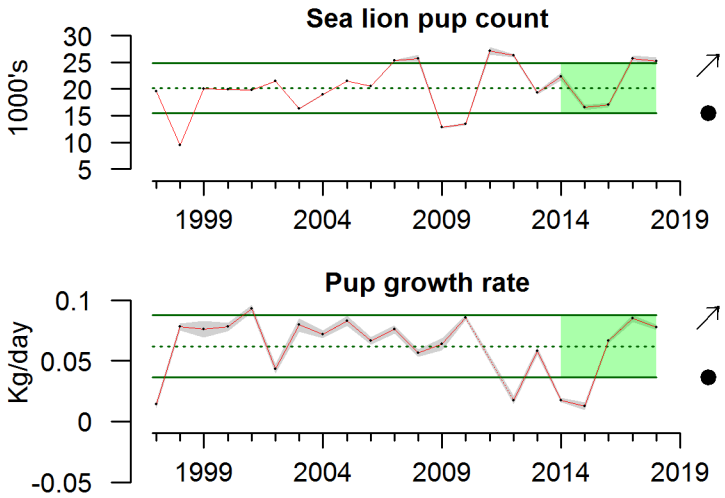

Figure 36. California sea lion pup counts, and estimated mean daily growth rate of female pups from 4–7 months of age on San Miguel Island for the 1997–2018 cohorts. Lines, colors, and symbols as in Figure 3a. California sea lion data were provided by S. Melin, NMFS/AFSC.

3.8.2. Whale entanglement

Starting with the anomalous warming of the CCE in 2014–16, observations of baleen whales entangled in fishing gear have occurred at levels far greater than in the preceding decade. Confirmed whale entanglements on the U.S. West Coast are shown in Figure 37 (derived from NOAA 2019). A "confirmed" observation represents a unique case of an entangled whale, including resightings, where the documentation provided to the NOAA Fisheries's West Coast Region's Marine Mammal Stranding Response Program is complete or compelling enough for NOAA Fisheries to conclude that a whale was observed entangled in some sort of human-made material. Confirmed entanglements were most numerous in 2015 (n = 50) and 2016 (n = 48), with the majority involving humpback whales (*Megaptera novaeanglidae*). Confirmed entanglements declined to 31 in 2017, but then increased to 46 in 2018. These annual entanglement rates are substantially higher than the annual average of about 10 confirmed entanglements per year in 2000–13. Of the 46 confirmed entanglements in 2018, 34 were humpback whales, 11 were gray whales (*Eschrichtius robustus*), and one was a fin whale (*Balaenoptera physalus*) (Figure 37). No confirmed entanglements of blue whales (*Balaenoptera musculus*) occurred along the West Coast in 2018.

The majority of entanglements occurred in gear that could not be identified visually. Of the portion that could be identified by visible tags or markings, most were pots and traps targeting Dungeness crab, along with a small number of traps targeting spot prawns (*Pandalus platyceros*) (NOAA 2019). There were no confirmed entanglements in fixed sablefish gear in 2018, unlike 2016 and 2017 when one confirmed entanglement in each year involved fixed sablefish gear. Gillnets have been observed as entangling gear each year since 2015. As in other years, most observations of entangled whales occurred in California waters, although confirmed reports were more widely distributed in 2018 than in other recent years. Importantly, the time and place of the observation does not necessarily coincide with the time and place of the actual entanglement event (NOAA 2019).

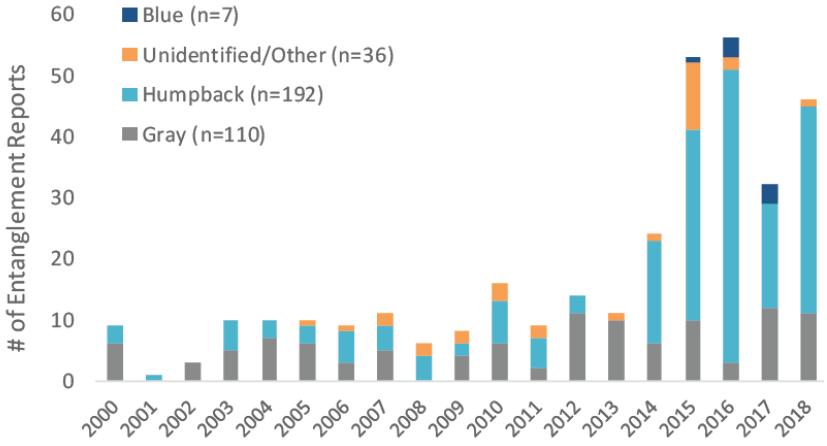

Figure 37. Confirmed numbers of whales (by species) reported as entangled in fishing gear and other sources along the U.S. West Coast from 2000–18. Whale entanglement data provided by D. Lawson, NMFS/WCR.

Many interacting factors could be causing the increased numbers of observed and reported entanglements, including shifts in oceanographic conditions and prey fields that brought the whales closer to shore, as well as changes in distribution and timing of fishing effort. Increased public awareness to look for and properly report entangled whales may also be playing a role. NOAA Fisheries's West Coast Region will continue to follow this issue as conditions in the CCE change, and the CCIEA team is collaborating with researchers from NOAA, other agencies, and academic partners on analyses of various biological, environmental, and anthropogenic factors that affect the dynamics of entanglement risk.

3.9. Seabirds

The seabird indicators (at-sea densities, productivity, diet, and mortality) constitute a portfolio of metrics that reflect population health and condition of seabirds as well as links to lower trophic levels and other conditions in the California Current Ecosystem. To highlight the status of different seabird guilds and relationships to their marine environment, multiple focal species are monitored throughout the CCE. The species we report on in the sections below represent a breadth of foraging strategies, life histories, and spatial ranges.

3.9.1. At-sea densities

Seabird densities on the water during the breeding season can track marine environmental conditions and may reflect regional production and availability of forage. Data from this indicator type can establish habitat use and may be used to detect and track seabird population movements or increases/declines as they relate to ecosystem change. We monitor and report on at-sea densities of three focal species in the northern, central, and southern regions of the CCE. Sooty shearwaters (*Ardenna grisea*) migrate to the CCE from the southern hemisphere in spring and summer to forage near the shelf break on a variety of small fish, squid and zooplankton. Common murres (*Uria aalge*) and Cassin's auklets (*Ptychoramphus aleuticus*) are resident species that feed primarily over the shelf; Cassin's auklets prey mainly on zooplankton and small fish, while common murres target a variety of pelagic fish (see Seabird diets).

At-sea density patterns varied within and across seabird species among the three regions of the CCE. Sooty shearwater at-sea density anomalies have undergone significant short-term declines in both the northern (NCC) and central (CCC) regions from 2014–18 and no short-term trend in the southern (SCC) region, where sooty shearwater densities have been relatively high over the past five years (Figure 38). The negative trends in the northern and central regions were driven by steep declines after 2015, although 2018 densities of sooty shearwaters rebounded and were above the long-term average in all three regions. Cassin's auklet at-sea density anomalies declined in the northern region from 2014–18 but showed no recent trends in the other regions, and recent average densities have been within 1 SD of the long-term regional means (Figure 38). The common murre at-sea density anomaly trend was neutral over the last five years in the northern CCE, but showed significant short-term increases in the central and southern regions (Figure 38). A record positive anomaly in 2018 and another strongly positive anomaly in 2015 resulted in above-average

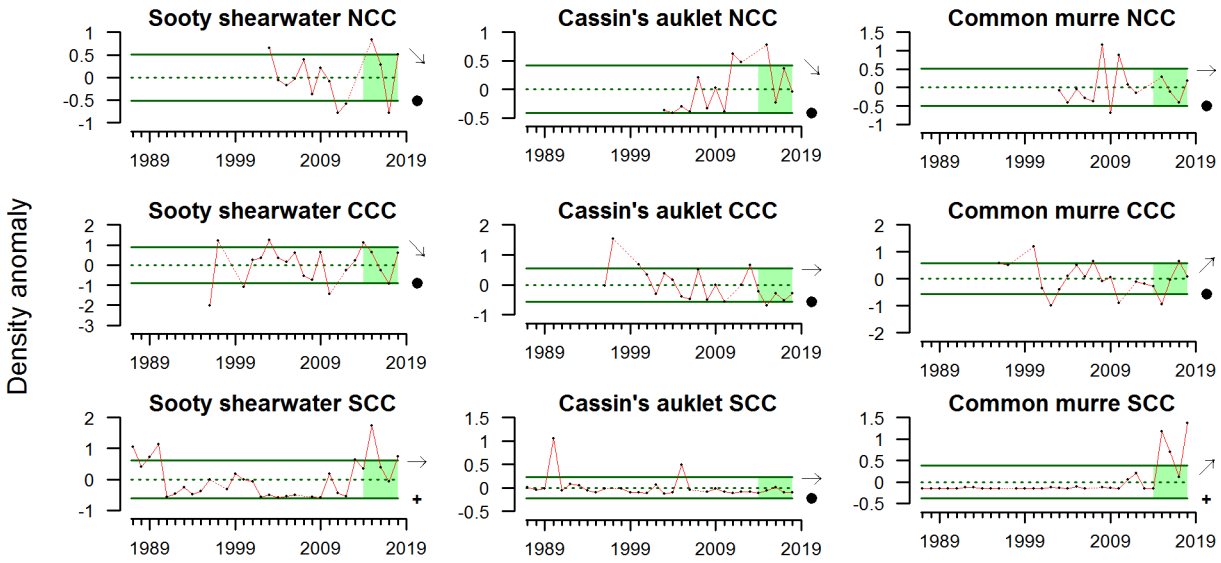

Figure 38. At-sea density anomalies of three seabird species during the spring/summer in three regions of the CCE through 2018. NCC = northern California Current, data from 2003–18; CCC = central California Current, data from 1996–2018; SCC = southern California Current, data from 1987–2018. Geographic regions correspond to Figure 4c. Lines, colors, and symbols as in Figure 3a. Seabird abundance data from NCC (collected on the NWFSC Salmon Ocean Ecology Survey) courtesy of J. Zamon, NMFS/NWFSC. Seabird abundance data from CCC (collected on SWFSC Rockfish Recruitment and Ecosystem Assessment Survey) and SCC (collected on CalCOFI surveys) courtesy of W. Sydeman, Farallon Institute. NCC data are from June surveys, CCC data are from May surveys, and SCC data are from April surveys, as no seabird data were collected during the summer survey.

common murre densities in the south, relative to the long-term mean (Figure 38). In the northern region, both sooty shearwaters and common murres were aggregated on a few transects at the Washington/Oregon border, likely attracted to forage fishes, squid, or krill abundant near the Columbia River mouth. In the southern region, it remains to be seen if sooty shearwaters and common murres will continue recent upticks in observed densities relative to the 1990s and much of the 2000s.

3.9.2. Seabird diets

Seabird diet composition during the breeding season tracks marine environmental conditions and often reflects production and availability of forage within regions. We monitor and report on five focal species in the northern and central regions of the CCE. Rhinoceros auklets (*Cerorhinca monocerata*) forage primarily on pelagic fishes in shallow waters over the continental shelf, generally within 50 km of breeding colonies, and they return to the colony after dusk to deliver multiple whole fish to their chicks. Common murres forage primarily on pelagic fishes in deeper waters over the shelf and near the shelf break, generally within 80 km of breeding colonies, and they return to the colony during daylight hours to deliver single whole fish to their chicks. Cassin's auklets forage primarily on zooplankton in shallow water over the shelf break, generally within 30 km of breeding

colonies; they forage at day and night and return to the colony at night to feed chicks regurgitated crustaceans from their throat pouch. Brandt's cormorants (*Phalacrocorax penicillatus*) forage primarily on pelagic and benthic fishes in waters over the shelf, generally within 20 km of breeding colonies, and they return to the colony during the day to deliver regurgitated fish to their chicks. Pigeon guillemots (*Cepphus columba*) forage primarily on small benthic and pelagic fish over the shelf, generally within 10 km of breeding colonies, and they return to the colony during the day to deliver a single fish to their chicks.

The proportion of anchovies in the diet of rhinoceros auklets provisioning chicks at Destruction Island (DI), off the Washington coast in the northern CCE, was below average in 2018 (Figure 39). The proportion of herring in DI rhinoceros auklet diet was above average in 2018, continuing to be the mirror image of anchovy proportion in the diet. The proportion of rockfish in DI rhinoceros auklet diet continued to be low since it peaked in 2016. The proportion of smelts (Osmeridae) in DI rhinoceros auklet diet was the highest that has been recorded, and showed a significant positive short-term trend.

The proportion of smelts in the diet of common murres provisioning chicks at Yaquina Head (YH), along the Oregon coast in the northern CCE, was below average in 2018, after six years of above-average values, and showed a significant negative short-term trend (Figure 40). The proportions of herring, sardine and Pacific sandlance

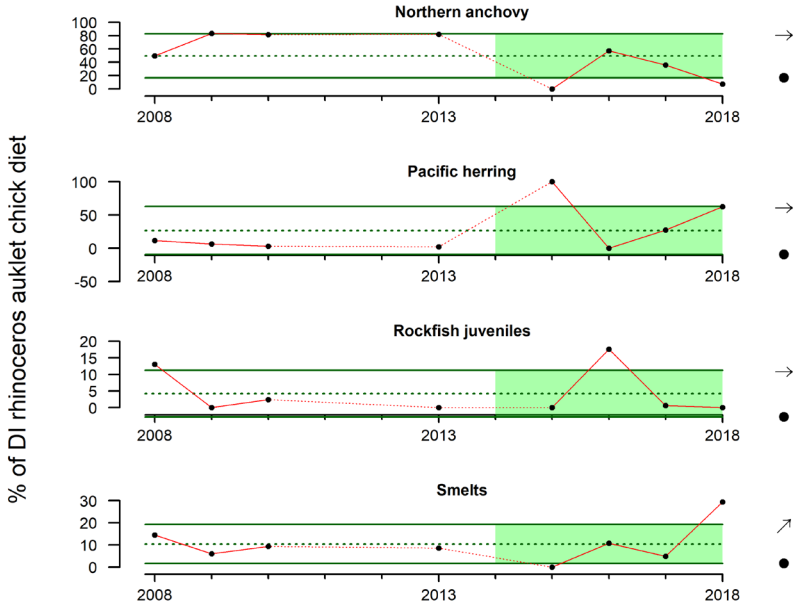

Figure 39. Rhinoceros auklet chick diets at Destruction Island (DI) through 2018. Data courtesy of the Washington Rhinoceros Auklet Ecology Project (scott.pearson@dfw.wa.gov). Lines, colors, and symbols as in Figure 3a.

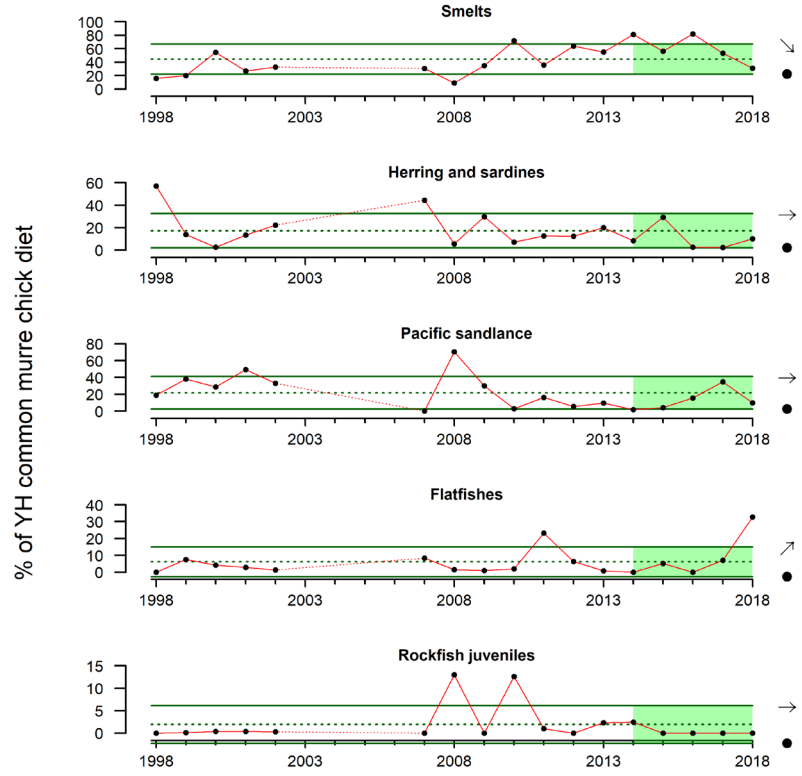

Figure 40. Common murre chick diets at Yaquina Head (YH) through 2018. Data provided by the Yaquina Head Seabird Colony Monitoring Project (rachael.orben@oregonstate.edu). Lines, colors, and symbols as in Figure 3a.

(*Ammodytes hexapterus*) in the YH murre diet were below average in 2018. The proportion of flatfishes in the YH murre diet in 2018 was the highest in the time series and showed a significant positive short-term trend. The proportion of rockfish in the YH murre diet in 2018 was zero for the fourth straight year, considerably lower than peaks in 2008 and 2010.

At Año Neuvo Island (ANI) off central California in the central CCE, the proportion of anchovy in the diet of rhinoceros auklets provisioning chicks was well above average in 2018, but showed no significant short-term trend due to other recent years with high proportions of anchovy as well (Figure 41). The proportion of YOY rockfish in the ANI rhinoceros auklet diet was below average in 2018 but has been highly variable over the last decade, dampening any short-term trend. The proportion of squid in the ANI rhinoceros auklet diet was slightly below average in 2018, while Pacific saury (*Cololabis saira*) have been missing from the observed diet since 2012 (Figure 41). Not only did northern anchovy dominate the composition of ANI rhinoceros auklet diet samples in 2018; the size of northern anchovy brought back to rhinoceros auklets chicks at ANI was slightly above average in 2018 and showed a significant short-term trend since below-average anchovy sizes in 2014–16 (Figure 42).

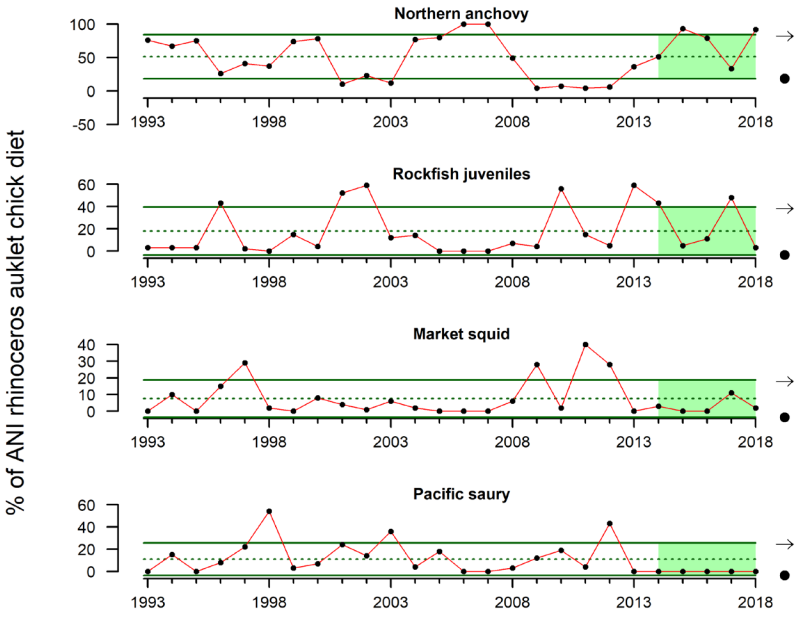

Figure 41. Rhinoceros auklet chick diets at Año Neuvo Island (ANI) through 2018. Data provided by Oikonos/Point Blue Conservation Science (ryan@oikonos.org). Lines, colors, and symbols as in Figure 3a.

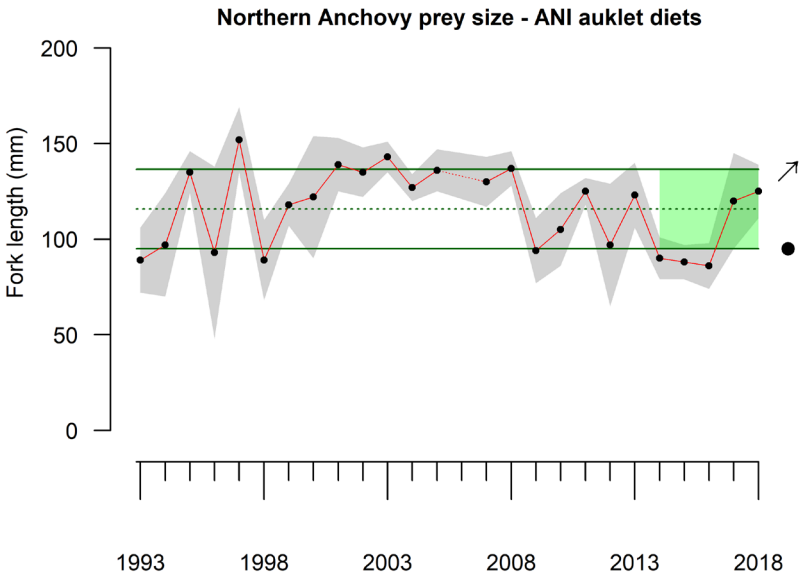

Figure 42. Fork length of northern anchovy brought to rhinoceros auklet chicks at Año Neuvo Island (ANI) through 2018. Data provided by Oikonos/Point Blue Conservation Science (ryan@oikonos.org). Lines, colors, and symbols as in Figure 3a.

In the Central CCE, there are diet trends for several seabirds from Southeast Farallon Island (SEFI), off central California (Figure 43). Among piscivores, there has been a trend of increasing reliance on anchovy and decreasing reliance on juvenile rockfish over the past five years. The proportion of anchovy in the SEFI rhinoceros auklet diet was above average in 2018, while the proportion of rockfish in their diet was well below average in 2018 and showed a significant negative

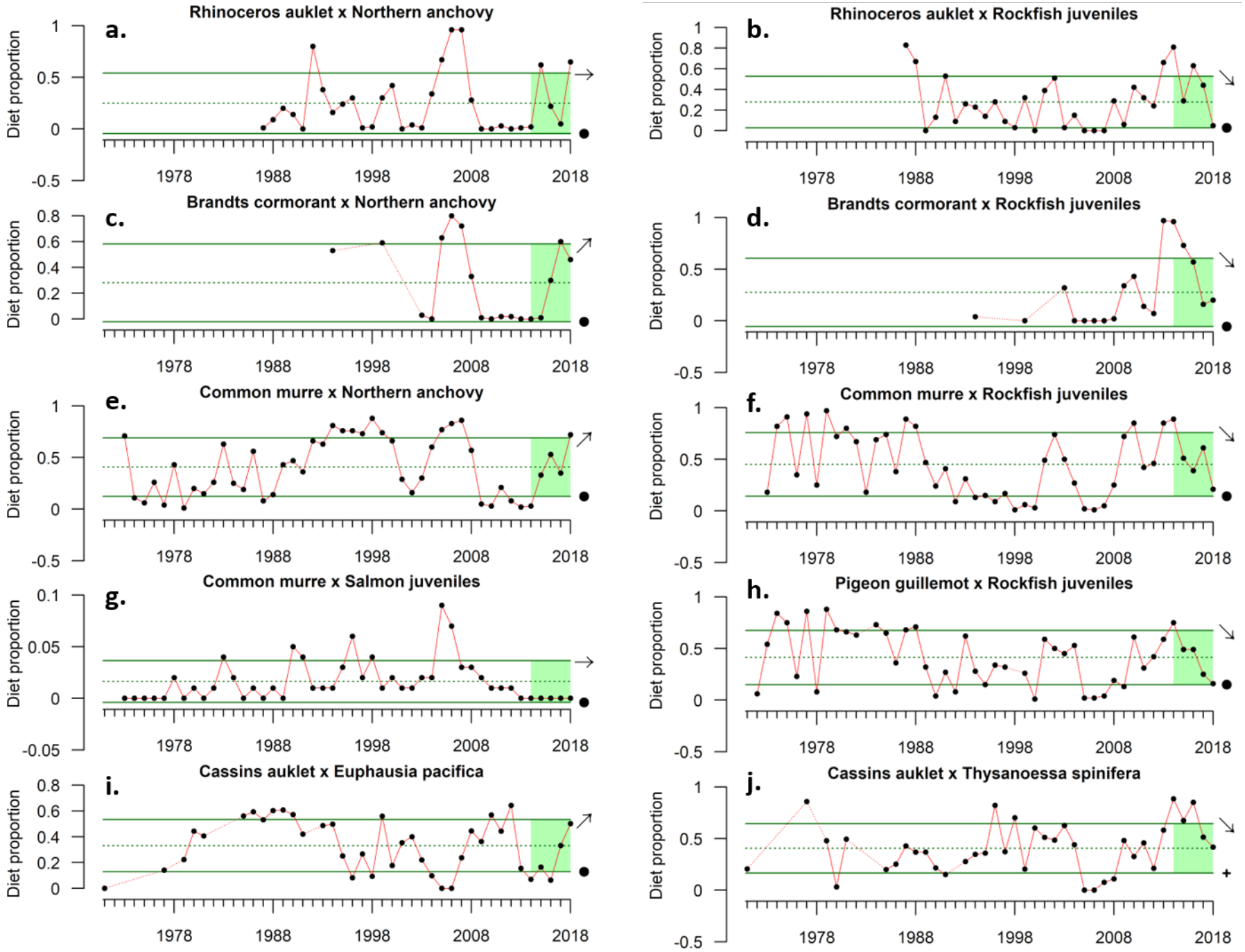

Figure 43. Diet of a–b) rhinoceros auklet, c–d) Brandt's cormorant, e–g) common murre, h) pigeon guillemot, and i–j) Cassin's auklet at Southeast Farallon Island through 2018. Data provided by Point Blue Conservation Science (jjahncke@pointblue.org). Lines, colors, and symbols as in Figure 3a.

short-term trend after peaks in 2014 and 2016 (Figure 43, a-b). The proportion of anchovy in the diet of Brandt's cormorants provisioning chicks on SEFI was above average in 2018 and showed a significant positive short-term trend, while the proportion of rockfish in their diet was close to the long-term average in 2018 but showed a significant negative short-term trend following a peak in 2013–14 (Figure 43, c-d). The proportion of anchovy in the SEFI common murre diet was above average in 2018 and showed a significant positive short-term trend, while the proportion of rockfish in their diet was well below average in 2018 and showed a significant negative short-term trend after peaking in 2014 (Figure 43, e-f). The proportion of salmonids in the SEFI common murre diet was zero in 2018, for the sixth year in a row (Figure 43g). The proportion of rockfish in the diet of SEFI pigeon guillemots was well below average in 2018 and showed a significant negative short-term trend since a 2014 peak (Figure 43h). The diets of Cassin's auklets on SEFI are only current through 2017. The proportion of *Euphausia pacifica* in the diet of SEFI Cassin's auklets was near the average and showed a significant positive short-term trend (Figure 43i), while the proportion of *Thysanoessa spinifera* in the SEFI Cassin's auklet diet was above average but showed a significant negative short-term trend (Figure 43j).

Collectively, these seabird diet indicators likely reflect both the variability of forage community composition and the plasticity or opportunistic nature of predator foraging and diet. While there have been shifts in dominant prey species over time, northern anchovy featured prominently in diets of multiple seabird predators in 2018, particularly in the central California Current, likely tracking availability as indexed by forage indicators (high anchovy and low rockfish) in the central CCE (see Figure 27 in Regional Forage Availability). On Año Nuevo Island, increased productivity of rhinoceros auklets in recent years appears to be tracking the proportion of anchovy in the diet (Jessie Beck, Oikonos, unpublished data).

3.9.3. Seabird population productivity

Seabird population productivity, as measured through variables related to reproductive success, tracks marine environmental conditions and often reflects forage production near breeding colonies. We monitor and report on five focal species on Southeast Farallon Island (SEFI) in the central region of the CCE. Here, productivity anomalies are defined as standardized measures of the annual number of chicks fledged per pair of breeding adults. By this metric, productivity was above average in 2018 for Brandt's cormorant, Cassin's auklet, and rhinoceros auklet breeding on SEFI (Figure 44). The fledgling rate for common murre was average in 2018, while productivity for pigeon guillemot on SEFI was below average in 2018 and showed a significant negative short-term trend. These mixed signals of productivity show that taking advantage of positive foraging conditions and focusing on available anchovy did not ensure success of seabird species across the board.

3.9.4. Seabird mortalities

Seabird mortality can track seabird populations as well as environmental conditions at regional and larger spatial scales. Monitoring beached birds (often by citizen scientists) provides information on the health of seabird populations, ecosystem health, and unusual mortality events. CCIEA reports from the anomalously warm and unproductive years of

2014–16 noted major seabird mortality events in each year. These "wrecks"—exceptional numbers of dead birds washing up on widespread beaches—impacted Cassin's auklets in 2014, common murres in 2015, and rhinoceros auklets in 2016.

In the northern CCE (WA to northern CA), the University of Washington-led Coastal Observation And Seabird Survey Team (COASST) documented beached birds at average to below-average levels for four focal species in 2018 (Figure 45). The Cassin's auklet encounter rate continued at baseline levels in 2018, as it has since the die-off in 2014. The sooty shearwater encounter rate in 2018 was below average, and both the common murre and northern fulmar (*Fulmarus glacialis*) encounter rates were below average in 2018 and showed significant negative short-term trends.

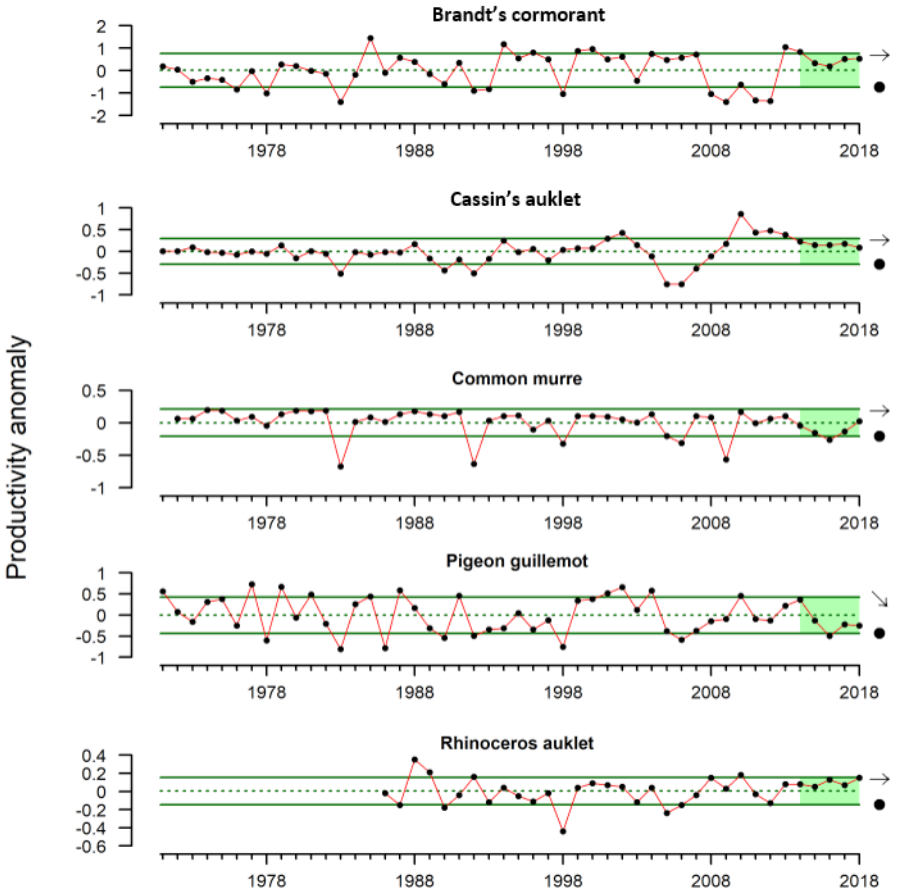

Figure 44. Standardized productivity anomalies (annual productivity, defined as the annual number of chicks fledged per pair of breeding adults, minus the long-term mean) for five seabird species breeding on Southeast Farallon Island through 2018. Data provided by Point Blue Conservation Science (jjahncke@pointblue.org). Lines, colors, and symbols as in Figure 3a.

In the central region of the CCE (Bodega Bay, CA to Point Año Nuevo, CA), the BeachWatch program documented beached birds at average to below average levels for five focal species in 2018 (Figure 46). The Cassin's auklet encounter rate continued at low baseline levels in 2018, as it has since a peak in 2014. The common murre encounter rate was just below average in 2018, and showed a significant negative trend due to the peak in 2015. The sooty shearwater encounter rate was average in 2018; the peak it also experienced in 2015 was not sharp enough to result in a short-term negative trend. The northern fulmar encounter rate was below average in 2018, as it has been since a peak in 2010. The Brandt's cormorant encounter rate was below average in 2018 and showed a significant negative short-term trend.

In another survey of beached seabirds on California beaches from Point Año Nuevo to Malibu, the BeachCOMBERS program documented beached birds at average to below average levels for same five focal species in 2018 (Figure 47). The BeachCOMBERS survey region is divided into three regions: north (Point Año Nuevo to Lopez Point, CA), central (Lopez Point to Rocky Point, CA), and south (Rocky Point to Malibu, CA). The Cassin's auklet encounter rate remained at low baseline levels in 2018 on both northern and central

beaches within the survey region, as they have since a peak in 2014, and showed significant negative short-term trends. Northern fulmar encounter rate on northern survey beaches was below average in 2018, as it has been since a peak in 2013, and showed a significant negative short-term trend. The common murre, sooty shearwater and Brandt's cormorant encounter rates were below average in 2018.

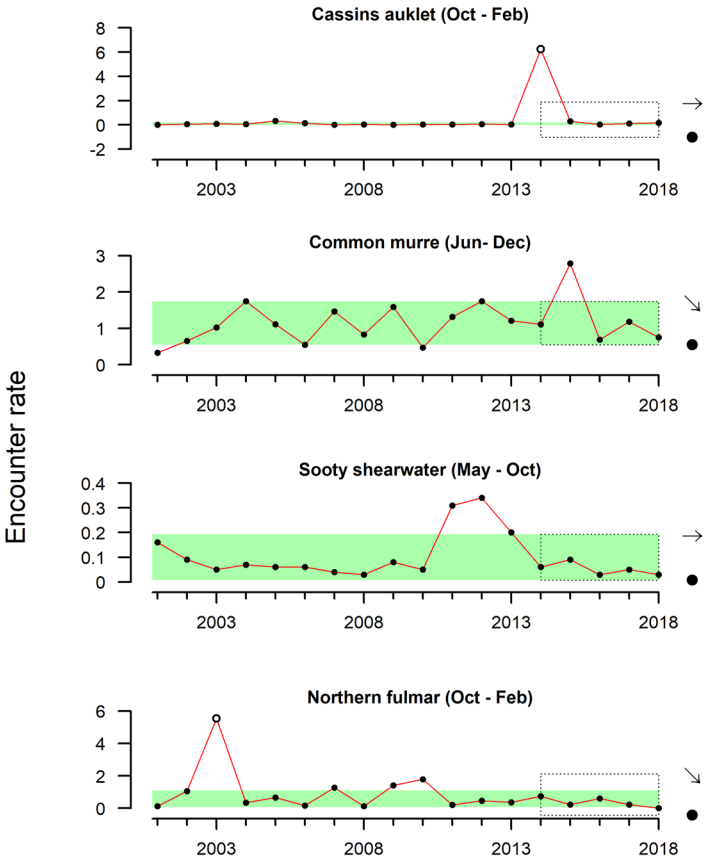

Figure 45. Encounter rate (birds/km) of bird carcasses on beaches from Washington to northern California. The mean and trend of the last five years is evaluated versus the mean and SD of the full time series without outliers (open circles). The green box indicates upper and lower SD of the full time series with outliers removed. The dotted-line box indicates the evaluation period and upper and lower SD of the full time series with the outliers included. Annual data for Cassin's auklet and northern fulmar are calculated through February of the following year. Data provided by the Coastal Observation and Seabird Survey Team (https://depts.washington.edu/coasst/). Lines, colors, and symbols as in Figure 3a.

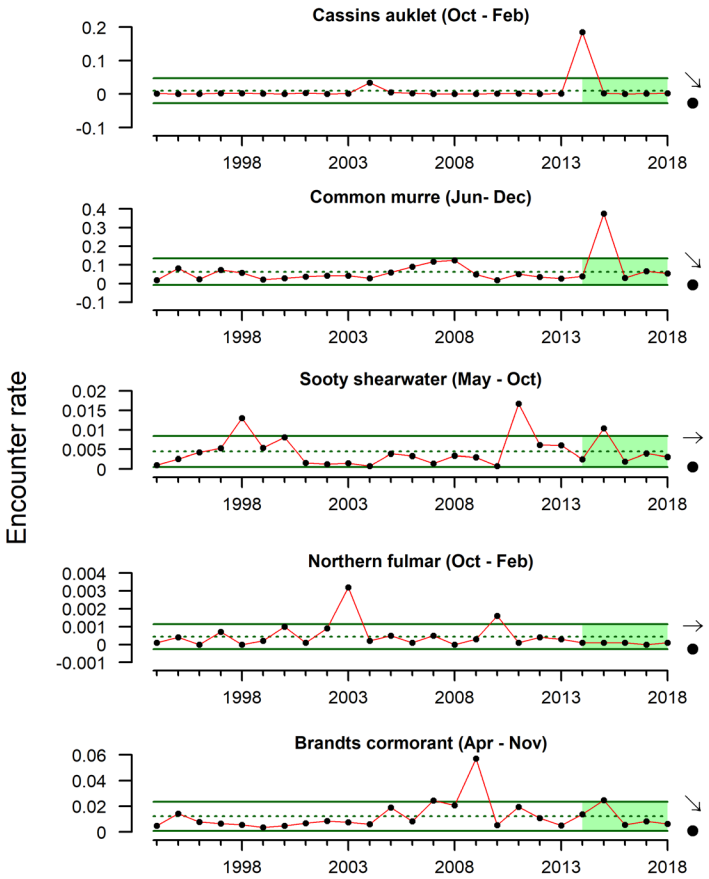

Figure 46. Encounter rate of bird carcasses on beaches in north-central California. Annual data for Cassin's auklet and northern fulmar are calculated through February of the following year. Data provided by BeachWatch (https://farallones.noaa.gov/science/beachwatch.html). Lines, colors, and symbols as in Figure 3a.

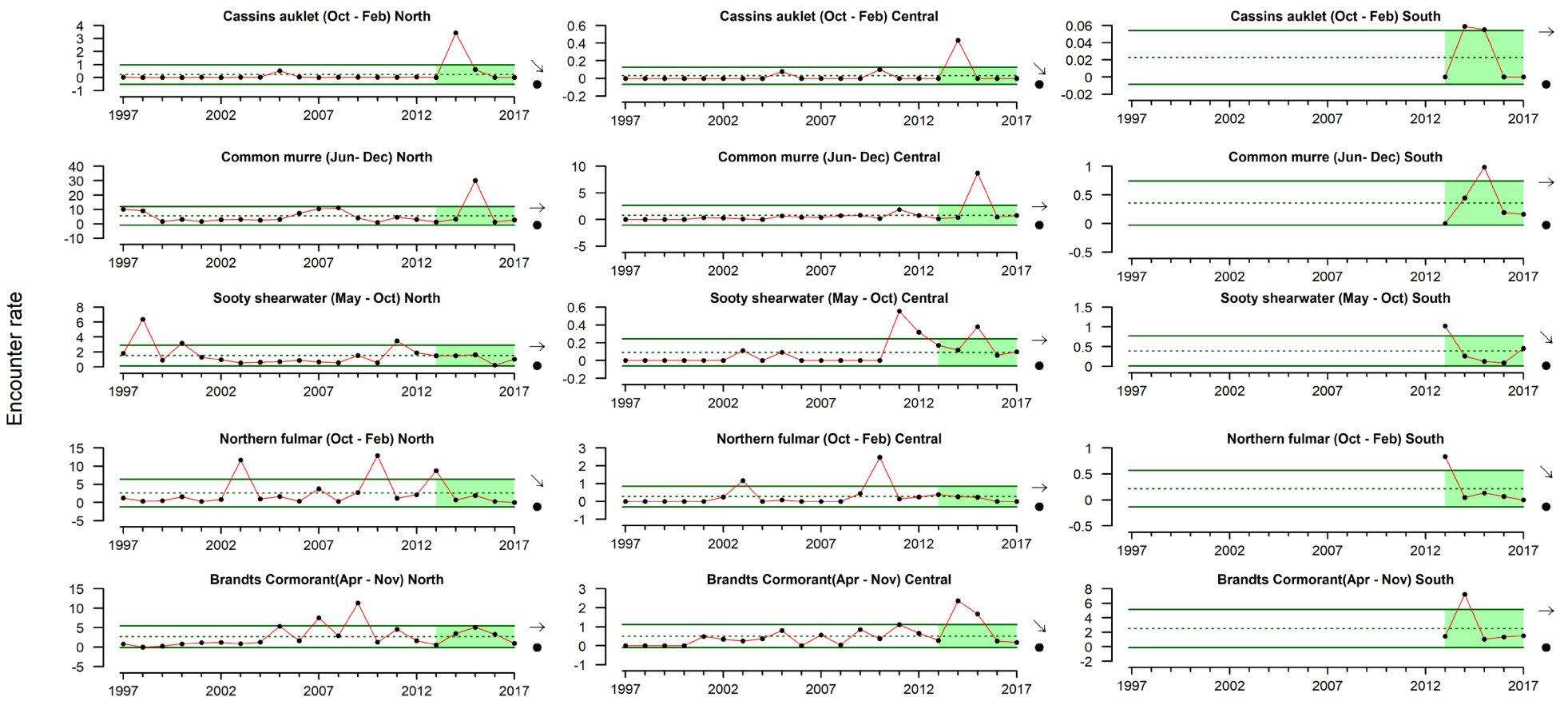

Figure 47. Encounter rate of bird carcasses on beaches from the northern (left), central (center), and southern (right) regions of the the BeachCOMBERS survey area of central-southern California. Annual data for Cassin's auklet and northern fulmar are calculated through February of the following year. Data provided by BeachCOMBERS (https://www.mlml.calstate.edu/beachcombers/about-us/). Lines, colors, and symbols as in Figure 3a.

4. Human Activities

4.1. Coastwide Landings by Major Fisheries

Fishery landings data are current through the end of 2018 (data accessed 03 May 2019). Overall, total commercial landings across the U.S. West Coast have been highly variable over the last five years, driven by low landings totals in 2015 and 2016 coupled with high landings in 2014 and 2017 (Figure 48). Landings of salmon, groundfish (excluding hake), highly migratory species and other species have been relatively constant and near the lower range of historical levels from 2014–18, although landings of groundfish (excluding hake) have increased modestly over the last two years. Landings of Pacific hake and crab have increased, with average hake landings exceeding historical levels by >1 SD over the last five years. Market squid and shrimp landings have decreased, but remained within ±1 SD of historical averages from 2014–2018. Coastal pelagic species (excluding market squid) have remained at historically low levels over the last five years.

Methods for calculating total landings in recreational fisheries have changed recently, leading to shorter comparable time series and different estimates from previous reports. Key components of the recreational fishery such as salmon and Pacific halibut (*Hippoglossus stenolepis*) from all states and HMS species from California are also missing due to inconsistent data (weights vs. numbers of fish and/or across-state methodological differences). Recreational landings coastwide decreased from 2014 to 2018 within historical averages (Figure 48), driven primarily by changes in landings of lingcod (*Ophiodon elongatus*) and Pacific yellowtail (*Seriola lalandi dorsalis*) in California and albacore and black rockfish in Oregon and Washington. Landings for recreationally caught salmon (Chinook and coho) showed no trends and were within historical averages, but landings were at the lower range of historical averages. State-by-state commercial and recreational landings (through 2017 only) are summarized in Appendix K of Harvey et al. (2019).

Total revenue across U.S. West Coast commercial fisheries (adjusted to 2018 dollars) varied near 1 SD above the upper historical average from 2014–18 (Figure 49). This pattern was driven primarily by interactions in the variation of revenue from the Pacific hake, market squid and crab fisheries. Revenue from salmon, groundfish (excluding hake), highly migratory species, other species, Pacific hake, and market squid fisheries showed no significant trends over the last five years of data, and were within ±1 SD of their respective historical averages. Coastal pelagic species revenue was consistently >1 SD below the historical average, while revenue from crab fisheries was >1 SD above its historical average over the last five years. The shrimp fisheries had a steep decrease in revenue from 2014 to 2018, but remained within 1 SD of the long-term average.

4.2. Bottom Trawl Contact with Seafloor

Benthic marine species, communities and habitats can be impacted by geological events (e.g., earthquakes, fractures, and slumping), oceanographic processes (e.g., internal waves, sedimentation, and currents), and human activities (e.g., bottom contact fishing, mining, and dredging). Such disturbances can lead to mortality of vulnerable benthic species and

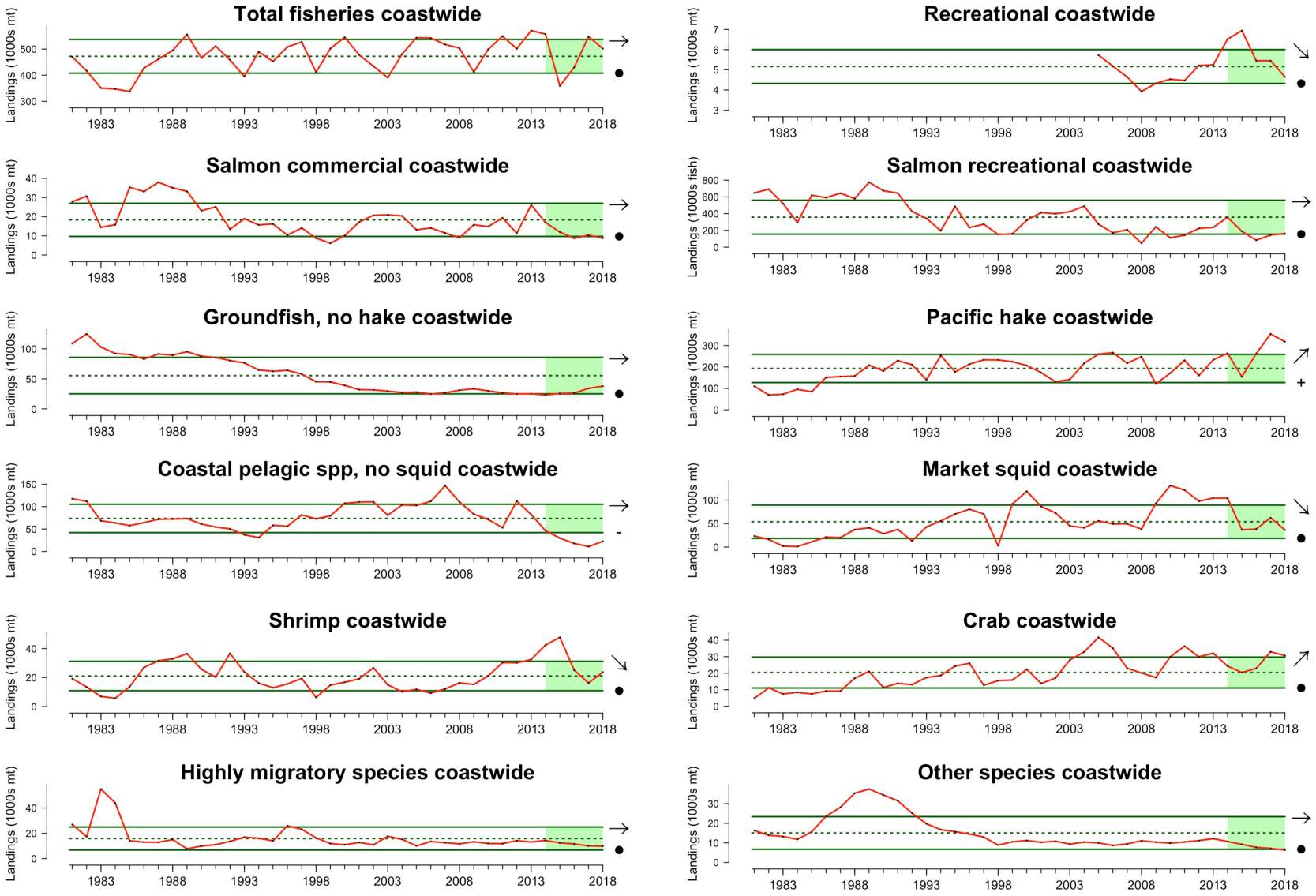

Figure 48. Annual landings of U.S. West Coast commercial (data from PacFIN; http://pacfin.psmfc.org) and recreational (data from RecFin; http://www.recfin.org/) fisheries, including total landings across all fisheries, 1981–2018. Lines, colors, and symbols as in Figure 3a.

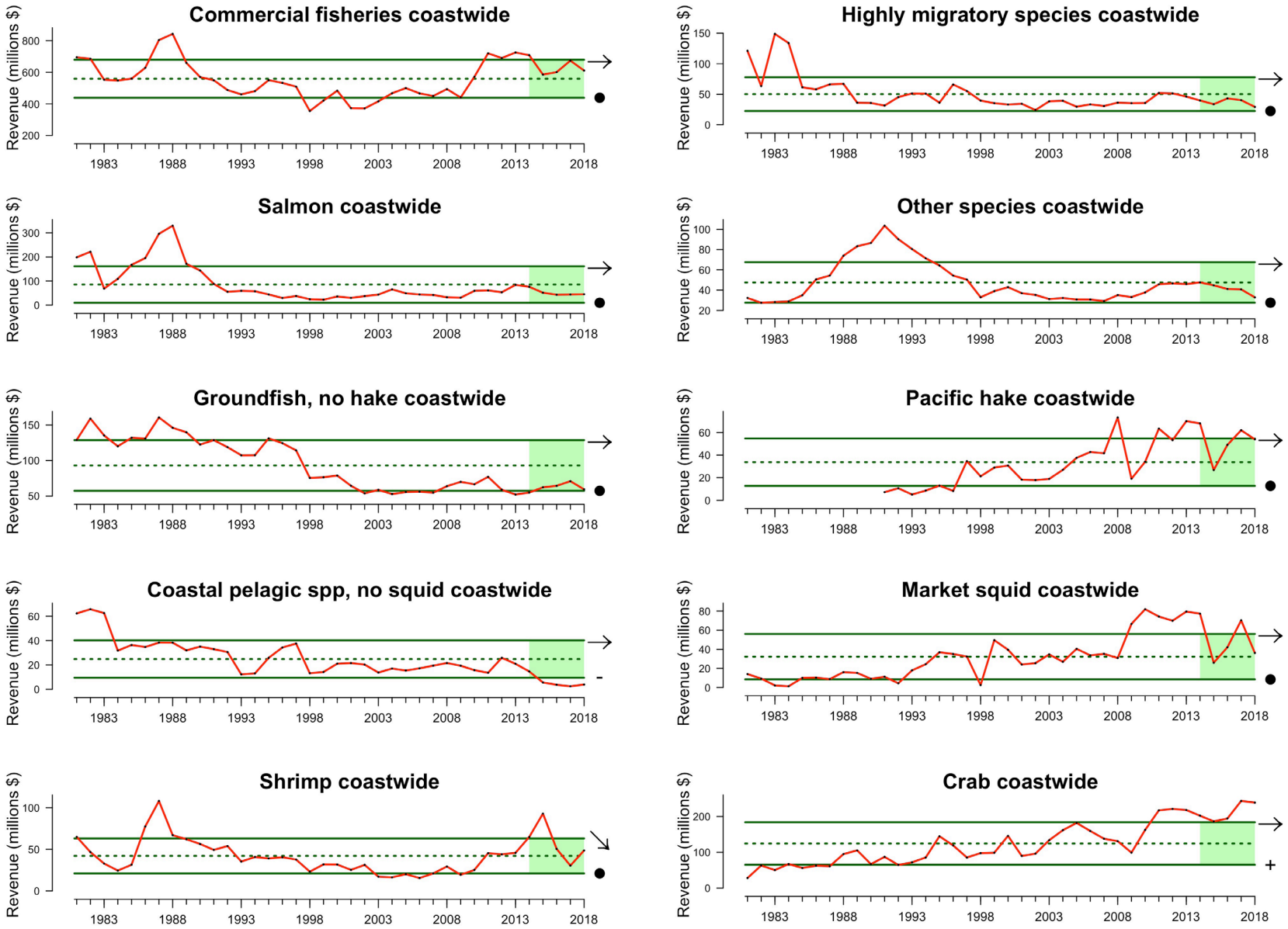

Figure 49. Annual revenue (ex-vessel value in 2018 dollars) of U.S. West Coast commercial fisheries (data from PacFin), 1981–2018. Pacific hake revenue includes shoreside and at-sea hake revenue values from PacFIN, NORPAC (North Pacific Groundfish Observer Program), and NMFS Office of Science and Technology. Lines, colors, and symbols as in Figure 3a.

disruption of food web processes. These effects may differ among physiographic types of habitat (e.g., hard, mixed, or soft sediments) and may be particularly dramatic in sensitive environments (e.g., seagrass, algal beds, coral and sponge reefs, or rocky substrates) relative to soft sediments. The exploration for resources (e.g., oil, gas, and minerals) and marine fisheries tend to operate within certain habitat types more than others, and long-term impacts of these activities may cause negative changes in biomass and the production of benthic communities. Thus, spatially explicit indicators are necessary to provide information for spatial management of specific human activities in relation to these resources.

We used estimates of coastwide distances exposed to bottom trawl fishing gear in federally managed fisheries along the ocean bottom from 1999–2016, the most recent year for which data were available. We calculated bottom trawl contact with the seafloor as straight-line distances between set and haul-back locations. Data come from state logbooks as reported to PacFIN and processed by the Northwest Fisheries Science Center's West Coast Groundfish Observer Program. Processing of the logbook data includes removing tows that appear to have errors in the logbook entries (e.g., set or haul-back location is on land; vessel speed necessary to make the tow was >5 knots; etc.). The data are presented here in two ways. The first is several time series of estimated bottom trawl contact, both at the coastwide scale and also subdivided into the northern, central and southern CCE, lumped by bottom type (hard, mixed, or soft) and general depth category (shelf or slope). The second approach presents much finer spatial resolution of bottom trawl contact (2×2-km grid cells across the shelf and slope).

At the coarsest scale of the entire West Coast, bottom trawl gear contact with seafloor habitat remained at historically low levels from 2012–16 (Figure 50, top). During this period, the vast majority of federally managed bottom trawl gear contact with seafloor habitat occurred in soft, upper slope and shelf habitats. The northern ecoregion experienced the most fishing gear contact with seafloor habitat with nearly four times the magnitude observed in the central ecoregion (Figure 50, bottom). Very little to no federally managed bottom trawling occurred in the southern ecoregion within the time series. A shift in federally managed trawling effort from shelf to upper slope habitats was observed during the mid-2000s, which in part corresponded to depth-related spatial closures implemented by PFMC.

To examine finer-scale bottom contact by bottom trawl gear in federally managed fisheries, we used the same logbook data to estimate total distance trawled on a 2×2-km grid from 2002 to 2016. We calculated distance trawled with straight-line distances between set and haul-back locations from the federally managed limited-entry and catch-share bottom trawl fisheries. Then for each grid cell, we mapped the 2016 anomaly from the long-term mean, the most recent 5-year average and the most recent 5-year trend (Figure 51); the number of cells included in the 5-year average and 5-year trend analyses is greater than in the 2016 anomaly analysis because there must be data from at least 3 vessels in a given cell for the period of analysis in order to conform to data confidentiality requirements. Off Washington, cells where distance trawled was above average in 2016 tended to be in central and southern waters (Figure 51, left; red cells), while northern cells mostly experienced below-average contact (blue cells). These patterns from 2016 were generally consistent with recent averages and trends for Washington over the period of 2012–16 (Figure 51, center and right). Off Oregon, red cells in 2016 and in the trend map were in several patches, the largest of which was off Newport, while blue cells in 2016 and the trend map were most concentrated to the north and south of Cape Blanco. Off California, the most notable

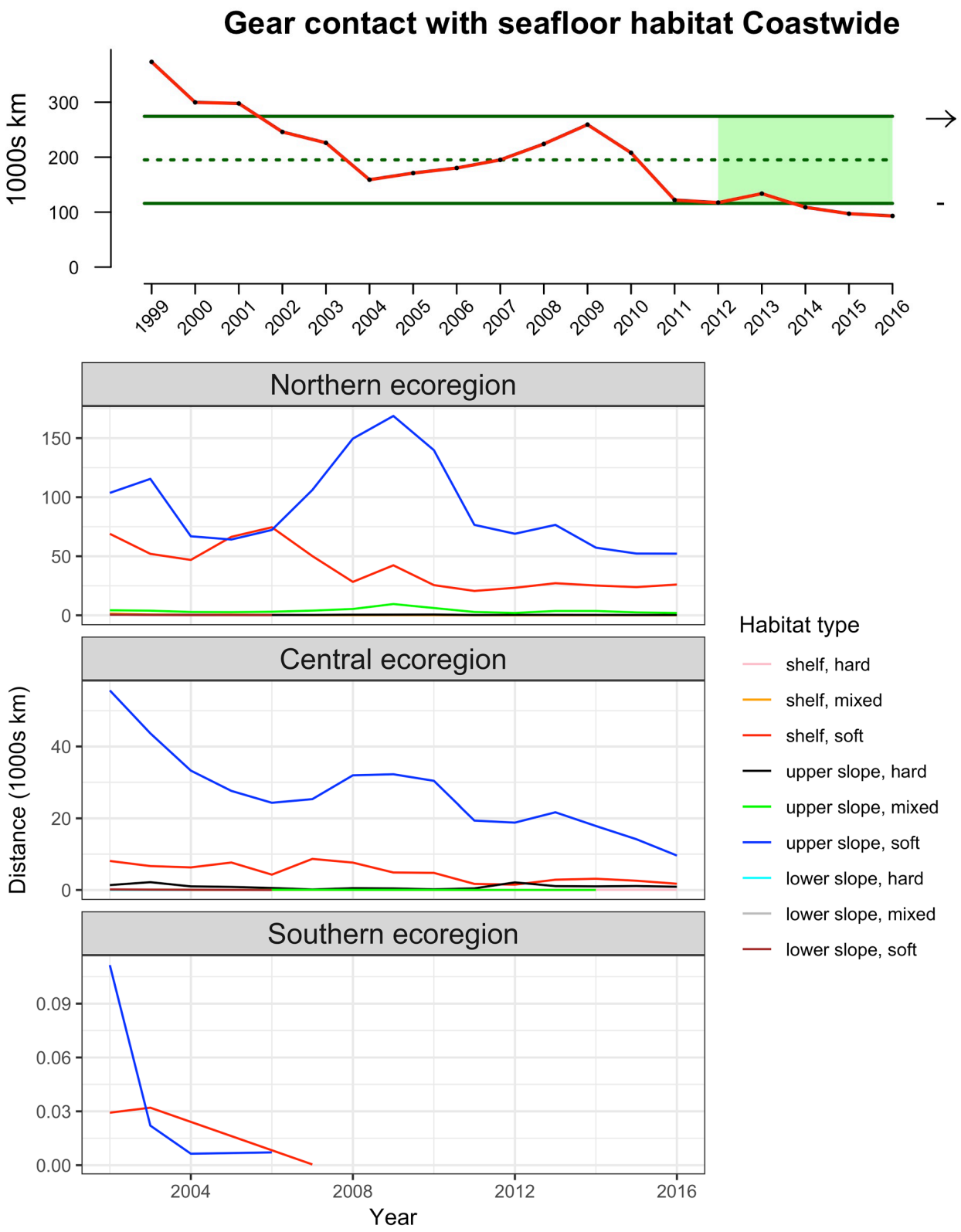

Figure 50. Estimated distance (1,000 km) of bottom trawl gear contact with seafloor habitat in federal fisheries across the entire CCE (top; 1999–2016) and within each ecoregion and habitat type (bottom three panels; 2002–16). Lines, colors, and symbols in top panel as in Figure 3a. Data for total benthic habitat distance contacted by federal bottom trawl fishing gear were calculated using state logbook data reported to PacFIN and processed by NWFSC's Fisheries Observation Science Program.

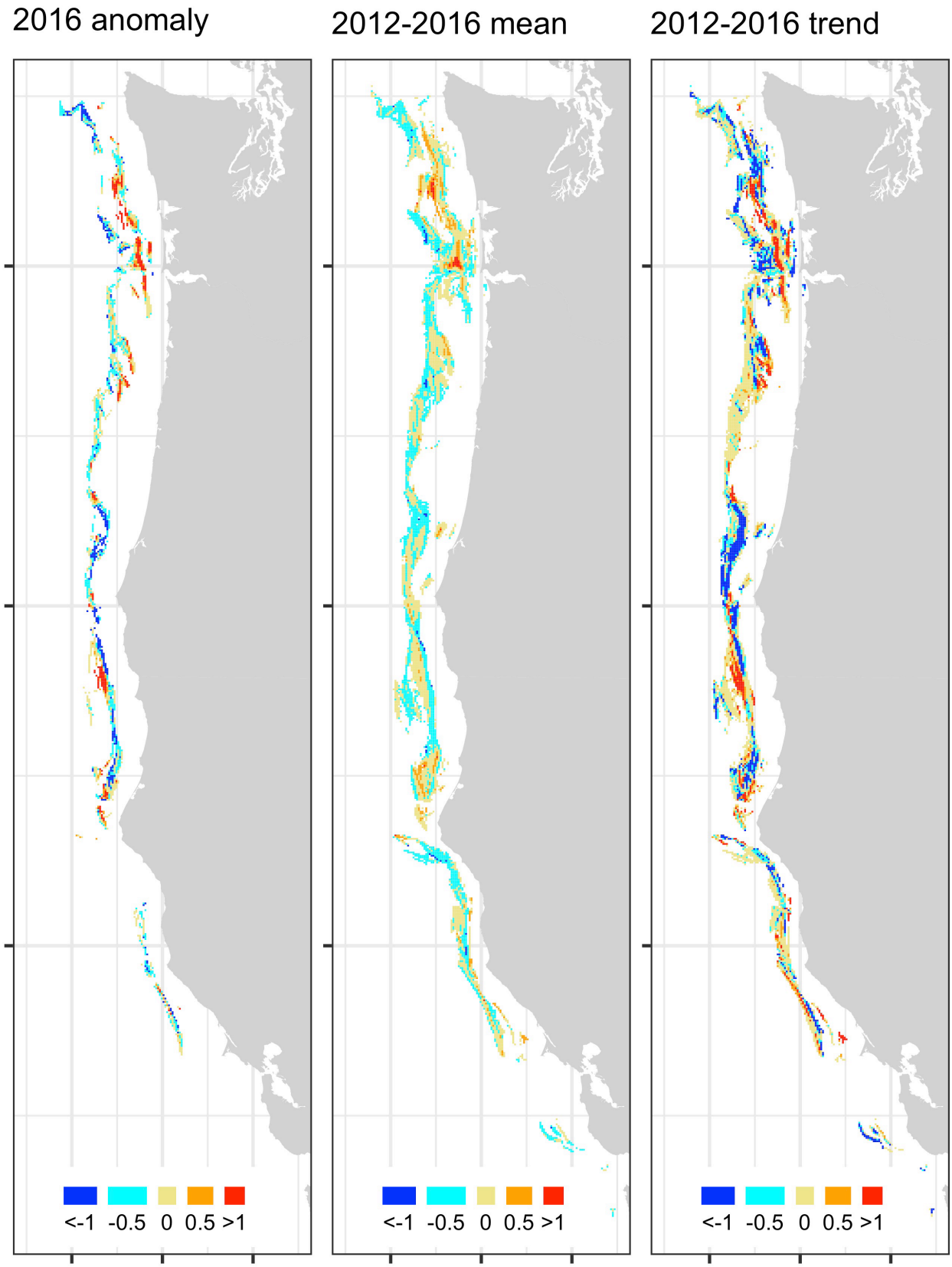

Figure 51. Spatial representation of seafloor contact by federal groundfish bottom trawl fishing gear, represented by annual distances trawled within each 2×2-km grid cell, 2002–16. Left: annual bottom contact anomalies. Middle: normalized mean values for the most recent five-year period (2012–16). Right: normalized trend values for the most recent five-year period. Grid cell values >1 (red) or <-1 (blue) represent a cell in which the 2016 anomaly, 5-year mean, or 5-year trend was at least 1 SD away from the long-term mean of that cell.

patches of red cells in 2016 were just north of Cape Mendocino, while cells with increasing or decreasing trends from 2012–16 were widespread. Because it highlights status and trends of federally managed trawling activity in specific areas, this spatial indicator is more informative than the time series of the total coastwide distance trawled, which indicated that federally managed bottom trawl contact with the seafloor was at historically low levels and had no trend from 2012–16 (Figure 50).

4.3. Aquaculture Production and Seafood Consumption

Aquaculture productivity is an indicator of seafood demand, and also may be related to some benefits (e.g., water filtration by bivalves, nutrition, or income and employment) or impacts (e.g., habitat conversion, waste discharge, or nonindigenous species introductions). Shellfish aquaculture production in the CCE consistently was at historically high levels from 2013–17 (Figure 52, top). These patterns are driven by production in Washington state, which is home to nearly >90% of coastwide shellfish production. Finfish aquaculture (of Atlantic salmon [*Salmo salar*]) has been variable, but was within 1 SD of the long-term mean after peaking above the average in 2014-15 (Figure 52, bottom).

Per capita seafood consumption in the U.S. was stable and near the upper end of the long-term average range from 2013–17 (Figure 53, top), while total seafood consumption was above average and continued the overall upward trend generally observed in both indicator's time series since the early 1970's (Figure 53, bottom). Total consumption in 2012–16 was above the historic average, while per capita consumption was within the historic range. With increasing human populations and recommendations in U.S. Dietary Guidelines[12] to increase seafood intake, total consumption of seafood products seems likely to continue increasing for the next several years, barring major changes in national or global economic drivers.

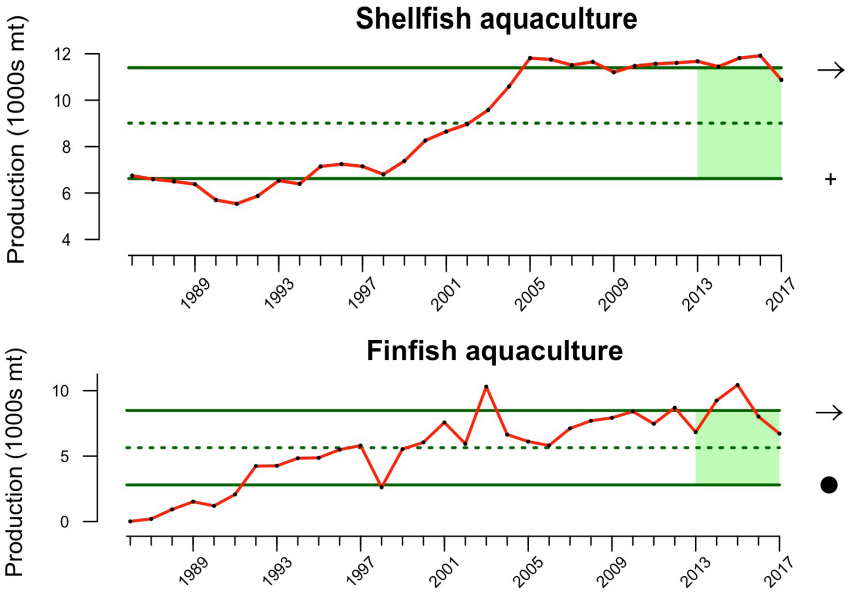

Figure 52. Aquaculture production of shellfish (clams, mussels, oysters) and finfish (Atlantic salmon) in CCE waters from 1986–2017. Lines, colors, and symbols as in Figure 3a. Shellfish production data were retrieved and summed together from Washington Department of Fish and Wildlife's Commercial Harvest Data Team, Oregon Department of Agriculture, and California Department of Fish and Game; finfish production data from Washington Department of Fish and Wildlife, Commercial Harvest Data Team.

[12] https://health.gov/dietaryguidelines/2015/guidelines/chapter-2/a-closer-look-at-current-intakes-and-recommended-shifts/#food-groups

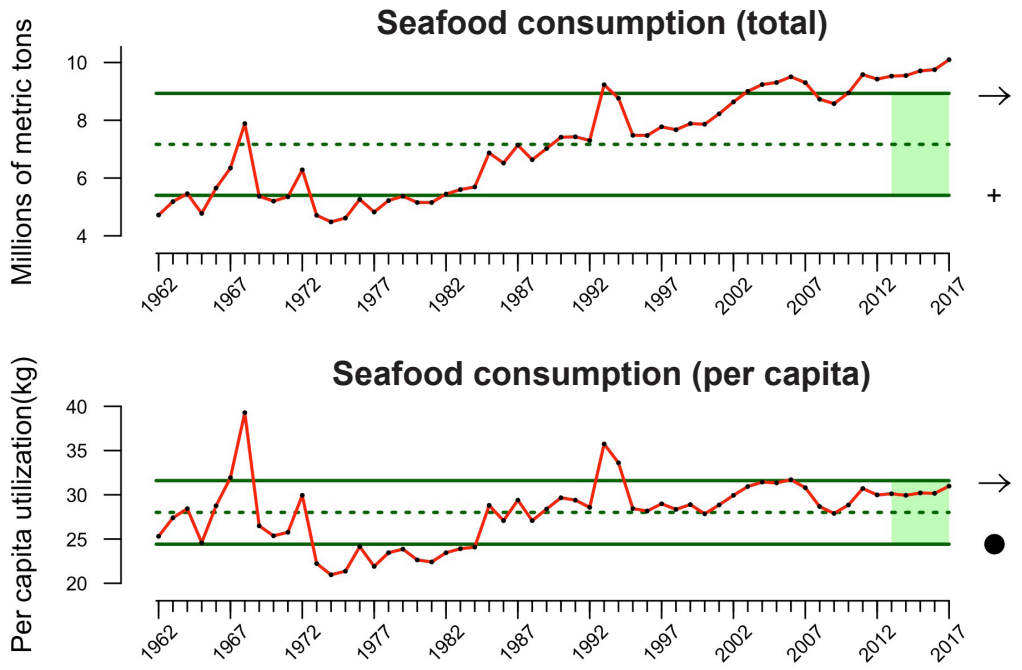

Figure 53. Total (metric tons) and per capita (kg) consumption of fisheries products in the U.S.A., 1962–2017. Lines, colors, and symbols as in Figure 3a. Data can be found in NOAA's annual Fisheries of the United States reports (http://www.st.nmfs.noaa.gov/st1/publications.html).

4.4. Nonfishing Human Activities

The CCIEA team compiles and regularly updates indicators of nonfishing human activities in the CCE, some of which may have effects on focal species, ecosystem processes and services, fisheries, and coastal communities. These activities relate to different ocean-use sectors like shipping and energy extraction, or to terrestrial sectors that result in nutrient inputs to coastal waters. We update many of these indicators annually, although some are updated less frequently due to the time required by the source agencies to release their data.

4.4.1. Commercial shipping

Approximately 90% of world trade is carried by the international maritime shipping industry. The volume of cargo moved through U.S. ports increased 3% per year from 2000 to 2017 (U.S. Army Corps of Engineers, Waterborne Commerce Statistics Center[13]), and is expected to continue to increase at that rate through 2030 (Lloyd's Register et al. 2013). Fisheries impacts associated with commercial shipping include interactions between fishing and shipping vessels; ship strikes of protected species; and underwater noise that affects reproduction, recruitment, migration, behavior, and communication of target and protected species.

Commercial shipping activity is measured by summing the total distances traveled by vessels traveling internationally within the CCE. Domestic traveling vessels are not included in this calculation because their trips make up only 10% of distances traveled, have no effect

[13] https://www.iwr.usace.army.mil/About/Technical-Centers/WCSC-Waterborne-Commerce-Statistics-Center/

on the overall status and trend, and are more difficult to update in a timely manner than international data. Commercial shipping activity in the CCE was at the lowest levels of the available time series over 2013–17, which are the most recent five years of available data (Figure 54). This contrasts drastically with global estimates of shipping activity, which are projected to increase nearly 250% between 2010 and 2030 (Lloyd's Register et al. 2013). However, most maritime shipping activity indicators are based on cargo volume and value of goods, thus capturing different attributes of the industry than we show here with distances traveled in the CCE, and we consider vessel activity as indicated by distance travel to be more relevant to CCE biota and human activities than the volume or value of the cargo on board. Changes in major trading routes and vessel characteristics (e.g. vessel length and cargo capacity) may also be responsible for the observed differences between global indicators and estimates for the CCE.

Figure 54. Distance transited by foreign commercial shipping vessels in the CCE, 1999–2017. Lines, colors, and symbols as in Figure 3a. Foreign vessel entrance and clearance data from https://publibrary.planusace.us/#/series/Waterborne%20Foreign%20Cargo.

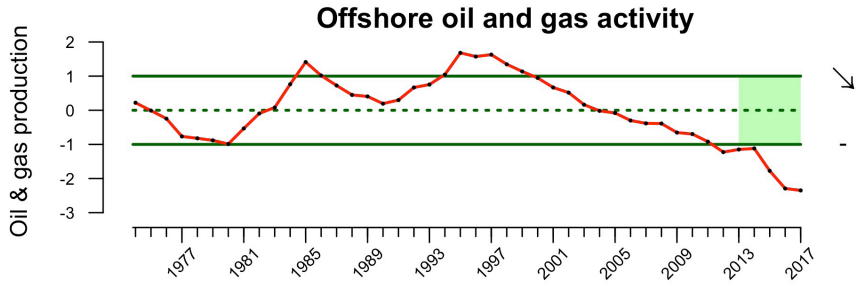

Figure 55. Normalized index of the sum of oil and gas production from state and federal offshore wells in California, 1974–2017. Lines, colors, and symbols as in Figure 3a. California State oil production data come from annual reports of the California State Department of Conservation's Division of Oil, Gas, and Geothermal Resources (ftp://ftp.consrv.ca.gov/../pub/oil/annual_reports/); federal oil production data come from the Bureau of Safety and Environmental Enforcement (https://www.data.bsee.gov/homepg/data_center/production/PacificFreeProd.asp); state and federal natural gas production data come from the U.S. Energy Information Administration (http://www.eia.gov/dnav/ng/ng_prod_sum_dcu_rcatf_a.htm).

4.4.2. Oil and gas activity

Oil and natural gas are extracted in offshore drilling in the CCE, with all active leases located in Southern California in the region of Point Conception and landward of the Channel Islands. Risks posed by offshore oil and gas activities include the release of hydrocarbons, smothering of benthos, sediment anoxia, benthic habitat loss, and the use of explosives. Petroleum products consist of thousands of chemical compounds such as polycyclic aromatic hydrocarbons (PAHs), which may impact marine fish health and reproduction. The effects of the physical presence of oil rigs on fish stocks are less conclusive, as rig structures may provide some habitat benefits.

Offshore oil and gas activity in the CCE declined and was below historical levels over 2013–17, the last five years of available data (Figure 55). Offshore oil and gas production has been decreasing steadily since the mid-1990s.

4.4.3. Nutrient loading

Nutrient input into coastal waters occurs through natural cycling of materials, as well as through loadings derived from human activities. Nutrient loading is a leading cause of contamination, eutrophication, and related impacts in streams, lakes, wetlands, estuaries, and groundwater throughout the United States. Nutrient input data into all CCE waters have not been updated since 2012, and are thus not presented here.

5. Human Wellbeing

Human wellbeing is inextricably linked to the marine, coastal, and upland environments of the CCE. These relationships are dependent on qualities of both the biophysical environment and the human social system. The marine ecosystem of the California Current supports human wellbeing through fisheries sustenance and income, aesthetic and recreational opportunities, and a variety of economically and socially discernible contributions. Human wellbeing may be measured at the individual, community and societal levels, and includes many component elements, some of which have been described and addressed within the output of a CCIEA-originated Social Wellbeing in Marine Management (SWIMM) working group (Breslow et al. 2017).

The subsections below outline several indicators of human wellbeing in the CCE. Community measures of social vulnerability are a way of partially assessing human wellbeing at the community level. Social vulnerability measures have been developed and applied to communities where commercial and recreational fishing are important, and the relative salience of marine fishing is likewise available through reliance and engagement indicators that tie communities to marine fishing within the California Current. Economically, the relative fishery diversity within commercial fishing income provides an indicator of wellbeing at both the individual vessel level, as well as the port and community levels. Finally, we introduce new metrics that characterize availability of fish stocks to different fishing communities, where availability is a function of changing stock abundance and spatial distribution.

5.1. Social Vulnerability

Coastal community vulnerability indices are generalized socioeconomic vulnerability metrics for communities. The Community Social Vulnerability Index (CSVI) is derived from social vulnerability data (demographics, personal disruption, poverty, housing characteristics, housing disruption, labor force structure, natural resource labor force, etc.; see methods in Jepson and Colburn (2013). The CCIEA team has been monitoring CSVI in West Coast communities dependent upon commercial and recreational fishing.

The commercial fishing *engagement* index is based on an analysis of variables reflecting commercial fishing engagement in 1,140 communities (e.g., fishery landings, revenues, permits, and processing). The commercial fishing *reliance* index applies the same factor analysis approach to these variables on a per capita basis; thus, in two communities with equal engagement, the community with the smaller population would have a higher reliance on its fisheries activities. Similarly, the recreational fishing engagement index is based on an analysis of variables reflecting a community's recreational fishing engagement (e.g., number of boat launches, number of charter boat and fishing guide license holders, number of charter boat trips, and a count of recreational fishing support businesses such as bait and tackle shops). The recreational fishing reliance index represents these variables for each community on a per capita basis. The plots shown in this report focus on indicators of fishing reliance (per capita dependence) within focal communities; for engagement plots, see Appendix M of Harvey et al. (2019).

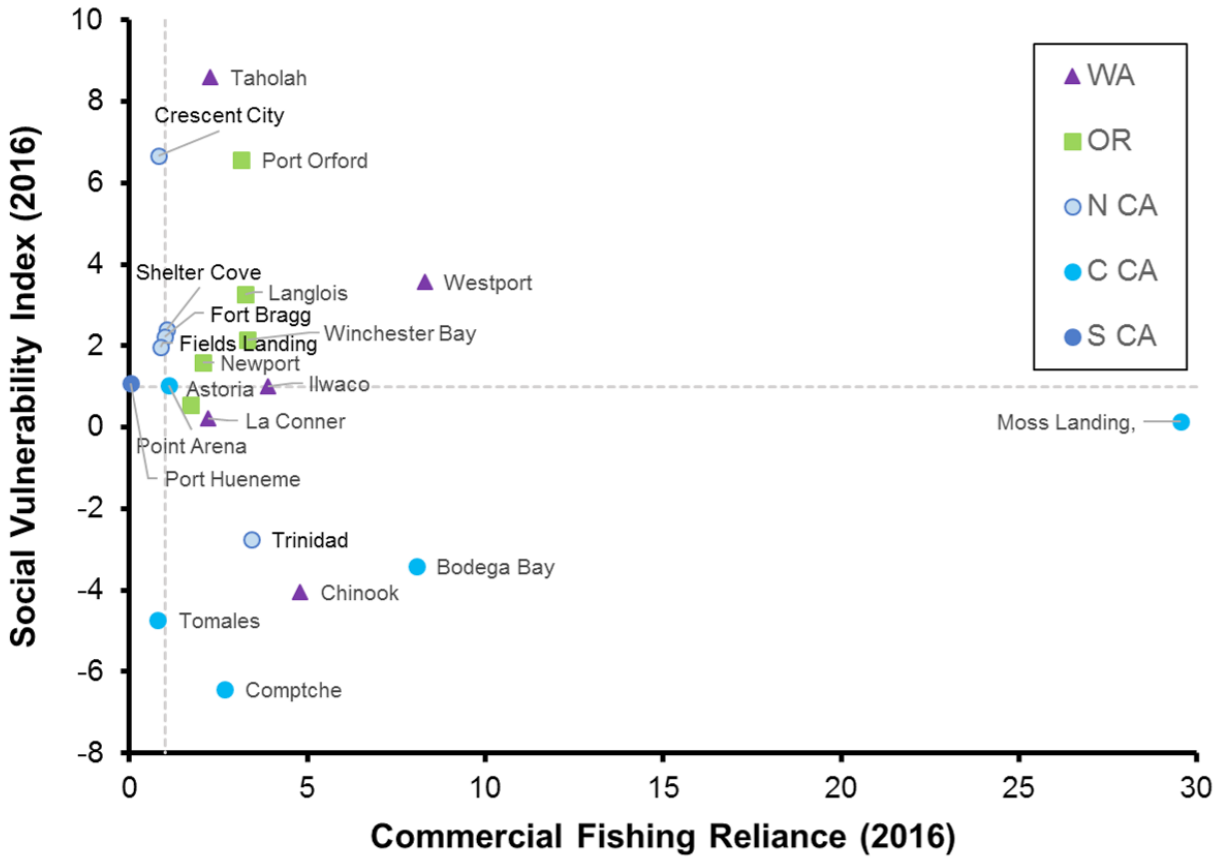

Figure 56. Commercial fishing reliance and social vulnerability scores plotted for twenty-five communities (five from each of the five regions of the CCE: Washington, Oregon, and Northern, Central, and Southern California). The top five highest-scoring communities for commercial fishing reliance were selected from each region. Community social vulnerability index (CSVI) and fishery reliance data were provided by K. Norman, NMFS/NWFSC, and A. Varney, PSMFC; these data were derived from the U.S. Census Bureau's American Community Survey (ACS; https://www.census.gov/programs-surveys/acs/) and PacFIN (http://pacfin.psmfc.org), respectively.

Figure 56 plots CSVI against per capita commercial fishery reliance for 2016 in communities most dependent on commercial fishing in Washington, Oregon, and Northern, central, and Southern California (five communities per region). Of note are communities that are above and to the right of the dashed lines, which indicate 1 SD above average levels of social vulnerability (horizontal dashed line) and commercial fishing reliance (vertical dashed line) of all U.S. West Coast communities. For example, Port Orford and Westport have high fishing reliance (4 and 9 SD above average) and high CSVI (6 and 4 SD above average) compared to other coastal communities. Commercial fishing downturns due to ecosystem changes or management actions may produce especially high individual- and community-level social stress in communities that are strong outliers in both indices. However, as we have discussed in past reports and discussions with PFMC, these data are difficult to ground-truth and require further study. We also lack data for many communities altogether, including many tribal communities.

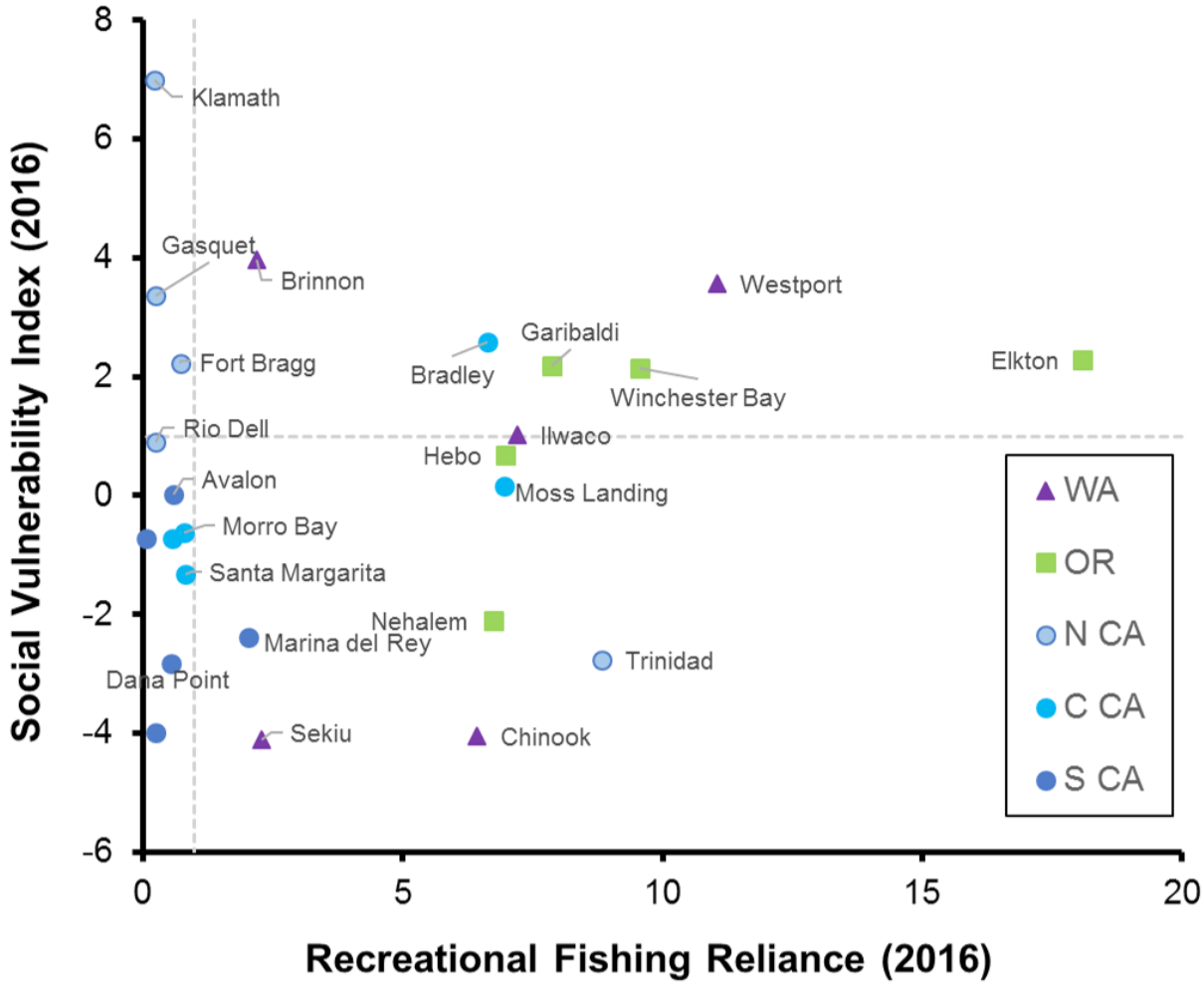

Figure 57. Recreational fishing reliance and social vulnerability scores plotted for twenty-five communities (five from each of the five regions of the CCE: Washington, Oregon, and Northern, Central, and Southern California). The top five highest-scoring communities for recreational fishing reliance were selected from each region. Community social vulnerability index (CSVI) and fishery reliance data were provided by K. Norman, NMFS/NWFSC, and A. Varney, PSMFC; these data were derived from the U.S. Census Bureau's American Community Survey (ACS; https://www.census.gov/programs-surveys/acs/) and PacFIN (http://pacfin.psmfc.org) and RecFIN (http://www.recfin.org/), respectively.

Figure 57 plots CSVI against the per capita recreational fishery reliance index for 2016 in the five communities most heavily dependent on recreational fishing in each of the same five geographic regions (note: this analysis does not differentiate between marine recreational fishing and inland recreational fishing, which may include anadromous salmonids of coastal commercial and recreational interest). Once again, of note are communities that appear above and to the right of the dashed lines, which indicate the 1 SD above average levels of recreational fishing reliance (vertical line) and social vulnerability (horizontal line) along the U.S. West Coast. Notable communities of this type include Westport, Washington; Elkton, Winchester Bay, and Garibaldi, Oregon; and Bradley, California. Also of note, several communities (Winchester Bay, Oregon; Westport and Ilwaco, Washington) appear in this portion of the plot for both the commercial and recreational sectors, which may imply some potential for management-related tradeoffs in those communities.

This is an emerging area of work, and more research will be required to ground-truth information and to understand the importance of these relationships. An effort to examine communities that may be particularly affected by ecosystem shifts, with respect to the Magnuson-Stevens Act's National Standard 8, is ongoing. Additional findings on these fishery engagement relationships are in Appendix M of Harvey et al. (2019).

5.2. Fishing Revenue Diversification Indices

Catches and prices from many fisheries exhibit high interannual variability leading to high variability in fishermen's revenue, but variability can be reduced by diversifying fishing activities across multiple fisheries or regions (Kasperski and Holland 2013). We use the effective Shannon index (ESI) to measure diversification among 28,000 fishing vessels on the U.S. West Coast and Alaska. The index has an intuitive meaning: ESI = 1 when all revenues are from a single species group and region; ESI = 2 if fishery revenues are spread evenly across 2 fisheries; and so on. It increases both as revenues are spread across *more* fisheries and as revenues are spread *more evenly* across fisheries.

In 2017 (the most recent year analyzed), revenue diversification of the fleet of vessels fishing on the U.S. West Coast and in Alaska changed little relative to 2016 (Figure 58). However, the fleet was less diverse on average than at any time in the preceding 36 years, and this was true for most home states, revenue categories, and size classes (Figure 58b-d). The long-term decline is due both to entry and exit of vessels, and to changes for individual vessels. Over time, less-diversified vessels have been more likely to exit, which would have a positive effect on diversification; however, vessels that remain in the fishery have also become less diversified, at least since the mid-1990s, and newer entrants have generally been less diversified than earlier entrants. The net result is a moderate decline in average diversification since the mid-1990s or earlier. Within the average trends, there are wide ranges of diversification levels and strategies within and across vessel classes, and some vessels remain highly diversified. Increased diversification from one year to the next may not always indicate an improvement. For example, if a class of vessels was heavily dependent on a single fishery with highly variable revenues (e.g., Dungeness crab), a decline in that fishery might force vessels into other fisheries, causing average diversification to increase.

As is true with individual vessels, the variability of landed value at the port level is reduced with greater diversification of landings. Diversification of fishing revenue has declined over the last several decades for some ports (Figure 59). Examples of ports where revenue diversification has declined in recent decades include Seattle and many ports in northern and southern California. However, a few ports have become more diversified, such as Bellingham. Diversification scores are highly variable year-to-year for some ports, particularly those in Southern Oregon (Brookings) and Northern California (Crescent City, Eureka) that depend heavily on the Dungeness crab fishery, which has highly variable landings. Many major ports saw a decrease in diversification between 2016 and 2017, but others saw an increase. No clear recent trends are apparent.

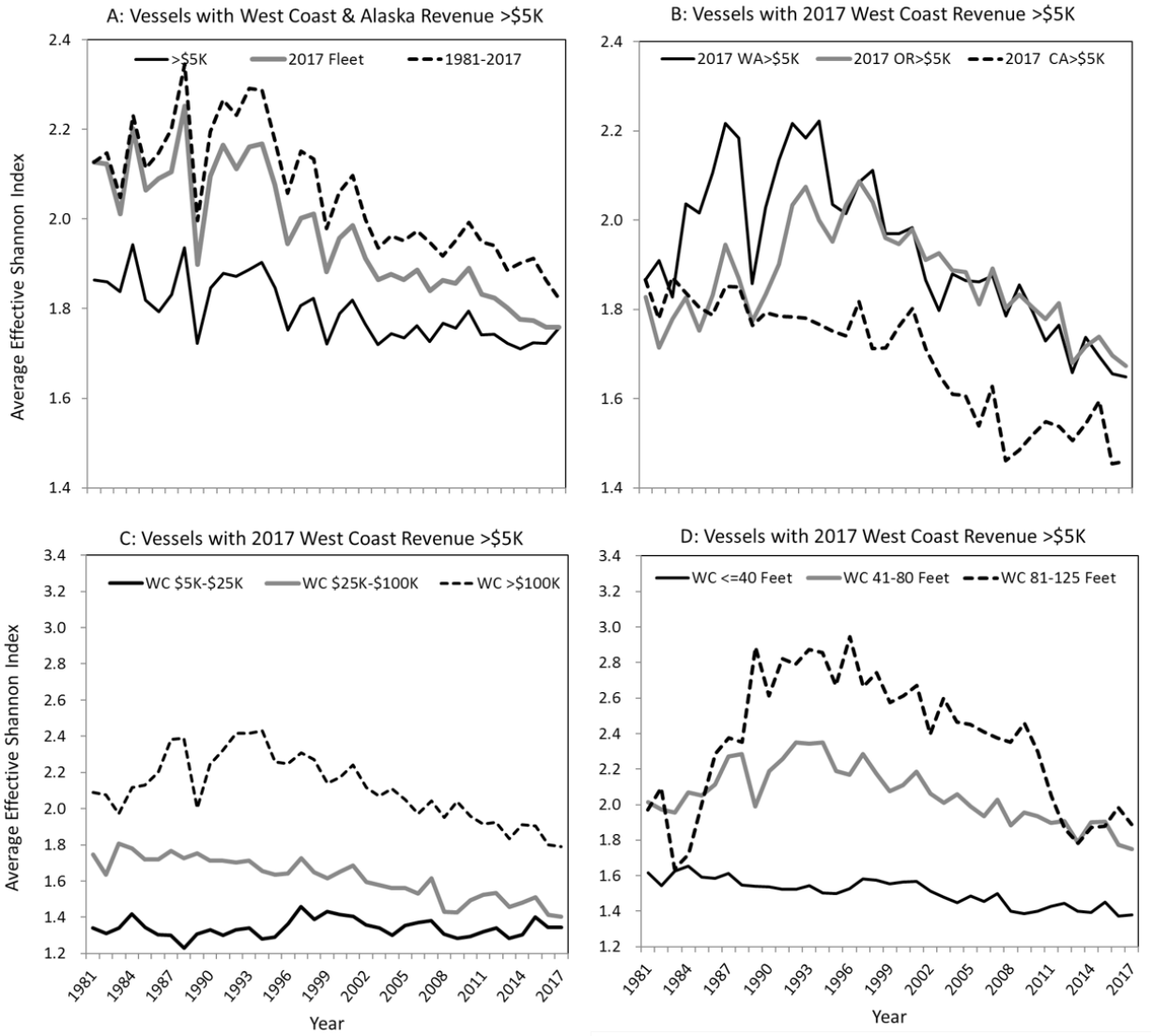

Figure 58. Trends in average diversification for U.S. West Coast and Alaskan fishing vessels with over $5K in average revenues (top left), and for vessels in the 2017 West Coast Fleet with over $5K in average revenues, broken out by state (top right), by average gross revenue classes (bottom left), and by vessel length classes (bottom right). Fishery diversification estimates were provided by D. Holland, NMFS/NWFSC, and S. Kasperski, NMFS/AFSC.

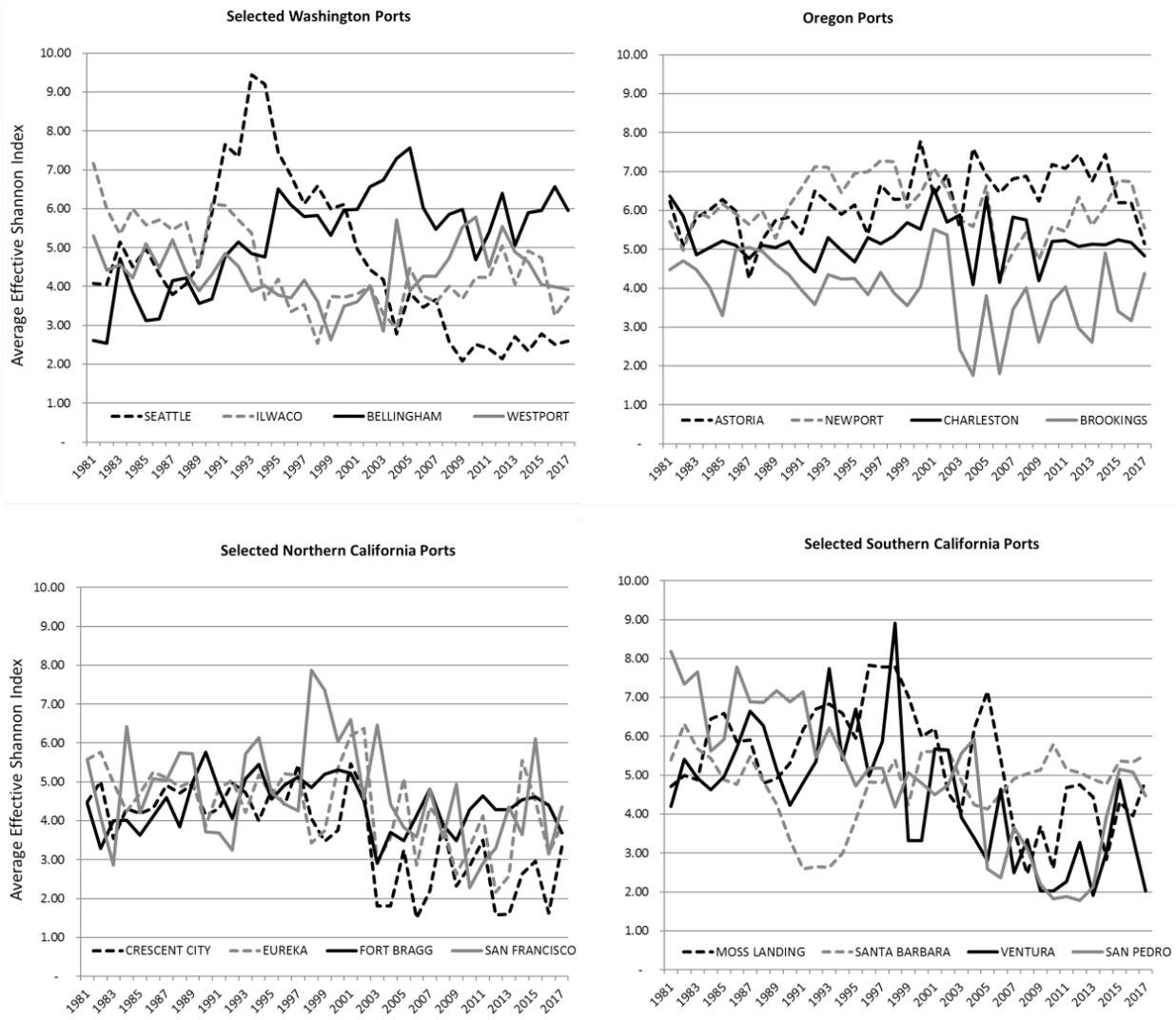

Figure 59. Trends in commercial fishing vessel revenue diversification in major U.S. West Coast ports for Washington, Oregon, and California. Fishery diversification estimates were provided by D. Holland, NMFS/NWFSC, and S. Kasperski, NMFS/AFSC.

5.3. Stock Spatial Distribution and Availability to Ports

Fishing communities must contend with changes in availability of important target stocks. Changes in availability may happen due to changes in the stock's population size, changes in its distribution, or both. To determine how fishing communities along the U.S. West Coast experience changes in the distribution of fish stocks, we estimated fluctuations in the relative availability of two groundfish species (sablefish and petrale sole [*Eopsetta jordani*]) to four west coast communities (Astoria, Coos Bay, Fort Bragg, and Morro Bay). This stock availability index represents the cumulative effects of changes in biomass and shifts in spatial distribution. While the qualitative trends in stock availability reflect trends in biomass reported in stock assessments, the four communities represented here experienced those trends quite differently depending on where they occur along the coast.

We estimated stock biomass for each species at each location within the spatial sampling domain of the NOAA Fisheries West Coast Groundfish Bottom Trawl Survey and any year from 1977–2017 (Selden et al., in press). To do so, we combined two sources of information. First, stock assessment estimates of total population biomass were developed based on many different data sources. The estimates account for age- and length-based selectivity and catchability within available survey data. By doing so, the assessment also estimates the proportion of total abundance that is not vulnerable to a given survey gear. Second, we estimated spatiotemporal biomass density within a 200-km radius of each port. These estimates were obtained from available survey data from NOAA Fisheries bottom trawl surveys operating from 1977–present. Spatiotemporal analysis using methods developed by Thorson et al. (2015) allowed us to estimate the spatial distribution of biomass vulnerable to each sampling gear.

Results from this analysis demonstrate the stark differences in access to different species that coastal communities experience (Selden et al., in press). While the coastwide biomass of petrale sole has increased everywhere along the coast since the early 2000s, the center of gravity of this stock is now farther north than it was historically. Thus, relative stock availability of petrale sole has tripled for Astoria and Coos Bay, but increased more modestly for Fort Bragg and Morro Bay (Figure 60, left). In contrast, the coastwide biomass of sablefish declined more than 50% since 1980, but the distribution of sablefish is centered further south today than it was in the early 1990s. This change in the center of gravity of the stock has counteracted the decline in sablefish biomass for southern ports (Fort Bragg and Morro Bay) over the last 25 years, such that stock availability was relatively stable compared to Astoria and Coos Bay (Figure 60, right).

Ecological, technological, management, economic, governance, and other social factors influence the availability of target species to fishing communities. This same set of considerations influences the capacity of these communities to respond to shifting availability of target species. Climate variability and change, in particular, challenge the capacities of fishing communities to keep pace with shifts in stock availability. Analyses like those presented here represent a first step toward evaluating the impacts of changing social and ecological conditions on the availability of target species and the individual fishing communities that depend upon them. In the future, this analysis can be updated annually for any west coast community and for groundfishes well sampled by the trawl survey, and can focus on the attribution of potential causes underlying the shifts in availability observed here.

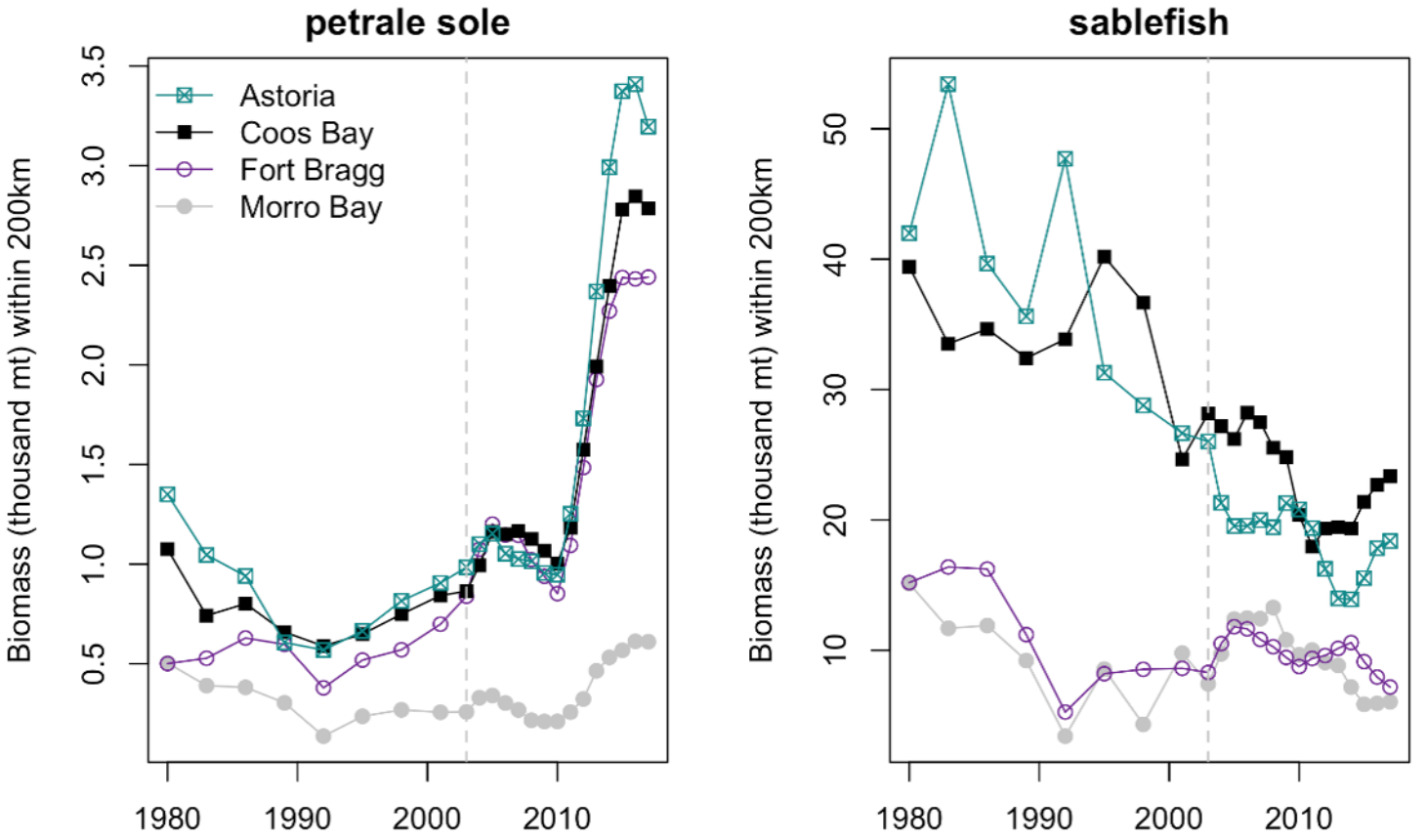

Figure 60. Time series of changes in availability of stock biomass to each focal port for petrale sole and sablefish, 1980–2017. Gray dashed lines indicate the year 2003, when the NOAA Fisheries bottom trawl survey transitioned from triennial to annual. Note differences in scale on y-axes. Stock availability estimates were provided by R. Selden, Rutgers University. From Selden et al. (in press).

6. Synthesis

6.1. Report Summary

As outlined in the Executive Summary, many indicators from the California Current Ecosystem in 2018 pointed toward a natural system that has moved away from the marine heat wave and El Niño of 2014–16 and closer to long-term average conditions. Within our indicators, this transition has been demonstrated by:

- Basin-scale climate indices, such as mostly neutral ONI and PDO values.
- Regional environmental indicators (i.e., average upwelling, snowpack, stream flow).
- Indicators of productivity at lower trophic levels (relatively average copepod community composition off Newport and krill size off northern California, subtle improvements in salmon indicators, no evidence of recent HABs off Washington, increases in anchovy).
- Indicators of predator foraging (improving conditions for sea lion pups; average or increasing densities of piscivorous seabirds).
- Recent increases in landings and revenues in several fisheries.

Furthermore, some variables that we had expected to be negatively affected by the warm conditions in 2014–16 actually exceeded those expectations, notably the large numbers of juvenile groundfish caught in pelagic surveys, suggesting that some parts of the CCE were resilient to the direct influence of the anomalous conditions.

Despite these signs of improvement, many indicators continued to suggest lingering effects of the anomalies of 2014–16, including persistence of subsurface warm water, high concentrations of pyrosomes, widespread ecologically and economically disruptive HABs off of Oregon and California, poor returns of salmon to some systems, and whale entanglements in fishing gear. Other concerning signs include persistently low NPGO anomalies, widespread hypoxic events, episodes of northeast Pacific warming (see Figure 9), and loss of fishery diversification. Finally, mild El Niño conditions are forecast to occur well into 2019.

As the CCE is highly variable in time, with climate and oceanographic patterns sometimes prevailing for one year and other times for a decade or more, we are unsure if the dynamics we have observed since the waning of the marine heat wave and El Niño will be a short transition that leads to more definitively productive or unproductive conditions, or a continuing regime of relatively average conditions. Our uncertainty about the overall status of the CCE underscores the importance of continued careful monitoring, modeling and analysis of indicators at appropriate scales; refinement of forecasting tools (see below); and maintaining communication between scientists, managers, and stakeholders. Indicators of the natural system also remind us that the California Current is a spatially diverse ecosystem. Meanwhile, indicators of the human system suggest that commercial fishery landings and revenue have begun to recover from the impact of the marine heat wave, though this is buoyed largely by Pacific hake and Dungeness crab. The diversification of fishery species providing revenue to the commercial fishery as a whole remains low, which may indicate that fishery sectors are more vulnerable to high interannual variability

in landings and price. The extent of the impacts of such vulnerability may differ across individual communities, depending on the diversification of their fleets and processing capabilities as well as the overall social vulnerability of each port, though this is an area where more information and dedicated research effort is needed.

6.2. Future Directions and Research Recommendations

In March 2015, PFMC approved FEP Initiative 2, "Coordinated Ecosystem Indicator Review" (PFMC 2015[14]), by which PFMC, advisory bodies, the public, and the CCIEA team would work jointly to refine the indicators in the annual ESRs to better meet PFMC objectives. Many of the recommendations that came out of Initiative 2 have been incorporated into this technical memorandum and also into the ESR that the CCIEA team presented to PFMC in March 2019 (see Appendix C in Harvey et al. 2019). We will continue to update and improve future ESRs and technical memorandums in collaboration with PFMC, as well as other end users with fisheries or other resource management mandates. The CCIEA team (and many other research teams) will also continue to focus research on how the recent anomalous conditions compare to historic conditions for key species and ecosystem processes in the CCE. Such work may help us identify ecosystem reference points in our indicators, i.e., points at which important ecosystem metrics experience disproportionate change that may require changes in management to mitigate impacts to ecological, economic, or social endpoints.

In the 2017 ESR to PFMC (Harvey and Garfield 2017), we were asked by PFMC to develop a list of general research recommendations that a) we believe are important, b) we could provide to PFMC in a reasonable time frame (e.g., one to three years), c) should support regional implementation of the NOAA EBFM Policy (NOAA 2018), and d) would provide added value to ecosystem indicators as they relate to management of FMP stocks and protected species. The recommendations also relate to key elements in the IEA framework (Figure 1). The six recommendations we generated were:

1. Continue an ongoing scoping process between PFMC and the CCIEA team.
2. Continue making improvements to indicator analysis.
3. Assess dynamics of fisheries adaptation to short-term climate variability.
4. Assess vulnerability of communities at sea to long-term climate change.
5. Use dynamic ocean management methods to reduce bycatch in HMS fisheries.
6. Assess the ecological and economic impacts of ocean acidification.

The CCIEA team is conducting integrative research and outreach activities related to each of these recommendations and will include outcomes in future reports as various activities are completed. We conclude this report with three examples of ongoing projects that support the recommendations. In the second technical memorandum of this series (Harvey et al. 2018), we described two projects related to research Recommendations 2 and 3 (development of an "early warning index" of major transitions in ecosystem state; an analysis to identify non-linear "thresholds" in relationships between stressor indicators and ecological

[14] https://www.pcouncil.org/ecosystem-based-management/fishery-ecosystem-plan-initiatives/coordinated-ecosystem-indicator-review-initiative/

components) and another project that was related to Recommendation 5 (nowcasts of the risk of bycatch of sea turtles and other non-target species in the California drift gillnet fishery). Research in these areas (and in relation to the other recommendations) is ongoing; CCIEA team members have published several management-relevant papers on these topics in the past year (Hazen et al. 2018, Scales et al. 2018, Mason et al. 2019, Welch et al. 2019a, Welch et al. 2019b), and anticipate publishing additional papers on them in the coming years.

In the next subsection, we add several analyses from another integrative project on developing short-term seasonal forecasts of ocean conditions and associated responses by important marine species. This project is most closely related to Recommendation 3, and it has promise to inform other recommendations as well. It also addresses feedback received from multiple PFMC advisory bodies during the FEP Initiative 2 process, namely that the CCIEA team provide management-relevant forecasts where possible.

6.3. Short-Term Seasonal Forecasts in the J-SCOPE Model

A set of forecasting tools has been developed in a partnership between academic scientists and CCIEA team members, and was reviewed in September 2018 by the PFMC Scientific and Statistical Committee's Ecosystem Subcommittee. The forecasting system was originally developed at the University of Washington Joint Institute for the Study of the Atmosphere and Ocean (JISAO), and the model system is called J-SCOPE (JISAO's Seasonal Coastal Ocean Prediction of the Ecosystem; www.nanoos.org/products/j-scope). The J-SCOPE forecast system provides short-term skilled forecasts of ocean conditions off of Washington and Oregon based on dynamically downscaled 6- to 9-month forecasts from the global-scale NOAA Climate Forecasting System model. J-SCOPE forecasts have been extended to include seasonal predictions of habitat quality for sardines (Kaplan et al. 2016, Siedlecki et al. 2016). Each January and April, the J-SCOPE modelers produce an ensemble of three forecasts that project ocean conditions through September and include variables like temperature, dissolved oxygen, chlorophyll, aragonite saturation state (ocean acidification), and sardine habitat, in addition to other dynamics such as the timing and intensity of upwelling.

According to the J-SCOPE ensemble forecast of the 2019 summer upwelling season (May–Aug):

- Sea surface temperatures were expected to be higher than average, with warm anomalies extending below the surface (related to the forecasted El Niño conditions).
- Dissolved oxygen on the bottom was expected to decline during the forecast period, with hypoxia (<2 mg/L) prominent over the Oregon shelf in June and spreading to Washington by July (Figure 61). Compared to previous years, oxygen was expected to be below average in Washington and near average in Oregon. The relative uncertainty in the forecast was low (10%) until the end of the upwelling season (July-August), when it increased to ~50%.
- Bottom waters were expected to be undersaturated with respect to aragonite (i.e., more corrosive) throughout the upwelling season for most of the region except for shallow nearshore Washington waters (Figure 62); surface waters were expected to be supersaturated throughout the season.
- Chlorophyll-a concentrations were forecast to be below average early in the upwelling season; later, chlorophyll was forecast to be above average over the Washington shelf and Heceta Bank, but below average over the rest of the Oregon shelf.

- Waters throughout the region were expected to be suitable for sardine (if sardines are present; the sardine population in U.S. waters has been very low throughout the 2010s).

The detailed forecasts for temperatures, chlorophyll and sardines can be viewed at the J-SCOPE website.[15] Additional forecasts for Pacific hake and Dungeness crab are being developed and will be available in future years, and similar types of seasonal forecasts at the spatial scale of the full California Current are expected in the future as well. By making these forecasts available to PFMC and other partners, we hope to provide useful, skilled forecast information that assists with decision making prior to the periods at which most productivity and harvest is occurring in key fishery sectors.

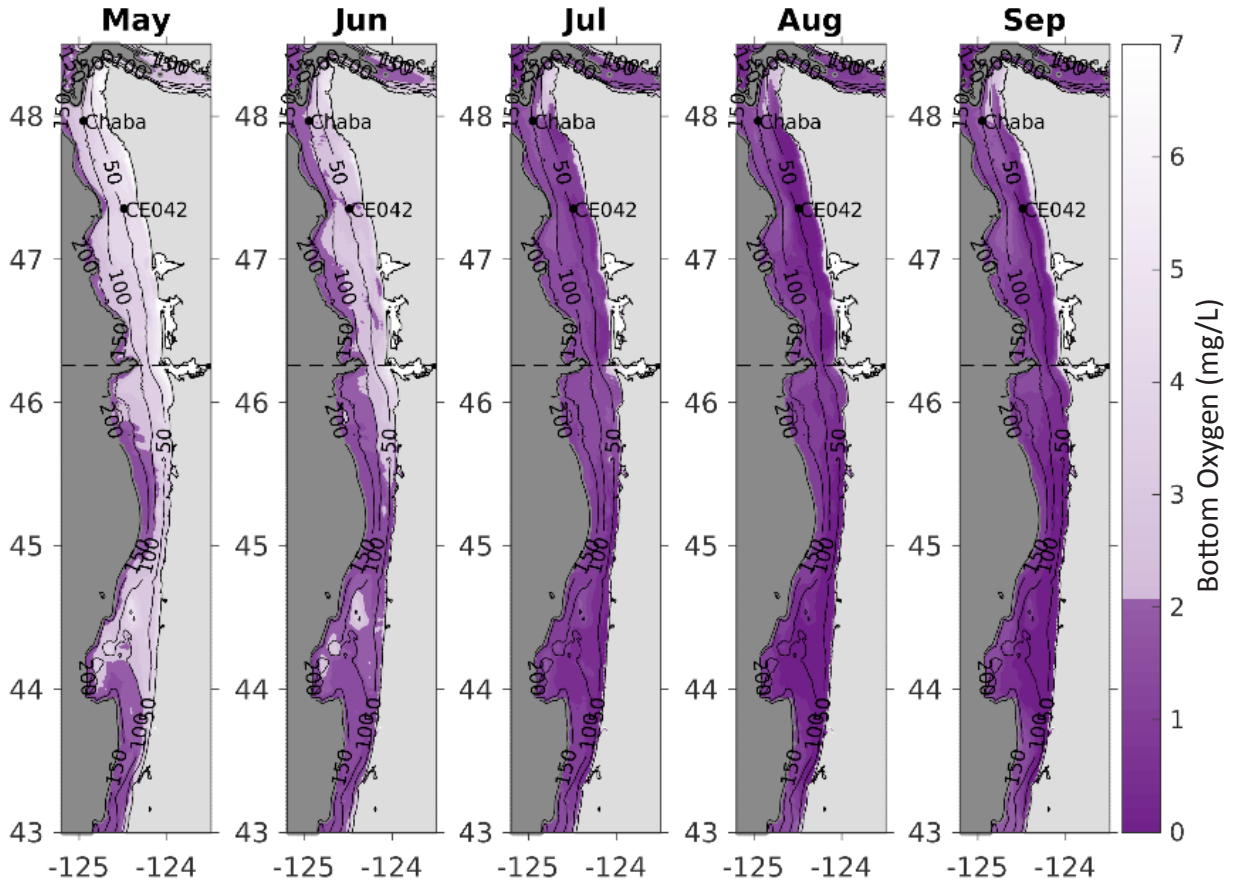

Figure 61. J-SCOPE forecasts of bottom dissolved oxygen (mg/L) for May–Sept 2019, averaged over all three ensemble members. Hypoxia (O_2 <2 mg/L) is shown in dark purple, and offshore areas are shaded dark gray. Black contours indicate bathymetry (m) on the shelf. J-SCOPE ensemble forecast maps were provided by S. Siedlecki, UCONN, and I. Kaplan, NMFS/NWFSC; http://www.nanoos.org/products/j-scope/forecasts.php.

[15] http://www.nanoos.org/products/j-scope/forecasts.php

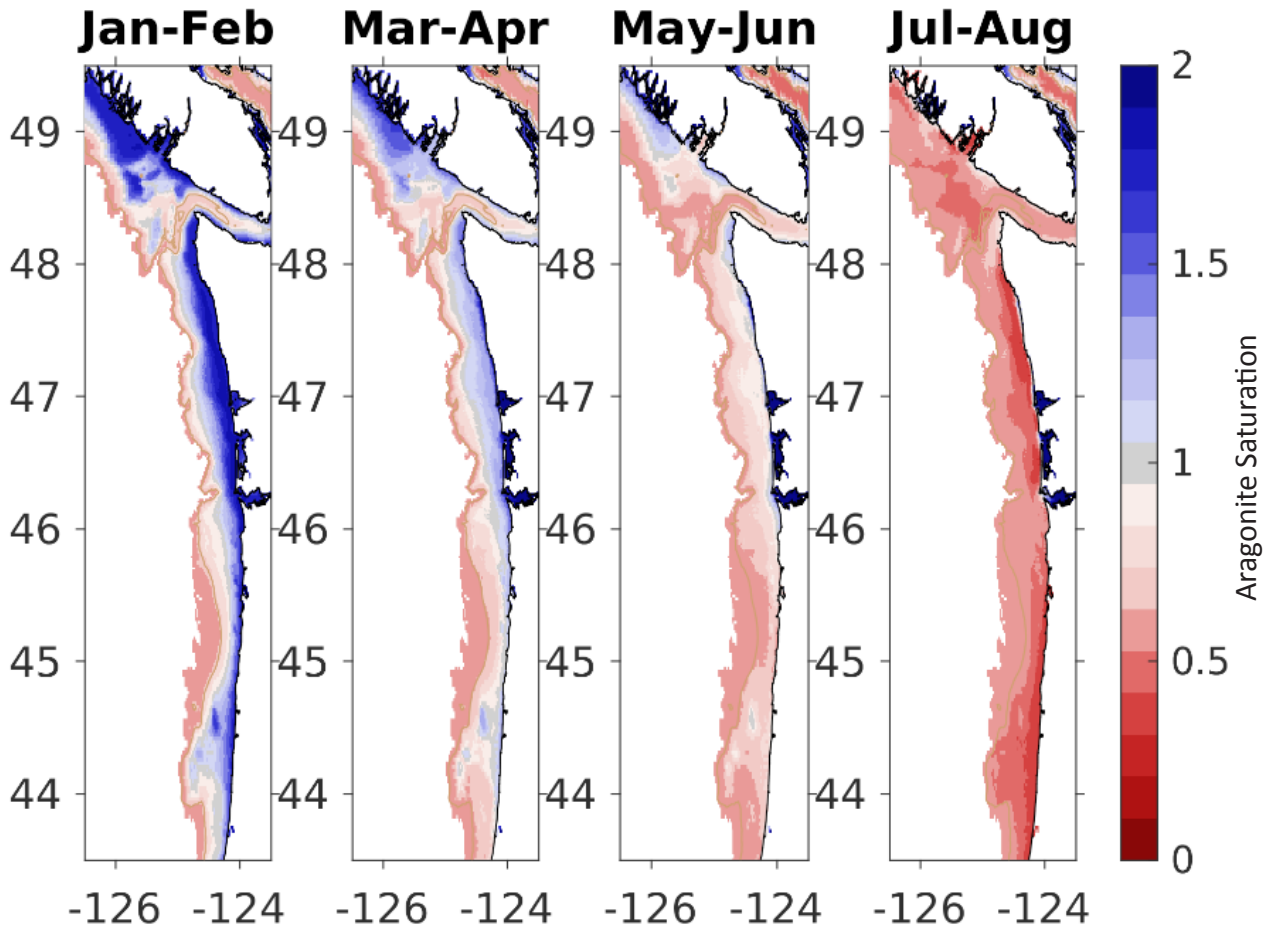

Figure 62. J-SCOPE forecasts of bottom aragonite saturation state for Jan–Aug 2019, averaged over all three ensemble members. For reference, aragonite saturation state = 1.0 is broadly considered the boundary between undersaturated and saturated conditions, although stressful conditions for juvenile oysters begin to occur when saturation state is ≤1.3. J-SCOPE ensemble forecast maps were provided by S. Siedlecki, UCONN, and I. Kaplan, NMFS/NWFSC; http://www.nanoos.org/products/j-scope/forecasts.php.

References

Abell, R., M. L. Thieme, C. Revenga, M. Bryer, M. Kottelat, N. Bogutskaya, B. Coad, N. Mandrak, S. C. Balderas, W. Bussing, M. L. J. Stiassny, P. Skelton, G. R. Allen, P. Unmack, A. Naseka, R. Ng, N. Sindorf, J. Robertson, E. Armijo, J. V. Higgins, T. J. Heibel, E. Wikramanayake, D. Olson, H. L. Lopez, R. E. Reis, J. G. Lundberg, M. H. S. Perez, and P. Petry. 2008. Freshwater ecoregions of the world: A new map of biogeographic units for freshwater biodiversity conservation. BioScience 58:403–414.

Alexander, J. D., S. L. Hallett, R. W. Stocking, L. Xue, and J. L. Bartholomew. 2014. Host and parasite populations after a ten year flood: *Manayunkia speciosa* and *Ceratonova* (syn *Ceratomyxa*) *shasta* in the Klamath River. Northwest Science 88:219–233.

Barton, A., B. Hales, G. G. Waldbusser, C. Langdon, and R. A. Feely. 2012. The Pacific oyster, *Crassostrea gigas*, shows negative correlation to naturally elevated carbon dioxide levels: Implications for near-term ocean acidification effects. Limnology and Oceanography 57:698–710.

Bednaršek, N., R. A. Feely, J. C. P. Reum, B. Peterson, J. Menkel, S. R. Alin, and B. Hales. 2014. *Limacina helicina* shell dissolution as an indicator of declining habitat suitability owing to ocean acidification in the California Current Ecosystem. Proceedings of the Royal Society B–Biological Sciences 281:20140123.

Bi, H. S., W. T. Peterson, and P. T. Strub. 2011. Transport and coastal zooplankton communities in the northern California Current system. Geophysical Research Letters 38.

Bradford, M. J., and J. S. Heinonen. 2008. Low flows, instream flow needs and fish ecology in small streams. Canadian Water Resources Journal 33:165–180.

Breslow, S. J., M. Allen, D. Holstein, B. Sojka, R. Barnea, X. Basurto, C. Carothers, S. Charnley, S. Coulthard, N. Dolsak, J. Donatuto, C. Garcia-Quijano, C. C. Hicks, A. Levine, M. B. Mascia, K. Norman, M. Poe, T. Satterfield, K. St. Martin, and P. Levin. 2017. Evaluating indicators of human well-being for ecosystem-based management. Ecosystem Health and Sustainability 3:1–18.

Brodeur, R. D., T. D. Auth, and A. J. Phillips. 2019. Major shifts in pelagic micronekton and macrozooplankton community structure in an upwelling ecosystem related to an unprecedented marine heatwave. Frontiers in Marine Science 6.

Brodeur, R. D., J. P. Fisher, R. L. Emmett, C. A. Morgan, and E. Casillas. 2005. Species composition and community structure of pelagic nekton off Oregon and Washington under variable oceanographic conditions. Marine Ecology Progress Series 298:41–57.

Browman, H., P. Cury, R. Hilborn, S. Jennings, H. Lotze, P. Mace, S. Murawski, D. Pauly, M. Sissenwine, K. Stergiou, and D. Zeller. 2004. Perspectives on ecosystem-based approaches to the management of marine resources. Marine Ecology Progress Series 274:269–303.

Chan, F., J. A. Barth, J. Lubchenco, A. Kirincich, H. Weeks, W. T. Peterson, and B. A. Menge. 2008. Emergence of anoxia in the California current large marine ecosystem. Science 319:920–920.

DeVries, P. 1997. Riverine salmonid egg burial depths: Review of published data and implications for scour studies. Canadian Journal of Fisheries and Aquatic Sciences 54:1685–1698.

Di Lorenzo, E., V. Combes, J. E. Keister, P. T. Strub, A. C. Thomas, P. J. S. Franks, M. D. Ohman, J. C. Furtado, A. Bracco, S. J. Bograd, W. T. Peterson, F. B. Schwing, S. Chiba, B. Taguchi, S. Hormazabal, and C. Parada. 2013. Synthesis of Pacific Ocean climate and ecosystem dynamics. Oceanography 26:68–81.

Dyson, K., and D. D. Huppert. 2010. Regional economic impacts of razor clam beach closures due to harmful algal blooms (HABs) on the Pacific coast of Washington. Harmful Algae 9:264–271.

Ecosystem Principles Advisory Panel. 1999. Ecosystem-based fishery management: A report to Congress by the Ecosystem Principles Advisory Panel. U.S. Dept. of Commerce, National Oceanic and Atmospheric Administration, National Marine Fisheries Service, Washington, D.C.

Feely, R. A., R. R. Okazaki, W. J. Cai, N. Bednarsek, S. R. Alin, R. H. Byrne, and A. Fassbender. 2018. The combined effects of acidification and hypoxia on pH and aragonite saturation in the coastal waters of the California current ecosystem and the northern Gulf of Mexico. Continental Shelf Research 152:50–60.

Feely, R. A., C. L. Sabine, J. M. Hernandez-Ayon, D. Ianson, and B. Hales. 2008. Evidence for upwelling of corrosive "acidified" water onto the continental shelf. Science 320:1490–1492.

Fisher, J. L., W. T. Peterson, and R. R. Rykaczewski. 2015. The impact of El Niño events on the pelagic food chain in the northern California Current. Global Change Biology 21:4401–4414.

Fluharty, D., M. Abbott, R. Davis, M. Donahue, S. Madsen, T. Quinn, J. Rice, and J. Sutinen. 2006. Evolving an ecosystem approach to science and management throughout NOAA and its partners: A report to the NOAA Science Advisory Board.

Grantham, B., F. Chan, K. Nielsen, D. Fox, J. Barth, A. Huyer, J. Lubchenco, and B. Menge. 2004. Upwelling-driven nearshore hypoxia signals ecosystem and oceanographic changes in the northeast Pacific. Nature 429:749–754.

Greene, C. M., D. W. Jensen, G. R. Pess, and E. A. Steel. 2005. Effects of environmental conditions during stream, estuary, and ocean residency on Chinook salmon return rates in the Skagit River, Washington. Transactions of the American Fisheries Society 134:1562–1581.

Harvey, C., and N. Garfield, editors. 2017. California Current Integrated Ecosystem Assessment (CCIEA) California Current Ecosystem Status Report, 2017. Report to the Pacific Fishery Management Council, Agenda Item F.1.a, March 2017. Available: http://www.pcouncil.org/wp-content/uploads/2017/02/F1a_NMFS_Rpt1_2017IEA_Main_Rpt_Final_Mar2017BB.pdf.

Harvey, C., N. Garfield, E. Hazen, and G. Williams, editors. 2014. The California Current Integrated Ecosystem Assessment: Phase III report. U.S. Department of Commerce, NOAA. Available: http://www.noaa.gov/iea/CCIEA-Report/index.

Harvey, C., N. Garfield, G. Williams, K. Andrews, C. Barcelo, K. Barnas, S. Bograd, R. Brodeur, B. Burke, J. Cope, L. deWitt, J. Field, J. Fisher, C. Greene, T. Good, E. Hazen, D. Holland, M. Jacox, S. Kasperski, S. Kim, A. Leising, S. Melin, C. Morgan, S. Munsch, K. Norman, W. T. Peterson, M. Poe, J. Samhouri, I. Schroeder, W. Sydeman, J. Thayer, A. Thompson, N. Tolimieri, A. Varney, B. Wells, T. Williams, and J. Zamon. 2017. Ecosystem status report of the California Current for 2017: A summary of ecosystem indicators compiled by the California Current Integrated Ecosystem Assessment Team (CCIEA). US Department of Commerce, NOAA Technical Memorandum NMFS-NWFSC-139.

Harvey, C., N. Garfield, G. Williams, N. Tolimieri, I. Schroeder, E. Hazen, K. Andrews, K. Barnas, S. Bograd, R. Brodeur, B. Burke, J. Cope, L. DeWitt, J. Field, J. Fisher, T. Good, C. Greene, D. Holland, M. Hunsicker, M. Jacox, S. Kasperski, S. Kim, A. Leising, S. Melin, C. Morgan, B. Muhling, S. Munsch, K. Norman, W. Peterson, M. Poe, J. Samhouri, W. Sydeman, J. Thayer, A. Thompson, D. Tommasi, A. Varney, B. Wells, T. Williams, J. Zamon, D. Lawson, S. Anderson, J. Gao, M. Litzow, S. McClatchie, E. Ward, and S. Zador. 2018. Ecosystem status report of the California Current for 2018: A summary of ecosystem indicators compiled by the California Current Integrated Ecosystem Assessment Team (CCIEA). U.S. Department of Commerce, NOAA Technical Memorandum NMFS-NWFSC-145.

Harvey, C., T. Garfield, G. Williams, and N. Tolimieri, editors. 2019. California Current Integrated Ecosystem Assessment (CCIEA) California Current ecosystem status report, 2019, Report to the Pacific Fishery Management Council. Available: https://www.integratedecosystemassessment.noaa.gov/regions/california-current/cc-publications-reports.

Hazen, E. L., K. L. Scales, S. M. Maxwell, D. K. Briscoe, H. Welch, S. J. Bograd, H. Bailey, S. R. Benson, T. Eguchi, H. Dewar, S. Kohin, D. P. Costa, L. B. Crowder, and R. L. Lewison. 2018. A dynamic ocean management tool to reduce bycatch and support sustainable fisheries. Science Advances 4.

Hodgson, E. E., I. C. Kaplan, K. N. Marshall, J. Leonard, T. E. Essington, D. S. Busch, E. A. Fulton, C. J. Harvey, A. J. Hermann, and P. McElhany. 2018. Consequences of spatially variable ocean acidification in the California Current: Lower pH drives strongest declines in benthic species in southern regions while greatest economic impacts occur in northern regions. Ecological Modelling 383:106–117.

Jacox, M. G., C. A. Edwards, E. L. Hazen, and S. J. Bograd. 2018. Coastal upwelling revisited: Ekman, Bakun, and improved upwelling indices for the US West Coast. Journal of Geophysical Research–Oceans 123:7332–7350.

Jeffries, K. M., S. G. Hinch, T. Sierocinski, T. D. Clark, E. J. Eliason, M. R. Donaldson, S. R. Li, P. Pavlidis, and K. M. Miller. 2012. Consequences of high temperatures and premature mortality on the transcriptome and blood physiology of wild adult sockeye salmon (*Oncorhynchus nerka*). Ecology and Evolution 2:1747–1764.

Jepson, M., and L. L. Colburn. 2013. Development of social indicators of fishing community vulnerability and resilience in the U.S. Southeast and Northeast regions. U.S. Dept. of Commerce, National Oceanic and Atmospheric Administration, National Marine Fisheries Service, NOAA Technical Memorandum NMFS-F/SPO-129.

Kaplan, I. C., G. D. Williams, N. A. Bond, A. J. Hermann, and S. A. Siedlecki. 2016. Cloudy with a chance of sardines: Forecasting sardine distributions using regional climate models. Fisheries Oceanography 25:15–27.

Kasperski, S., and D. S. Holland. 2013. Income diversification and risk for fishermen. Proceedings of the National Academy of Sciences of the United States of America 110:2076–2081.

Keister, J. E., E. Di Lorenzo, C. A. Morgan, V. Combes, and W. T. Peterson. 2011. Zooplankton species composition is linked to ocean transport in the Northern California Current. Global Change Biology 17:2498–2511.

Keller, A. A., V. Simon, F. Chan, W. W. Wakefield, M. Clarke, J. A. Barth, D. Kamikawa, and E. L. Fruh. 2010. Demersal fish and invertebrate biomass in relation to an offshore hypoxic zone along the US West Coast. Fisheries Oceanography 19:76–87.

Keller, A. A., J. R. Wallace, and R. D. Methot. 2017. The Northwest Fisheries Science Center's West Coast Groundfish Bottom Trawl Survey: History, design and description. U.S. Dept. of Commerce, National Oceanic and Atmospheric Administration, National Marine Fisheries Service, NOAA Technical Memorandum NMFS-NWFSC-136.

Kershner, J., J. F. Samhouri, C. A. James, and P. S. Levin. 2011. Selecting indicator portfolios for marine species and food webs: A Puget Sound case study. PLOS ONE 6.

Lefebvre, K. A., S. Bargu, T. Kieckhefer, and M. W. Silver. 2002. From sanddabs to blue whales: The pervasiveness of domoic acid. Toxicon 40:971–977.

Leising, A. W., I. D. Schroeder, S. J. Bograd, J. Abell, R. Durazo, G. Gaxiola-Castro, E. P. Bjorkstedt, J. Field, K. Sakuma, R. R. Robertson, R. Goericke, W. T. Peterson, R. Brodeur, C. Barcelo, T. D. Auth, E. A. Daly, R. M. Suryan, A. J. Gladics, J. M. Porquez, S. McClatchie, E. D. Weber, W. Watson, J. A. Santora, W. J. Sydeman, S. R. Melin, F. P. Chavez, R. T. Golightly, S. R. Schneider, J. Fisher, C. Morgan, R. Bradley, and P. Warybok. 2015. State of the California Current 2014–15: Impacts of the Warm-Water "Blob". California Cooperative Oceanic Fisheries Investigations Reports 56:31–68.

Leising, A. W., I. D. Schroeder, S. J. Bograd, E. P. Bjorkstedt, J. Field, K. Sakuma, J. Abell, R. R. Robertson, J. Tyburczy, W. T. Peterson, R. Brodeur, C. Barcelo, T. D. Auth, E. A. Daly, G. S. Campbell, J. A. Hildebrand, R. M. Suryan, A. J. Gladics, C. A. Horton, M. Kahru, M. Manzano-Sarabia, S. McClatchie, E. D. Weber, W. Watson, J. A. Santora, W. J. Sydeman, S. R. Melin, R. L. Delong, J. Largier, S. Y. Kim, F. P. Chavez, R. T. Golightly, S. R. Schneider, P. Warzybok, R. Bradley, J. Jahncke, J. Fisher, and J. Peterson. 2014. State of the California Current 2013–14: El Niño Looming. California Cooperative Oceanic Fisheries Investigations Reports 55:51–87.

Levin, P. S., M. J. Fogarty, G. C. Matlock, and M. Ernst. 2008. Integrated ecosystem assessments. U.S. Dept. of Commerce, National Oceanic and Atmospheric Administration, National Marine Fisheries Service, NOAA Technical Memorandum NMFS-NWFSC-92.

Levin, P. S., M. J. Fogarty, S. A. Murawski, and D. Fluharty. 2009. Integrated ecosystem assessments: Developing the scientific basis for ecosystem-based management of the ocean. PLOS Biology 7:23–28.

Levin, P. S., and F. B. Schwing, editors. 2011. Technical background for an integrated ecosystem assessment of the California Current: Groundfish, salmon, green sturgeon, and ecosystem health. U.S. Dept. of Commerce, National Oceanic and Atmospheric Administration, National Marine Fisheries Service, NOAA Technical Memorandum NMFS-NWFSC-109.

Levin, P. S., B. K. Wells, and M. B. Sheer, editors. 2013. California Current Integrated Ecosystem Assessment: Phase II Report. Available: https://www.integratedecosystemassessment.noaa.gov/regions/california-current/cc-publications-reports/phaseIIIReport2013.

Lindgren, F., and H. Rue. 2015. Bayesian spatial modelling with R-INLA. Journal of Statistical Software 63:1–25.

Link, J. 2017. A conversation about NMFS' Ecosystem-Based Fisheries Management Policy and Road Map. Fisheries 42:498–503.

Lloyd's Register, QinetiQ, and University of Strathclyde. 2013. Global marine trends 2030. Available: https://www.lr.org/en-us/insights/global-marine-trends-2030/.

Long, R., A. Charles, and R. Stephenson. 2015. Key principles of marine ecosystem-based management. Marine Policy 57:53–60.

Marine, K. R., and J. J. Cech. 2004. Effects of high water temperature on growth, smoltification, and predator avoidance in Juvenile Sacramento River Chinook salmon. North American Journal of Fisheries Management 24:198–210.

Marshall, K. N., I. C. Kaplan, E. E. Hodgson, A. Hermann, D. S. Busch, P. McElhany, T. E. Essington, C. J. Harvey, and E. A. Fulton. 2017. Risks of ocean acidification in the California Current food web and fisheries: Ecosystem model projections. Global Change Biology 23:1525–1539.

Mason, J. G., E. L. Hazen, S. J. Bograd, H. Dewar, and L. B. Crowder. 2019. Community-level effects of spatial management in the California drift gillnet fishery. Fisheries Research 214:175–182.

McCabe, R. M., B. M. Hickey, R. M. Kudela, K. A. Lefebvre, N. G. Adams, B. D. Bill, F. M. D. Gulland, R. E. Thomson, W. P. Cochlan, and V. L. Trainer. 2016. An unprecedented coastwide toxic algal bloom linked to anomalous ocean conditions. Geophysical Research Letters 43:10366–10376.

McClatchie, S. 2014. Regional fisheries oceanography of the California Current system. Springer, Dordrecht.

McClatchie, S., R. Goericke, A. Leising, T. Auth, E. Bjorkstedt, R. R. Robertson, R. Brodeur, X. Du, E. A. Daly, C. Morgan, F. Chavez, A. Debich, J. Hildebrand, J. Field, K. Sakuma, M. Jacox, M. Kahru, R. Kudela, C. Anderson, B. E. Lavaniegos, J. Gomez-Valdes, S. Jimenez-Rosenberg, R. McCabe, S. R. Melin, M. D. Ohman, L. Sala, B. Peterson, J. Fisher, I. Schroeder, S. J. Bograd, E. Hazen, S. Schneider, R. T. Golightly, R. M. Suryan, A. J. Gladics, S. Loredo, J. M. Porquez, A. Thompson, E. D. Weber, W. Watson, V. Trainer, P. Warzybok, R. Bradley, and J. Jahncke. 2016. State of the California Current 2015–16: Comparisons with the 1997–98 El Niño. CalCOFI Reports 57:5–61.

McFadden, K., and C. Barnes. 2009. The implementation of an ecosystem approach to management within a federal government agency. Marine Policy 33:156–163.

McKibben, S. M., W. Peterson, M. Wood, V. L. Trainer, M. Hunter, and A. E. White. 2017. Climatic regulation of the neurotoxin domoic acid. Proceedings of the National Academy of Sciences of the United States of America 114:239–244.

Melin, S. R., A. J. Orr, J. D. Harris, J. L. Laake, and R. L. DeLong. 2012. California sea lions: An indicator for integrated ecosystem assessment of the California Current system. California Cooperative Oceanic Fisheries Investigations Reports 53:140–152.

Morgan, C. A., B. R. Beckman, L. A. Weitkamp, and K. L. Fresh. 2019. Recent Ecosystem Disturbance in the Northern California Current. Fisheries. DOI: 10.1002/fsh.10273.

Munsch, S., C. Greene, R. Johnson, W. Satterthwaite, H. Imaki, and P. Brandes. 2019. Warm, dry winters truncate timing and size distribution of seaward-migrating salmon across a large, regulated watershed. Ecological Applications 29:e01880.

Neveu, E., A. M. Moore, C. A. Edwards, J. Fiechter, P. Drake, W. J. Crawford, M. G. Jacox, and E. Nuss. 2016. An historical analysis of the California Current circulation using ROMS 4D-Var: System configuration and diagnostics. Ocean Modelling 99:133–151.

NMFS. 2016. Fisheries of the United States, 2015. US Department of Commerce, NOAA Current Fishery Statistics No. 2015. Available: https://www.st.nmfs.noaa.gov/Assets/commercial/fus/fus15/documents/FUS2015.pdf.

NOAA. 2016. Ecosystem-based fisheries management policy of the National Marine Fisheries Service. U.S. Department of Commerce, National Oceanic and Atmospheric Administration. Available: http://www.st.nmfs.noaa.gov/Assets/ecosystems/ebfm/Draft_EBFM_Policy_9.9.2015_for_release.pdf.

NOAA. 2018. Ecosystem-based fisheries management policy of the National Marine Fisheries Service. NOAA Fisheries Policy 01-120. U.S. Department of Commerce, National Oceanic and Atmospheric Administration. Available: https://www.fisheries.noaa.gov/resource/document/ecosystem-based-fisheries-management-policy.

NOAA. 2019. 2018 West Coast whale entanglement summary. US Department of Commerce, National Oceanic and Atmospheric Administration, National Marine Fisheries Service. Available: https://www.fisheries.noaa.gov/resource/document/2018-west-coast-whale-entanglement-summary.

Peterson, W. T., J. L. Fisher, J. O. Peterson, C. A. Morgan, B. J. Burke, and K. L. Fresh. 2014. Applied fisheries oceanography ecosystem indicators of ocean condition inform fisheries management in the California Current. Oceanography 27:80–89.

Peterson, W. T., J. L. Fisher, P. T. Strub, X. N. Du, C. Risien, J. Peterson, and C. T. Shaw. 2017. The pelagic ecosystem in the Northern California Current off Oregon during the 2014–2016 warm anomalies within the context of the past 20 years. Journal of Geophysical Research–Oceans 122:7267–7290.

PFMC. 2013. Pacific Coast Fishery Ecosystem Plan for the U.S. portion of the California Current large marine ecosystem. Pacific Fishery Management Council, Portland, OR.

PFMC. 2019. Status of the Pacific Coast coastal pelagic species fishery and recommended acceptable biological catches. Stock assessment and fishery evaluation for 2018. Pacific Fishery Management Council, Portland, OR.

Richter, A., and S. A. Kolmes. 2005. Maximum temperature limits for Chinook, coho, and chum salmon, and steelhead trout in the Pacific Northwest. Reviews in Fisheries Science 13:23–49.

Ritzman, J., A. Brodbeck, S. Brostrom, S. McGrew, S. Dreyer, T. Klinger, and S. K. Moore. 2018. Economic and sociocultural impacts of fisheries closures in two fishing-dependent communities following the massive 2015 US West Coast harmful algal bloom. Harmful Algae 80:35–45.

Rogers-Bennett, L., and C. I. Juhasz. 2014. The rise of invertebrate fisheries and the fishing down of marine food webs in California. California Fish and Game 100:218–233.

Sainsbury, K., P. Gullestad, and J. Rice. 2014. The use of national frameworks for sustainable development of marine fisheries and conservation, ecosystem-based management and integrated ocean management. Pages 301–316 in S. Garcia, J. Rice, and A. Charles, editors. Governance of Marine Fisheries and Biodiversity Conservation: Interaction and Coevolution. John Wiley & Sons, Chichester, UK.

Sakuma, K. M., J. C. Field, N. J. Mantua, S. Ralston, B. B. Marinovic, and C. N. Carrion. 2016. Anomalous epipelagic micronekton assemblage patterns in the neritic waters of the California Current in spring 2015 during a period of extreme ocean conditions. California Cooperative Oceanic Fisheries Investigations Reports 57:163–183.

Santora, J. A., I. D. Schroeder, J. C. Field, B. K. Wells, and W. J. Sydeman. 2014. Spatio-temporal dynamics of ocean conditions and forage taxa reveal regional structuring of seabird–prey relationships. Ecological Applications 24:1730–1747.

Scales, K. L., E. L. Hazen, M. G. Jacox, F. Castruccio, S. M. Maxwell, R. L. Lewison, and S. J. Bograd. 2018. Fisheries bycatch risk to marine megafauna is intensified in Lagrangian coherent structures. Proceedings of the National Academy of Sciences of the United States of America 115:7362–7367.

Schroeder, I. D., J. A. Santora, S. J. Bograd, E. L. Hazen, K. M. Sakuma, A. M. Moore, C. A. Edwards, B. K. Wells, and J. C. Field. 2019. Source water variability as a driver of rockfish recruitment in the California Current Ecosystem: Implications for climate change and fisheries management. Canadian Journal of Fisheries and Aquatic Sciences 76:950–960.

Schwing, F., M. O'Farrell, J. Steger, and K. Baltz. 1996. Coastal upwelling indices, west coast of North America 1946–95. U.S. Department of Commerce, NOAA Technical Memorandum NMFS-SWFSC-231.

Selden, R. L., J. T. Thorson, J. F. Samhouri, S. J. Bograd, S. Brodie, G. Carroll, M. A. Haltuch, E. L. Hazen, K. K. Holsman, M. L. Pinsky, N. Tolimieri, and E. Willis-Norton. In press. Coupled changes in biomass and distribution drive trends in availability of fish stocks to U.S. West Coast ports. ICES Journal of Marine Science.

Siedlecki, S. A., I. C. Kaplan, A. J. Hermann, T. T. Nguyen, N. A. Bond, J. A. Newton, G. D. Williams, W. T. Peterson, S. R. Alin, and R. A. Feely. 2016. Experiments with seasonal forecasts of ocean conditions for the northern region of the California Current upwelling system. Scientific Reports 6.

Slater, W., G. DePiper, J. Gove, C. Harvey, E. Hazen, S. Lucey, M. Karnauskas, S. Regan, E. Siddon, E. Yasumiishi, S. Zador, M. Brady, M. Ford, R. Griffis, R. Shuford, H. Townsend, T. O'Brien, J. Peterson, K. Osgood, and J. Link. 2017. Challenges, opportunities and future directions to advance NOAA Fisheries ecosystem status reports (ESRs): Report of the National ESR Workshop. U.S. Dept. of Commerce, National Oceanic and Atmospheric Administration, National Marine Fisheries Service, NOAA Technical Memorandum NMFS-F/SPO-174.

Sutherland, K. R., H. L. Sorensen, O. N. Blondheim, R. D. Brodeur, and A. W. E. Galloway. 2018. Range expansion of tropical pyrosomes in the northeast Pacific Ocean. Ecology 99:2397–2399.

Thompson, A., C. Harvey, W. Sydeman, C. Barceló, S. Bograd, R. Brodeur, J. Fiechter, J. Field, N. Garfield, T. Good, E. Hazen, M. Hunsicker, K. Jacobson, M. Jacox, A. Leising, J. Lindsay, S. Melin, J. Santora, I. Schroeder, J. Thayer, B. Wells, and G. Williams. 2019. Indicators of pelagic forage community shifts in the California Current large marine ecosystem, 1998–2016. Ecological Indicators 105:215–228.

Thompson, A., I. Schroeder, S. Bograd, E. Hazen, M. Jacox, A. Leising, B. Wells, J. Largier, J. Fisher, K. Jacobson, S. Zeman, E. Bjorkstedt, R. Robertson, F. Chavez, M. Kahru, R. Goericke, S. McClatchie, C. Peabody, T. Baumgartner, B. Lavaniegos, J. Gomez-Valdes, R. Brodeur, E. Daly, C. Morgan, T. Auth, B. Burke, J. Field, K. Sakuma, E. Weber, W. Watson, J. Coates, R. Schoenbaum, L. Rogers-Bennett, R. Suryan, J. Dolliver, S. Loredo, J. Zamon, S. Schneider, R. T. Golightly, P. Warzybok, J. Jahncke, J. Santora, S. Thompson, W. Sydeman, and S. Melin. 2018. State of the California Current 2017–2018: Still not quite normal in the north and getting interesting in the south. California Cooperative Oceanic Fisheries Investigations Report 59:1–66.

Thorson, J. T., A. O. Shelton, E. J. Ward, and H. J. Skaug. 2015. Geostatistical delta-generalized linear mixed models improve precision for estimated abundance indices for West Coast groundfishes. ICES Journal of Marine Science 72:1297–1310.

True, K., A. Voss, and J. Foott. 2017. Myxosporean parasite (*Ceratonova shasta* and *Parvicapsula minibicornis*) prevalence of infection in Klamath River basin juvenile Chinook salmon, March–August 2017. U.S. Fish and Wildlife Service, California–Nevada Fish Health Center, Anderson, CA.

Walther, Y. M., and C. Möllmann. 2014. Bringing integrated ecosystem assessments to real life: A scientific framework for ICES. ICES Journal of Marine Science 71:1183–1186.

Waples, R. S. 1995. Evolutionarily significant units and the conservation of biological diversity under the Endangered Species Act. Evolution and the Aquatic Ecosystem: Defining Unique Units in Population Conservation 17:8–27.

Welch, H., E. L. Hazen, S. J. Bograd, M. G. Jacox, S. Brodie, D. Robinson, K. L. Scales, L. Dewitt, and R. Lewison. 2019a. Practical considerations for operationalizing dynamic management tools. Journal of Applied Ecology 56:459–469.

Welch, H., E. L. Hazen, D. K. Briscoe, S. J. Bograd, M. G. Jacox, T. Eguchi, S. R. Benson, C. C. Fahy, T. Garfield, D. Robinson, J. A. Seminoff, and H. Bailey. 2019b. Environmental indicators to reduce loggerhead turtle bycatch offshore of Southern California. Ecological Indicators 98:657–664.

Wells, B. K., I. D. Schroeder, S. J. Bograd, E. L. Hazen, M. G. Jacox, A. Leising, N. Mantua, J. A. Santora, J. Fisher, W. T. Peterson, E. Bjorkstedt, R. R. Robertson, F. P. Chavez, R. Goericke, R. Kudela, C. Anderson, B. E. Lavaniegos, J. Gomez-Valdes, R. D. Brodeur, E. A. Daly, C. A. Morgan, T. D. Auth, J. C. Field, K. Sakuma, S. McClatchie, A. R. Thompson, E. D. Weber, W. Watson, R. M. Suryan, J. Parrish, J. Dolliver, S. Loredo, J. M. Porquez, J. E. Zamon, S. R. Schneider, R. T. Golightly, P. Warzybok, R. Bradley, J. Jahncke, W. Sydeman, S. R. Melin, J. A. Hildebrand, A. J. Debich, and B. Thayre. 2017. State of the California Current 2016–17: Still anything but "normal" in the north. California Cooperative Oceanic Fisheries Investigations Reports 58:1–55.

Wells, B. K., I. D. Schroeder, J. A. Santora, E. L. Hazen, S. J. Bograd, E. P. Bjorkstedt, V. J. Loeb, S. Mcclatchie, E. D. Weber, W. Watson, A. R. Thompson, W. T. Peterson, R. D. Brodeur, J. Harding, J. Field, K. Sakuma, S. Hayes, N. Mantua, W. J. Sydeman, M. Losekoot, S. A. Thompson, J. Largier, S. Y. Kim, F. P. Chavez, C. Barcelo, P. Warzybok, R. Bradley, J. Jahncke, R. Goericke, G. S. Campbell, J. A. Hildebrand, S. R. Melin, R. L. Delong, J. Gomez-Valdes, B. Lavaniegos, G. Gaxiola-Castro, R. T. Golightly, S. R. Schneider, N. Lo, R. M. Suryan, A. J. Gladics, C. A. Horton, J. Fisher, C. Morgan, J. Peterson, E. A. Daly, T. D. Auth, and J. Abell. 2013. State of the California Current 2012–13: No such thing as an "average" year. California Cooperative Oceanic Fisheries Investigations Reports 54:37–71.

Zimmerman, M. S., C. Kinsel, E. Beamer, E. J. Connor, and D. E. Pflug. 2015. Abundance, survival, and life history strategies of juvenile Chinook salmon in the Skagit River, Washington. Transactions of the American Fisheries Society 144:627–641.

Contributors

Corresponding authors

Dr. Chris Harvey	chris.harvey@noaa.gov
Dr. Newell (Toby) Garfield	toby.garfield@noaa.gov
Mr. Gregory Williams	greg.williams@noaa.gov
Dr. Nick Tolimieri	nick.tolimieri@noaa.gov
Dr. Isaac Schroeder	isaac.schroeder@noaa.gov

All contributors, by affiliation

NOAA Fisheries—NWFSC

Dr. Chris Harvey
Mr. Kelly Andrews
Ms. Katie Barnas
Dr. Richard Brodeur
Dr. Brian Burke
Dr. Jason Cope
Mr. Peter Frey
Dr. Thomas Good
Dr. Correigh Greene
Dr. Daniel Holland
Dr. Kym Jacobson
Dr. Isaac Kaplan
Dr. Stephanie Moore
Dr. Stuart Munsch
Dr. Karma Norman
Dr. Jameal Samhouri
Dr. Kayleigh Somers
Dr. Nick Tolimieri
Dr. Vera Trainer
Mr. Curt Whitmire
Ms. Margaret Williams
Dr. Jeannette Zamon

NOAA Fisheries—SWFSC

Dr. Newell (Toby) Garfield
Dr. Eric Bjorkstedt
Dr. Steven Bograd
Ms. Lynn deWitt
Dr. John Field
Dr. Elliott Hazen
Dr. Michael Jacox
Dr. Andrew Leising
Mr. Keith Sakuma
Dr. Andrew Thompson
Dr. Brian Wells
Dr. Thomas Williams

NOAA Fisheries—AFSC

Dr. Stephen Kasperski
Dr. Sharon Melin
Dr. Jim Thorson

NOAA Fisheries—West Coast Region

Mr. Dan Lawson

Pacific States Marine Fisheries Commission

Mr. Gregory Williams
Ms. Anna Varney

Oregon State University

Ms. Jennifer Fisher
Ms. Cheryl Morgan
Ms. Samantha Zeman

University of California, Santa Cruz

Dr. Barbara Muhling
Dr. Isaac Schroeder
Dr. Desiree Tommasi

Humboldt State University

Ms. Roxanne Robertson

University of Connecticut

Dr. Samantha Siedlecki

Rutgers University

Dr. Rebecca Selden

Farallon Institute

Dr. William Sydeman

Washington Department of Health

Ms. Audrey Coyne

Oregon Department of Fish and Wildlife

Mr. Matthew Hunter

Oregon Department of Agriculture

Mr. Alex Manderson
Dr. Judy Dowell

California Department of Fish and Wildlife

Ms. Christy Juhasz
Dr. Laura Rogers-Bennett

Recently published by the Northwest Fisheries Science Center

NOAA Technical Memorandum NMFS-NWFSC-

148 **Sharma, R., C. E. Porch, E. A. Babcock, M. Maunder, and A. E. Punt, editors. 2019.** Recruitment: Theory, Estimation, and Application in Fishery Stock Assessment Models. U.S. Department of Commerce, NOAA Technical Memorandum NMFS-NWFSC-148. NTIS number PB2019-100745. https://doi.org/10.25923/1r2p-hs38

147 **Sloan, C. A., B. Anulacion, K. A. Baugh, J. L. Bolton, D. Boyd, P. M. Chittaro, D. A. M. da Silva, J. B. Gates, B. L. Sanderson, K. Veggerby, and G. M. Ylitalo. 2019.** Quality Assurance Plan for Analyses of Environmental Samples for Polycyclic Aromatic Hydrocarbons, Persistent Organic Pollutants, Dioctyl Sulfosuccinate, Estrogenic Compounds, Steroids, Hydroxylated Polycyclic Aromatic Hydrocarbons, Stable Isotope Ratios, and Lipid Classes. U.S. Department of Commerce, NOAA Technical Memorandum NMFS-NWFSC-147. NTIS number PB2019-100744. https://doi.org/10.25923/kf28-n618

146 **Jannot, J. E., K. A. Somers, V. Tuttle, J. McVeigh, and T. P. Good. 2018.** Seabird Mortality in U.S. West Coast Groundfish Fisheries, 2002–16. U.S. Department of Commerce, NOAA Technical Memorandum NMFS-NWFSC-146. NTIS number PB2019-100330. https://doi.org/10.25923/qeyc-0r73

145 **Harvey, C., N. Garfield, G. Williams, N. Tolimieri, I. Schroeder, E. Hazen, K. Andrews, K. Barnas, S. Bograd, R. Brodeur, B. Burke, J. Cope, L. deWitt, J. Field, J. Fisher, T. Good, C. Greene, D. Holland, M. Hunsicker, M. Jacox, S. Kasperski, S. Kim, A. Leising, S. Melin, C. Morgan, B. Muhling, S. Munsch, K. Norman, W. Peterson, M. Poe, J. Samhouri, W. Sydeman, J. Thayer, A. Thompson, D. Tommasi, A. Varney, B. Wells, T. Williams, J. Zamon, D. Lawson, S. Anderson, J. Gao, M. Litzow, S. McClatchie, E. Ward, and S. Zador. 2018.** Ecosystem Status Report of the California Current for 2018: A Summary of Ecosystem Indicators Compiled by the California Current Integrated Ecosystem Assessment Team (CCEIA). U.S. Department of Commerce, NOAA Technical Memorandum NMFS-NWFSC-145. NTIS number PB2019-100284. https://doi.org/10.25923/mvhf-yk36

144 **Fonner, R., and A. Warlick. 2018.** Marine Protected Resources on the U.S. West Coast: Current Management and Opportunities for Applying Economic Analysis. U.S. Department of Commerce, NOAA Technical Memorandum NMFS-NWFSC-144. NTIS number PB2019-100285. https://doi.org/10.25923/vprp-1507

143 **Harsch, M., L. Pfeiffer, E. Steiner, and M. Guldin. 2018.** Economic Performance Metrics: An Overview of Metrics and the Use of Web Applications to Disseminate Outcomes in the U.S. West Coast Groundfish Trawl Catch Share Program. U.S. Department of Commerce, NOAA Technical Memorandum NMFS-NWFSC-143. NTIS number PB2019-100087. https://doi.org/10.25923/a4g5-cq83

142 **Jannot, J. E., T. Good, V. Tuttle, A. M. Eich, and S. Fitzgerald, editors. 2018.** U.S. West Coast and Alaska Trawl Fisheries Seabird Cable Strike Mitigation Workshop, November 2017: Summary Report. U.S. Department of Commerce, NOAA Technical Memorandum NMFS-NWFSC-142. NTIS number PB2018-101082. https://doi.org/10.7289/V5/TM-NWFSC-142

NOAA Technical Memorandums NMFS-NWFSC are available from the NOAA Institutional Repository, https://repository.library.noaa.gov.

U.S. Secretary of Commerce
Wilbur L. Ross, Jr.

Acting Under Secretary of Commerce
for Oceans and Atmosphere
Dr. Neil Jacobs

Assistant Administrator for Fisheries
Chris Oliver

October 2019

www.nmfs.noaa.gov

OFFICIAL BUSINESS

National Marine
Fisheries Service
Northwest Fisheries Science Center
2725 Montlake Boulevard East
Seattle, Washington 98112